Design and Performance Analysis of Urban Traffic Control Systems

Rui Sha

A thesis submitted in partial fulfilment

of the requirements for the degree of

Doctor of Philosophy

of

University College London

Department of Civil, Environmental & Geomatic Engineering

Centre for Transport Studies

University College London

December 2017

Declaration

I, Rui Sha, declare that this thesis titled, ‘Design and Performance Analysis of Urban Traffic Control Systems’ and the work presented in it are my own. I confirm that:

- This work was done wholly or mainly while in candidature for a research degree at University College London.
- Where I have consulted the published work of others, this is always clearly attributed.
- Where I have quoted from the work of others, the source is always given. With the exception of such quotations, this thesis is entirely my own work.
- I have acknowledged all main sources of help.

Signed:

____

Date:

____

If you make more roads, you will have more traffic.

by Jan Gehl

Acknowledgements

I would like to express my sincere gratitude to my supervisor Dr Andy Chow for his academic support and insightful advices through my PhD study. His support helped me to work productively and think a question from different perspectives. My sincere thanks also go to my second supervisor Dr Tohid Erfani. I want to thank him for his valuable opinions and encouragement. I would like to thank Dr. Kamalasudhan Achuthan, Dr Kostantinos Ampountolas, Dr Panagiotis Angeloudis, Dr Bani Anvari and Dr Peter Wagner for their comments on this study, and Angela Cooper for her help on the thesis writing. I am very grateful to UCL Faculty of Engineering Sciences and China Scholarships Council for funding this study.

A special thanks to my friends and UCL colleagues: Atiyeh Ardakanian, Huanfa Chen, Fernanda Garcia Alba Garciadiego, Taha Ghasempour, Sam Ghazizadeh, Yuanyuan Huang, David Huynh, Xianzhe Li, Kun Liu, Shuqiong Luo, Stylianos Minas, Arash Nassirpour, Aris Pavlides, Sascha Pohoryles, Li Shuai, Palak Shukla, Peter Soi, Alexandra Tsioulou, Fang Xu and Ying Li. They have been great companies in the past four years and have given me fond memories.

Finally, I want to thank my family, especially my wife Lifei Liu for both her emotional and academic support. I also would like to express my gratitude to my parents, parents in law, and daughter for their love, care and joy throughout the study and life in general.

Abstract

This study aims to investigate the design and performance of different architectures for urban traffic control with consideration of variations and uncertainties in traffic flow. The architectures, which ranging from centralised, semi-centralised to decentralised, are applied to different road networks. Both macroscopic and microscopic flow models are developed and used to calculate the performance of the systems. The macroscopic model is capable of generating essential traffic dynamics, such as traffic queues' spillover, formation and dissipation. The control systems' are tested under varies traffic demand levels. The results suggest that the centralised systems generally can outperform the decentralised systems, and the most benefit gained in the centralised control comes from its setting of signal offsets. On the other hand, the microscopic flow model captures the movement of each individual vehicle and drivers' rerouting behaviour with respect to traffic conditions. The test results showed that the drivers' response to the traffic condition can help a decentralised system perform as well as a centralised system. This study brings a new insight into cooperative transport management, and contributes to the state-of-the-art of urban traffic system design.

Contents

List of Figures

Abbreviations

BF	**B**rute **F**orce
CTM	**C**ell **T**ransmission **M**odel
FIT	**Fit**ness
GA	**G**enetic **A**lgorithm
GHR	**G**azis-**H**erman-**R**othery
HC	**H**ill-**C**limbing
HJB	**H**amilton-**J**acobi-**B**ellman
LQR	**L**inear-**Q**uadratic **R**egulator
LWR	**L**ighthill and **W**hitham-**R**ichards
MP	**M**ax-**P**ressure
SUMO	**S**imulation of **U**rban **Mo**bility
TND	**T**otal **N**etwork **D**elay
TRANSYT	**Tra**ffic **N**etwork **S**tud**y** **T**ool
TUC	**T**raffic-responsive **U**rban **C**ontrol

VDT	**V**ehicle **D**istance **T**ravelled
VHT	**V**ehicle **H**ours **T**ravelled
VISSIM	**V**erkehr **I**n **S**tÃd’dten - **SIM**ulationsmodel

Notation

C	cycle time	[sec]
$\mathbf{C}$	a set of all cells in a network	
C^N	nominal cycle time	[sec]
$C_{\min}$	minimum cycle time	[sec]
$C_{\max}$	maximum cycle time	[sec]
CI	converted integer cycle time	[sec]
c	cell (or road section) index	
c_l, c_m	relaxation constant and anticipation constant in Payne's second order flow model	
c_s	magnification parameter of performance differences between chromosomes	
c_v, c_κ	sensitivity parameters in METANET flow model	
c_α	a fundamental relationship parameter in METANET flow model	
c_β	a sensitivity coefficient of a stimulus-response model	

d	standstill distance between two successive vehicles	[m]
d_{min}	minimum distance between two successive vehicles	[m]
d_{crit}	critical distance between two successive vehicles	[m]
$\mathbb{G}$	a set of green phases	
GI	converted integer green split	[sec]
g	green split	[sec]
g^N	nominal green split	[sec]
g_{min}	minimum green split	[sec]
g^*	scaled green split	[sec]
$\dot{g}$	gravitational acceleration	[$\mathrm{m}^2/\mathrm{sec}$]
H	sum of demand to saturation flow ratio for all signal stages	
h	demand to saturation flow ratio	
$\mathbf{I}$	a set of all network roads (links)	
$\mathbf{I}^{\mathrm{in}}$	a set of all the inflow roads (links) to an intersection (node)	
$\mathbf{I}^{\mathrm{out}}$	a set of all the outflow roads (links) to an intersection (node)	
i	road (link) index	
j	intersection index	
K_c	the parameter of cycle time control intensity	
k	cycle index	
$\mathbf{L}$	control gain matrix	

LT	lost time	[sec]
l^{cell}	cell length	[m]
l^{link}	link length	[m]
l^{veh}	vehicle length	[m]
$\bar{l}^{\text{veh}}$	mean vehicle length	[m]
m	vehicle index	
n	intersection (node) index	
o	offset	[sec]
o^*	optimal offset	[sec]
Q	maximum flow or saturation flow	[veh/hr]
q	traffic flow rate	[veh/hr]
$\mathbb{R}$	a set of red phases	
R	a set of routes	
T	time period	
t	time step index	
$\mathbf{U}$	a set of signal timing plans	
u	average road (link) travel time	
v	vehicle speed	[m/sec]
v_{des}	vehicle's desired speed	[m/sec]
v_{final}	vehicle's final speed	[m/sec]
v_{max}	vehicle's maximum speed	[m/sec]
v_{safe}	vehicle's safe speed	[m/sec]
w	shockwave speed	

x	road (link) queue length	[veh]
x_{max}	road (link) capacity	[veh]
α	vehicle acceleration or deceleration rate	[m^2/sec]
γ	degree of congestion	
ε	drivers' imperfection factor	
ζ	turning ratio	
η	sensitivity parameter of pressure	
Θ	a set of all stages	
θ	stage index	
ι	stage switch indicator	
Λ	traffic demand profile	
λ	demand magnitude parameter	[veh/hr]
μ	a friction coefficient between vehicle and road surface	
ξ	ratio of queue length to the road (link) queue capacity	
ρ	traffic density, the number of vehicles at a unit length of a road	[veh/m]
ρ_{crit}	critical density	[veh/m]
ρ_{jam}	jam density	[veh/m]
τ	driver's reaction time	
σ	traffic spatial distribution parameter	
υ	average traffic speed	[m/sec]

υ_{f}	free flow speed	[m/sec]
υ_{crit}	critical speed	[m/sec]
$\upsilon_{\mathrm{equal}}$	an equilibrium speed for high order flow model	[m/sec]
χ	vehicle location	
ψ	pressure in Max-pressure control	[veh^2/sec]

Chapter 1

Introduction

1.1 General background

According to the United Nations' statistics record [1], 54 percent of the world population live in cities. This ratio is projected to reach to 66% by 2050, where it was only 34% in the 1960s. The continuous growth in the urban population will lead to the increase in traffic volume. As reported by the Department of Transport, the traffic across the UK will rise 19%-55% during the period from 2010 to 2040 [2]. The growth of traffic challenges the operation of existing urban transport infrastructure and aggravates the traffic congestion problem in large cities like London. Traffic congestion not only has negative impacts on economic growth and social development, but also has severe effects on citizens'daily activities. The traffic information company INRIX found the time wasted in traffic congestion over 2016 is 73.4 hours in London, 65.3 hours in Paris and 39.4 hours in Manchester per passenger per year [3].

Figure 1.1: The urban traffic control system monitors more than 450 of the intersections in Nottingham (Source: World Highways, 2010)

For an urban road network, the expansion of road infrastructure to improve the operation capacity can certainly match the needs for the growth in road traffic. However, it is not a sustainable solution due to the limited land resource and expensive construction. Improving the performance of traffic control systems can be an alternative solution to minimise the congestion and reduce the delays of travel. An urban traffic control system takes traffic count via road detectors and computes control plans to traffic signals. Figure 1.1 is an urban traffic control centre in Nottingham and Figure 1.2 is one of the widely used urban traffic control systems known as SCOOT. A recent study by Chow *et al* [4] indicates that 25%-30% of urban congestion can be reduced by effective traffic control.

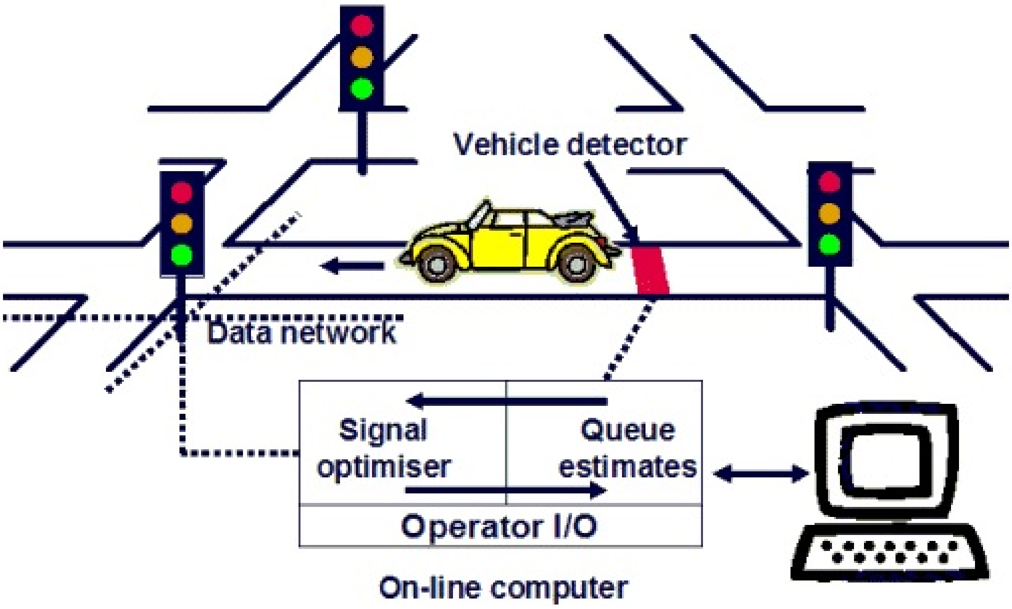

Figure 1.2: An example of urban traffic control system: SCOOT

(Source: Peek Traffic Ltd, Siemens PLC and TRL Limited [5])

Traffic control systems for urban areas are different in structure and can be classified into centralised and decentralised control structures (see Figure 1.3). A centralised control system focuses on finding a global plan for all the traffic signals across the controlled area. However, it is known that the computational time to derive the global plan grows dramatically with the increase in the size of the controlled region. On the other hand, a decentralised system computes the local optimal solutions for each intersection separately in the controlled area. To obtain the global plan, the traffic status for the entire network is essential while the local optimal plans can be derived by knowing the local traffic status. The benefit of using the centralised control system comes from the use of a global optimal plan, and using the decentralised control system provides fast reaction and high scalability. Recently, there has been much research focused on the decentralised control structure [6, 7, 8, 9, 10] for urban

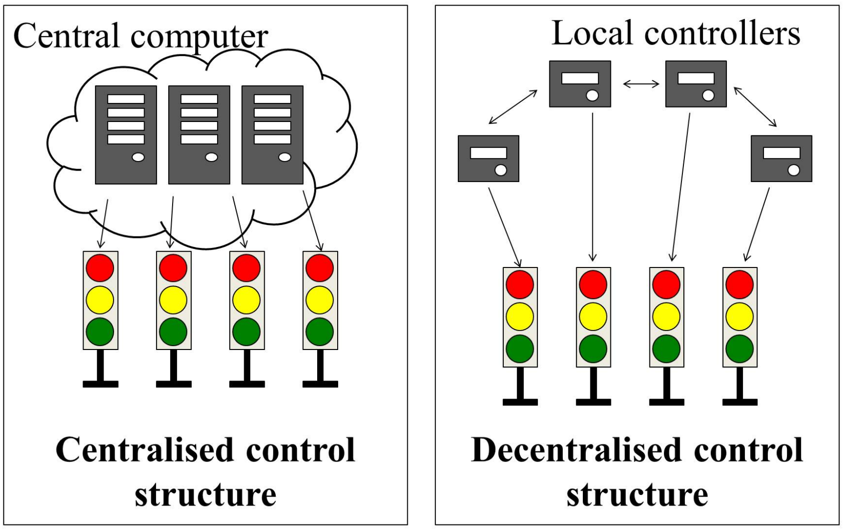
Central computer
Centralised control structure
Local controllers
Decentralised control structure

Figure 1.3: Different control structures of traffic control systems

road traffic. A number of studies [10, 11, 12] have suggested that the performance of a decentralised system would not be significantly outperformed by a centralised one. However, there are limited studies to compare the nature and performance of the centralised and decentralised control structures.

1.2 Research objectives

This study focuses on the performance difference between centralised and decentralised control systems for urban traffic management. The performance difference can provide important insights and guidance on how to design the decentralised control system and bridge the gap with the centralised system. The main objectives of this study are shown as follows:

1. Review the control structures of existing urban traffic control systems and identify the differences in design between centralised and decentralised ones.
2. Build a test platform which can evaluate the performance of traffic control systems.
3. Compare the performances between the centralised and decentralised traffic control systems under different traffic demand with variation and uncertainty.
4. Propose feasible methods to bridge the efficiency gap between the centralised and decentralised systems based on the findings of the previous objective.

1.3 Report outline

The remainder of this report is organised as follows:

Chapter 2 is a review of different types of traffic flow models, urban control systems and traffic signal optimisation techniques. A traffic flow model is a mathematical representation of traffic dynamics, and is a common tool used for traffic modelling and forecasting. The review of the flow model discusses the features of each flow model and determines the ones which are appropriate to use for this study. The review of the urban traffic control system explains the developments of the system and different control structures. The review of the optimisation techniques discussed the use of exact methods and heuristic methods in traffic signal control problems.

Chapter 3 analyses the control principles of selected centralised and decentralised traffic control systems. Two searching techniques are used to derive global signal plans which represent the centralised systems. TUC and Hybrid systems are semi-decentralised systems, where parts of the signal plan are derived from decentralised controllers. Max-pressure controller is a decentralised system which only uses local traffic information to operate traffic signals.

Chapter 4 investigates the performance of the control systems. A macroscopic flow model is used to describe the traffic dynamics. The experiment is carried out in three networks with a range of traffic demands from undersaturation to oversaturation.

Chapter 5 investigates the performance of the control systems at a deeper level. The movement of individual vehicles are simulated by a microscopic flow model, and drivers' rerouting behaviour respecting real-time traffic condition is captured. The experiment is performed on four networks with different demand levels and spatial distributions.

Chapter 6 is a conclusion of the thesis and outlines the future work of this study.

Chapter 2

Literature review

2.1 Introduction

This chapter is a review of traffic flow models, traffic control systems, and traffic signal optimisation methods . A traffic flow model is an essential tool for transport planning and operation, since it is a mathematical representation of traffic dynamics and an analytic expression of traffic forecast. Traffic control systems have been used as the main measure to improve traffic flow in urban road networks. They prevent the traffic movement conflicts at intersections and give appropriate traffic signals to reduce travel delays. Optimisation methods show the insight of the traffic control systems and how traffic signal plans are derived. Section 2.2 reviews different types of traffic flow models, Section 2.3 presents the development made in urban traffic control systems and Section 2.4 discusses the differences between various implemented optimisation methods.

2.2 Traffic flow models

The traffic flow model is a mathematical description of traffic dynamics. It is used to analyse traffic phenomena and to provide efficient traffic operations. The development of the flow model has been carried out for half a century, hence, there exist a wide range of models. The level of detail (microscopic or macroscopic) is commonly used as a criterion to categorise traffic flow models. This section reviews microscopic and macroscopic traffic flow models and discusses their features to determine which ones are suitable to use in this study.

2.2.1 Microscopic flow models

A microscopic traffic flow model considers detailed movements of each individual vehicle, such as lane change, acceleration and other drivers' behaviour. As a modelled vehicle in the flow model has a strong relation to its front vehicle, the microscopic flow model is also known as the car-following model. Some main types of car-following models are: the stimulus-response model, safety-distance model, and psycho-physical model [13]. They base on different assumptions of driving behaviours.

Stimulus-response models

The stimulus-response models describe the response of a driver as a product of a stimulus and the driver's sensitivity to the stimulus. A general form of the stimulus-response model suggested by Chandler *et al* [14] is:

$$\alpha_{m+1}(t+1) = c_\beta[v_m(t) - v_{m+1}(t)] \tag{2.1}$$

c_β is a sensitivity coefficient of vehicle m to the stimulus, which is the difference in speeds $v_m(t) - v_{m+1}(t)$ between the successive vehicles m and $m+1$. The acceleration (deceleration) α of the follower vehicle $m+1$ is a response to the stimulus. The response at a time step $t+1$ is calculated from the stimulus at time step t, since there is a time lag between the response and the stimulus. As the driver may become more sensitive to the stimulus when vehicles are close to each other, Gazis *et al* [15] modified Equation 2.1 to:

$$\alpha_{m+1}(t+1) = \frac{c_\beta}{\chi_m(t) - \chi_{m+1}(t)}[v_m(t) - v_{m+1}(t)] \tag{2.2}$$

The expression of the sensitivity becomes to $\frac{c_\beta}{\chi_m(t)-\chi_{m+1}(t)}$, which is affected by the distances between the successive vehicles m and $m+1$. Equation 2.2 is subsequently generalised as:

$$\alpha_{m+1}(t+1) = \frac{c_\beta v_m(t+1)_l^c}{[\chi_m(t) - \chi_{m+1}(t)]_m^c}[v_m(t) - v_{m+1}(t)] \tag{2.3}$$

Equation 2.3 is known as the Gazis-Herman-Rothery (GHR) model [16], and the parameters c_l and c_m are calibrated with fields data in several studies, such as [17] and [18]. Although the stimulus-response model has been proposed since the late

1950s, it had been used less frequently until the mid-1990s due to the findings on the parameter values contradict with each other [19].

Safety-distance models

The second type of car-following models is the safety-distance model. Different from the stimulus-response model, a safety-distance model is based on the assumption that successive vehicles maintain a safe distance with each other to avoid collision. The early safety-distance model proposed by Pipe [20] expresses the location of two successive vehicle m and $m+1$ as:

$$\chi_m = \chi_{m+1} + d + l_m^{\text{veh}} + \tau v_{m+1} \tag{2.4}$$

In Equation 2.4, d is the standstill distance between the vehicles, l^{veh} is the vehicle length and τv_{n+1} represents the travel distance. The travel distance is calculated as the product of the driver's reaction time τ and its travel speed v_{m+1} of the vehicle $m+1$. The whole part of $d + l_m^{\text{veh}} + \tau v_{m+1}$ forms the safe distance between the vehicles m and $m+1$. Comparing to the traffic data measured from field, the Pipe's model has less headway distance when vehicles travel at the speed close to minimum or maximum allowed speed [21]. Leutzbach [22] modifies the Pipe's model by introducing a breaking distance $\frac{v_{m+1}^2}{2\mu \dot{g}}$, and the new expression is shown as:

$$\chi_m = \chi_{m+1} + l_m^{\text{veh}} + \tau v_{m+1} + \frac{v_{m+1}^2}{2\mu \dot{g}} \tag{2.5}$$

where the μ is friction coefficient between vehicle and road surface and $\dot{g}$ stands for gravitational acceleration rate.

One development in the safety-distance model includes a time lag between the change in space headway with the front vehicle and the follower vehicle's reaction [23]. This model has been developed into a hybrid flow model [24] by combining with the LWR model (introduced in Section 2.2.2).

Psycho-physical models

The psycho-physical model is another branch of the car-following models and are also known as the action point model. It is similiar to safety-distance model, but with a more detailed description on drivers' behaviour. In previous mentioned microscopic models, drivers strictly react to the headway change $\chi_m - \chi_{m+1}$ and relative speed change $v_m - v_{m+1}$ which are not the same in real life. A driver will not actively react to the front vehicle when the two vehicles are far apart. If the two vehicles are close to each other, the motion will be small for a driver to respond to changes in relative speed or headway so that the driver may not react as well. The first psycho-physical model is proposed by Wiedemann [25] and is the foundation of the widely used microscopic simulation software VISSIM [26]. In Wiedemann's model, perception thresholds are introduced (see Figure 2.1) to determine whether drivers will obey the car-following rules or not.

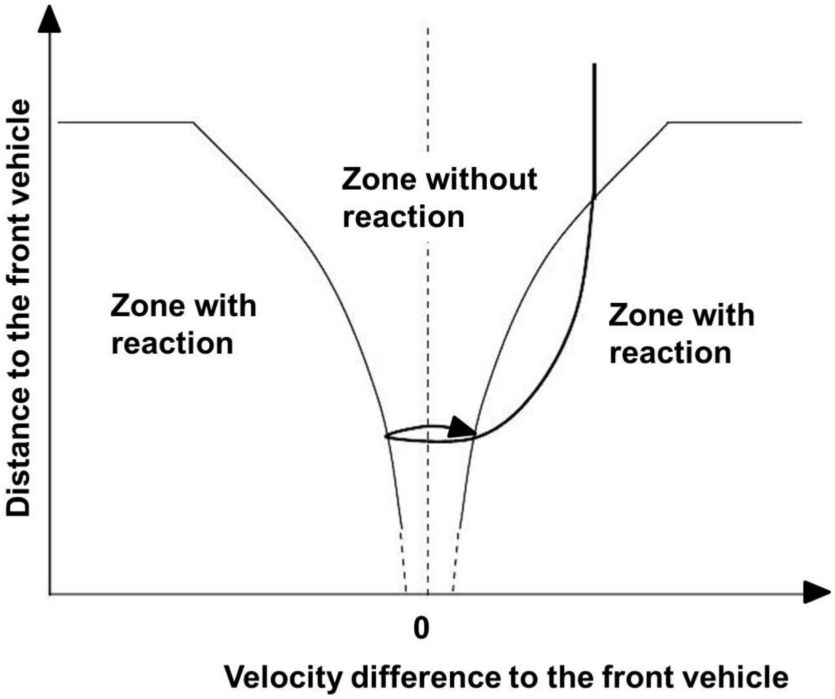
Distance to the front vehicle
Zone without reaction
Zone with reaction
Zone with reaction
0
Velocity difference to the front vehicle

Figure 2.1: An example of perception threshold of the psycho-physical model

(Source: Olstam and Tapani, 2004 [13])

2.2.2 Macroscopic flow models

While the microscopic model is a space-time representation of individual vehicles, the macroscopic traffic flow model represents traffic as a continuous fluid. Before introducing the macroscopic models, a fundamental relation of traffic flow is discussed, which is the foundation of both the macroscopic and microscopic models. In this review of the macroscopic flow models, two types of model are introduced: kinematic wave model and higher-order model. The kinematic wave model is the first macroscopic model, and the higher-order model is the latest branch of the kinematic wave model which considers speed dynamics.

Fundamental relation of traffic flow

The development of the macroscopic model starts from the fundamental relations of traffic flow. Greenshields [27] first studies the fundamental relation of traffic flow and used three quantity terms (the density ρ, flow q and speed υ) to describe the continuous traffic flow. The relationships among the three terms are known as fundamental diagrams (see Figure 2.2 as an example). The density ρ is defined as the number of vehicles at a unit length of a road, the flow q is defined as the number of vehicle passed in a unit of time and the speed υ is the average speed of the traffic. The relation of the three terms can be expressed as:

$$q = \rho \upsilon \tag{2.6}$$

In Figure 2.2, the speed and the density have a linear relationship, and a high-density traffic corresponds to a low moving speed. The relationship between the flow and the density is nonlinear, where a low flow rate corresponds two density status. Before the density reaches a critical value ρ_{crit}, the flow increases with the growth of density. When the density is higher than ρ_{crit}, the growth of density slows down the flow. Consequently, the relationship between the speed and the flow is also nonlinear. The fundamental relationships in Figure 2.2 are not unique, where various shapes of fundamental diagrams are proposed and can be found in [28, 29, 30, 31].

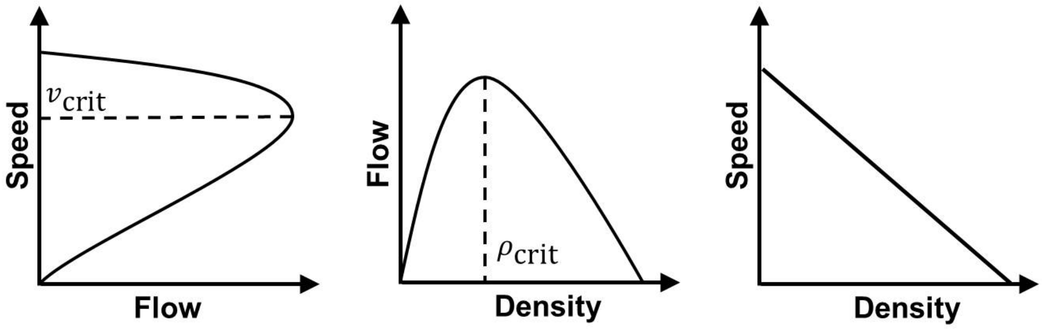

Figure 2.2: Fundamental diagrams

Kinematic wave models

The first macroscopic flow model is proposed by Lighthill, Whitham and Richards [32, 33], which is known as the LWR model or kinematic wave model. The LWR model is a conservation law where no vehicle can be created or removed within a closed road section. Any changes in traffic (Δq and $\Delta \rho$) have to be the same during time interval Δt in the closed road section. The following expression is found for the conservation law:

$$\frac{\Delta \rho}{\Delta t} + \frac{\Delta q}{\Delta \chi} = 0 \tag{2.7}$$

$\Delta \chi$ is the length of the road section. When $\Delta \chi$ and Δt approach to 0, Equation 2.7 converts to the general expression of the LWR model:

$$\frac{\partial \rho}{\partial t} + \frac{\partial q}{\partial \chi} = 0 \tag{2.8}$$

In order to solve the LWR model, several approaches have been proposed such as: Godunov method [34] and Cell Transmission Model (CTM) [31]. The CTM is one of the most popular methods, which dicretise each road into a collection of cells. According to the conservation law (Equation 2.8), the traffic density ρ of each cell i at time t can be expressed as:

$$\rho_c(t+1) = \rho_c(t) + \frac{\Delta t}{l_c^{\text{cell}}} \left[q_{c-1}(t) - q_c(t) \right], \tag{2.9}$$

where $q_c(t)$ is the outflow from cell c. Cell $c-1$ is the upstream cell, where traffic flows from cell $c-1$ into cell c. Δt is one time step and l_c^{cell} is the length of cell c. The step size Δt has to satisfy $\Delta t \leq \min(\frac{l^{\text{cell}}}{\upsilon})$, which means the traffic can not travel more than one cell per time step.

CTM has a piecewise linear relationship with the traffic flow q and density ρ between each pair of successive cells $(c, c+1)$. The maximum flow rate (saturation flow rate) for each cell is Q, and the maximum density (jam density) of each cell is ρ_{jam}. When there is no congestion, traffic moves through cells at a maximum speed (free flow speed). With the piecewise linear relationship, the outflow $q_c(t)$ from cell c to its downstream $c+1$ is determined as:

$$q_c(t) = \min\left\{ \upsilon_c \rho_c(t), Q_c, Q_{c+1}, w_{c+1} \left[\rho_{\text{jam},c+1} - \rho_{c+1}(t) \right] \right\}, \tag{2.10}$$

where w is a shockwave speed which refers to the backward propagation speed of traffic. Equation 2.10 can be considered as an expression of the triangular flow-density relationship. In addition, the effect of traffic signals is formulated as a binary variable at cell c:

$$Q_c(t) = \begin{cases} Q_c, & t \in \mathbb{G} \\ 0, & t \in \mathbb{R} \end{cases} \tag{2.11}$$

$\mathbb{G}$ and $\mathbb{R}$ stand of the green and red phases. The setting of $\mathbb{G}$ and $\mathbb{R}$ use a timing plan derived from the signal control system.

The LWR model is sufficient to describe the basic flow dynamics such as formation and dissipation of traffic congestion. However, due to its simplicity, LWR has several issues such as the limitations in describing vehicle's speed dynamics and formulating the capacity drop phenomenon. The solution to address the dynamics of vehicle's speed is the higher-order model.

Higher-order models

Higher-order models are developed to overcome the limitation of the LWR model in mean speed dynamics. The LWR flow model contains one partial differential equation. Payne [35] proposed a second order flow model which contains the LWR's partial differential equation (conservation of vehicles) Equation 2.8 and another partial differential equation to describe mean speed dynamics. In the Payne's model, the average speed of traffic on a road section is not only affected by the traffic density but also by the neighbour traffic conditions. The expression of mean speed dynamics in Payne's model is as follows:

$$\frac{\partial \upsilon}{\partial t} + \upsilon \frac{\partial \upsilon}{\partial \chi} = \frac{(\upsilon_{\text{equal}}(\rho) - \upsilon)}{c_l} - \frac{c_m^2}{\rho}\frac{\partial \rho}{\partial \chi} \tag{2.12}$$

where $\upsilon_{\text{equal}}(\rho)$ is an equilibrium speed associated with density ρ. c_l and c_m are relaxation constant and anticipation constant respectively. The term $\upsilon \frac{\partial \upsilon}{\partial \chi}$ stands for the convection of traffic. Given a road section where vehicles are travel from its upstream road section, the average speeds of the two sections may not be the same. In this case, the vehicles have to accelerate or decelerate $\frac{\partial v}{\partial x}$ to adapt the traffic speed. In terms of the $\frac{(\upsilon_{\text{equal}}(\rho)-\upsilon)}{c_1}$, this is a relaxation term where the vehicles will try to reach the equilibrium speed υ_{equal} of the road section. The last term $\frac{c_2^2}{\rho}\frac{\partial \rho}{\partial \chi}$ represents drivers' anticipation to their downstream road section. When the density ρ at the downstream road section is higher, the driver will anticipate to slow down.

A METANET [36] is a popular software used Payne's model for motorway modelling. It separates each road into a group of sections, and the length of each road section is l. Both fundamental relation of traffic flow (Equation 2.6) and conservation law (Equation 2.9) are considered. The mean speed dynamics of the METANET's model is as follows:

$$\begin{aligned} \upsilon_c(t+1) =& \upsilon_c(t) + \frac{\Delta t}{\tau}[\upsilon_{\text{equal},c}(\rho_c(t)) - \upsilon_c(t)] - \frac{\Delta t}{l}\upsilon_c(t)[\upsilon_{c-1}(t) - \upsilon_c(t)] \\ & - \frac{c_v \Delta t}{\tau l}\frac{\rho_{c+1}(t) - \rho_c(t)}{\rho_c(t) + c_\kappa} \end{aligned} \tag{2.13}$$

The relaxation term $\frac{\Delta t}{\tau}[\upsilon_{\text{equal},c}(\rho_c(t)) - \upsilon_c(t)]$ describes the behaviour of the drivers.

Drivers will try to achieve the equilibrium speed $\upsilon_{\text{equal},c}(\rho_c(t))$ of the road section. τ is the reaction time for drivers to realise the equilibrium speed of the road section, and when τ value is small the drivers can response quicker. The convection term $\frac{\Delta t}{l}\upsilon_c(t)[\upsilon_{c-1}(t)-\upsilon_c(t)]$ captures the impact of the driver's speed change from the upstream road section $c-1$. The last term $\frac{c_v \Delta t}{\tau l}\frac{\rho_{c+1}(t)-\rho_c(t)}{\rho_c(t)+c_\kappa}$ is the anticipation term to consider drivers' speed change with respect to downstream road density. c_v and c_κ are sensitivity parameters and they allow the model to be more sensitive to medium or high density. The equilibrium mean speed in the relaxation term is derived from:

$$\upsilon_{\text{equal},c}[(\rho_c(t))] = \upsilon_{\text{f},c}\text{exp}(-\frac{1}{c_\alpha}(\frac{\rho_c(t)}{\rho_{\text{crit}}})^{c_\alpha}) \tag{2.14}$$

where $\upsilon_{\text{f},c}$ is the free flow speed of road section c. c_α is a parameter which helps to form a non-linear fundamental relationship between the density and the mean speed.

Apart from the second order model, the higher order model can be further extended to a third order model proposed by Helbing [37]. The third order model introduces speed variance to take the chaotic feature of traffic into account.

2.2.3 Discussion

Section 2.2.1 (Microscopic Flow Models) and Section 2.2.2 (Macroscopic Flow Models) have reviewed the main types of traffic flow models. Three types of microscopic flow models are introduced: stimulus-response model, safe-distance model and psycho-physical model. The microscopic models captures detailed vehicle movements and drivers' behaviour, however, there are many parameters used in the models. Some of the parameters do not have physical meanings and could be difficult to calibrate with traffic flow data (e.g. c_l and c_m of the GHR model). In terms of the macroscopic flow models, the kinematic wave model (LWR model) is developed as a prototype and the high order flow models were purposed for capturing more details traffic dynamics. A high accuracy in the macrscopic flow models is difficult to achieve. This is due to a fact that the drivers' behaviours change over the times [38]. Therefore, choosing a flow model need to consider the model's accuracy and level of description.

This study is going to use both macroscopic and microscopic flow models to avoid the aforementioned issues in model accuracy and parameter calibration. A macroscopic model CTM will be used to derive preliminary results for implementing time-consuming traffic control systems. SUMO is a microscopic simulation platform with a safety-distance mode. It will be used to verify the results from CTM and to perform further experiments with more detailed vehicle movements. A detailed description of the SUMO is in Section 5.2.

2.3 Urban traffic control systems

Urban road traffic control systems are implemented in many cities around the world to manage the traffic efficiently and meet passengers' travel demand. A traffic control system generally uses traffic signals to control traffic flow at intersections and uses historical and real-time measured data to derive signal plans. The conventional system is the fixed-time control system where the signal plans are calculated offline and can not adapt to real-time disruptions in traffic flow. The modern system are traffic-responsive, which could update signal plans according to measure live traffic data on controlled roads.

A traffic signal at an intersection could have red, amber and green lights to give orders to road traffic. Following the order of the signal, traffic can make allowed movements to pass the intersection. The term phase is used to refer to one or multiple traffic movements which receive identical traffic signals at an intersection. Figure 2.3 is an example where 6 different phases are set for the signalised intersection. The term stage is defined as a compatible group of phases where they can process together without having conflict. Figure 2.4 shows how the 6 phases are grouped into 3 stages.

There are three control variables which are generally used for the traffic signal settings: split, offset and cycle time. The duration of a stage is equivalent to the green light given to the traffic movements and known as split. Offset is the time difference between adjacent signals for coordination. The total time required is for a complete

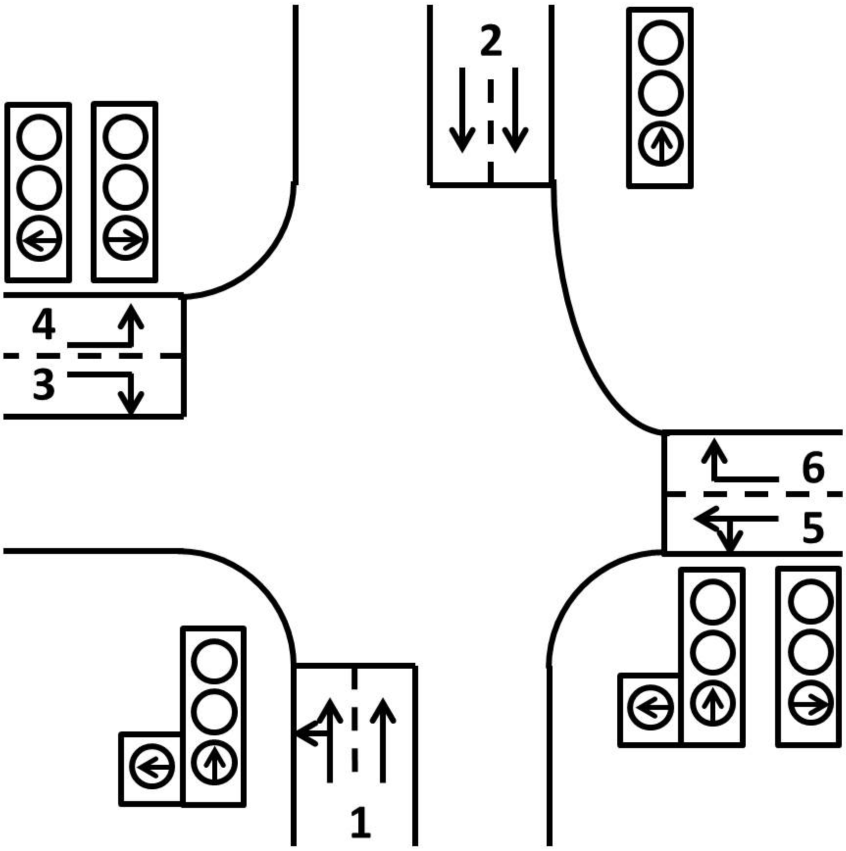

Figure 2.3: Different phases of a signalised intersection

operation of all stages in the cycle time. Figure 2.5 shows the signal settings of two coordinated traffic signals and the split, offset and cycle time settings.

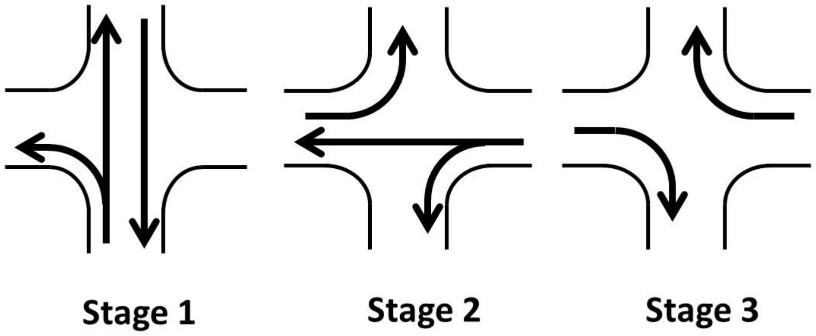

Figure 2.4: Different stages of a signalised intersection

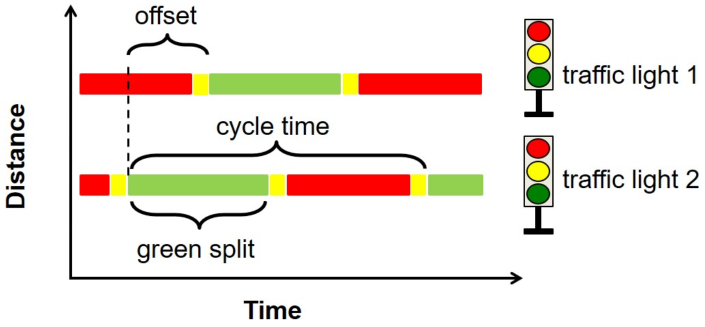

Figure 2.5: An illustration of signal settings

2.3.1 Fixed-time control systems

As the name suggests, the fixed-time control systems are not changing the signal setting rapidly with the measured traffic status, but using predefined settings basing on historical data.

Webster's Method

Webster's method [39] is the foundation of the fixed-time control method which can calculate the cycle time and green split of a signalised intersection. The cycle time C is expressed as:

$$C = \frac{1.5LT + 5}{1 - H} \tag{2.15}$$

where LT is the lost time, and lost time is the time not operating under full efficiency during the change between stages. H is the sum of demand to saturation flow ratio h for each stage θ. Θ is a set of all stages, so it has $\theta \in \Theta$. The expression of H is shown as follows:

$$H = \sum_{\theta \in \Theta}^{K} h_\theta \text{ , and } h_\theta = \max[\frac{q_\theta}{Q_\theta}] \tag{2.16}$$

q stands for demand flow rate and Q is the saturation flow rate. The split for each stage is calculated as:

$$g_\theta = (C - L)\frac{h_\theta}{H} \tag{2.17}$$

The split timing plan calculated balances the demand to saturation ratio for all stages, so that the delay of the traffic through this signalised intersection can be reduced. However, traffic demand in practice will not be constant, and it varies over time. The Webster method is relatively simple and does not consider other important factors such as the coordination with other signals and road blockage.

TRANSYT - Traffic Network Study Tool

A centralised fixed-time system, which has been widely used in practice, is the Traffic Network Study Tool (TRANSYT) [40, 41]. TRANSYT optimises the signal plans for all traffic signals within the controlled area. It can estimate network performance via a platoon dispersion model, and uses a hill climbing search algorithm to look for the signal timing plans that give the best performance. The search algorithm evaluates different split and offset values in order to bring an improvement to the performance. The process of finding the signal plan is similar with other studies on the fixed-timing system [42, 43] and can be summarised as the following optimisation problem:

$$\min_{\mathbf{U}} f(\mathbf{q}, \mathbf{U}) \tag{2.18}$$

where **q** is the traffic flows in the network, and **U** is the signal timing plans which include split, offset, cycle time for each intersection.

Fixed-time systems can achieve coordination in traffic signals and provide reasonable plans for the controlled network. It modifies the plans for busy roads and peak hours of a day. As fixed-time systems relying on historical data, the challenges come from the unpredictable incidents and dynamic travel demands. Incidents like car accident and signal failure can lead to rapid changes in driving routes. Meanwhile, the historical data has to be updated regularly. Bell and Bretherton [44] found the ageing of fixed-time plans causes 3% per year in performance drop. Under the pressure of the above issues, traffic-responsive control systems became more and more popular.

2.3.2 Traffic-responsive control systems

Traffic-responsive control systems process the collect flow data and derive efficient signal plans to the traffic signals in the controlled network. Comparing to the fixed-time control, it can response to traffic fluctuation and adjust plans actively. The traffic-responsive control system generally requires a centralised control for coordination between traffic signals.

SCOOT - Split Cycle Offset Optimisation Technique

SCOOT (Split Cycle Offset Optimisation Technique) is a real-time centraliased control system, and the traffic information are collected from road detectors. SCOOT has three key features: measuring cyclic flow profiles, updating queues continuously for online control and use of incremental optimization for deriving signal plans. Based on the traffic status across an urban network, the system continuously optimises and updates the traffic signal plans to minimise stops and delays of vehicles. Within the network controlled by SCOOT, signal plans for all signal controllers are optimised together by a central computer. Therefore, SCOOT has a centralised control structure. While updating traffic signal plans, SCOOT can have a frequency of 10,000 times per hour for modifying 100 traffic signals within one network [45]. The advantage of using SCOOT is to adapt to the short-term changes of traffic. A previous study showed that additional 12% of the delay can be reduced by SCOOT compared to an up-to-date fixed time system [46].

SCATS - Sydney Coordinated Adaptive Traffic System

SCATS (Sydney Coordinated Adaptive Traffic System) is a centralised hierarchical control system [47, 48], and generally consists of one central management computer, regional computers and local controllers (see Figure 2.6). SCATS is a phase-based control system, and uses cycle time, phase split and offset as control parameters. Regional computers make strategic decisions at the upper control level which is to determine all the control parameters based on its control area's traffic conditions. The local controller makes tactical decisions at the lower control level, and it can terminate the green light earlier or skip the entire phase when the locally measured traffic demand is low. As local controllers control the signal settings, it can not modify the control settings made from a higher control level. For example, when it is necessary need to coordinate traffic signals for a main road, local controllers can not omit the green phase on the main road. This is due to a common cycle time needed for the coordination. The value range of signal timings that a local controller can modify depends on the regional computer.

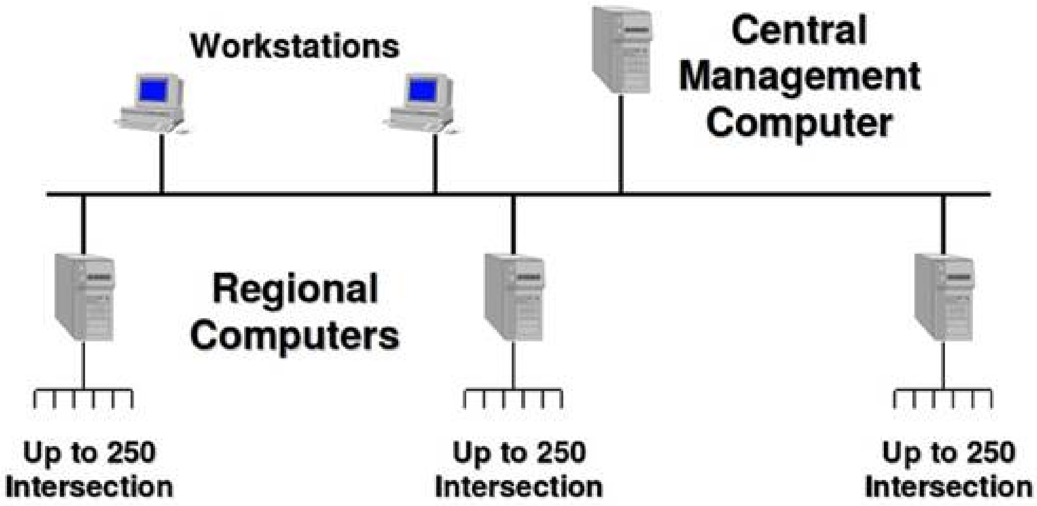

Figure 2.6: Architecture of a SCATS system

(Source: Roads and Maritime Services, 2011 [48])

OPAC - Optimisation Policies for Adaptive Control

OPAC (Optimisation Policies for Adaptive Control) is a real-time adaptive traffic control system, which was developed in the early 1980s [49]. OPAC can support both decentralisation of individual intersection control and the control coordination of intersections within the network. As the control algorithm works independently at each intersection, OPAC can be viewed as a decentralised control system. OPAC uses dynamic programming to compute optimal control plans, and uses maximum and minimum green splits as constraints. Without requiring a fixed cycle time, only spit and offset are used for signals control. The objective of OPAC is to minimise vehicle delays and stops (performance measures) by using both historical data and online data from upstream detectors. OPAC aims to provide up to date signal plans by continuously optimising system performance [50].

Other control systems with centralised structure are RHODES (Real-Time Hierarchical Optimized Distributed Effective System) [51, 52], TUC (Traffic-Responsive Urban Control) [53, 54]. With a decentralised structure, the UTOPIA (Urban Traffic Optimisation by Integrated Automation) [55, 56] system has been implemented in several cities in Europe. Each of its signal controllers is integrated with a industrial computer named SPOT (System for Priority and Optimisation of Traffic). This SPOT unit determines control parameters (cycle time, offset, split) according to the detected local traffic volumes. SPOT units share the signal plans and traffic data with adjacent ones. Public transport forecast, coordination criteria and other control parameters are established by the central computer. Recently, researches have paid great attention to developing the decentralised control systems [57, 6, 58, 9, 59, 11, 60, 10]. Lammer and Helbing [59, 10] introduced a decentralised self-organised control system with a stabilisation mechanism. Max-pressure [6, 8, 61] (also known as BackPressure) is a decentralised control system which operates through the upstream and downstream queuing at each intersections. A leader-follower coordination framework [58] has been proposed to enhance the cooperation between decentralised controllers.

MOVA - Microprocessor Optimised Vehicle Actuation

MOVA (Microprocessor Optimised Vehicle Actuation) [62] is a control system developed by Transport Research Laboratory. Typically, it is used as a standalone intersection controller which adapts to traffic by using loop detectors. At an intersection, MOVA requires two loop detectors (see Figure 2.7) to count vehicle numbers and measure the presence of the coming vehicles. One loop detector is located at around

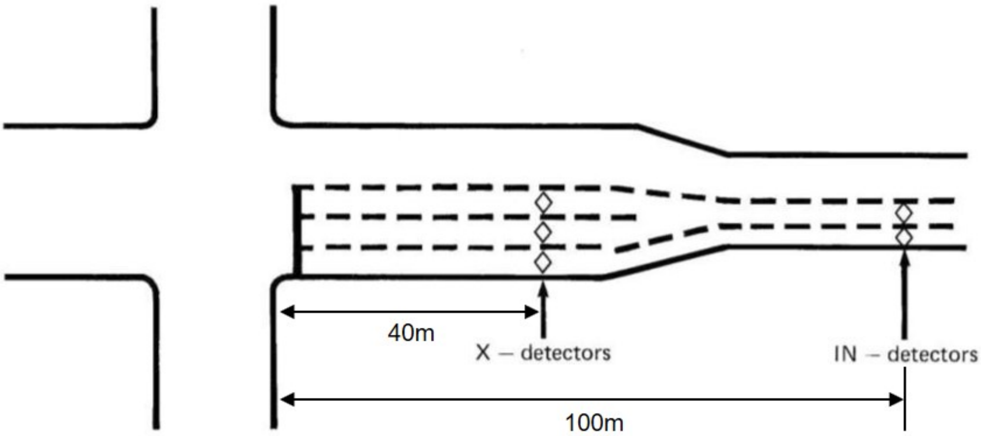

Figure 2.7: Locations of MOVA system's loop detectors

(Source: Crabtree, 2011 [62])

40m from the stopline which is referred to as ‘X-detector’. Another loop detector, known as ‘IN-detector’, is located around 100m from the stopline. MOVA has two operation modes, where it minimises the vehicle delay and stops in the undersaturated condition and maximises the capacity in the oversaturated condition. In the undersaturated condition, the decision on switch to the next stage or extend the current stage is based on whether change can benefit the traffic on reducing delays and stops. In the oversaturated condition, MOVA prioritises the oversaturated road by extending its green light time, consequently, the signal is likely to operate with a longer cycle time.

2.3.3 Discussion

This section has discussed the urban traffic control systems with different control structures. The fixed-time system is first used to operate traffic signals in urban areas. It is an offline control and uses predefined signal plans which rely on historical data. The common challenge of the fixed-time system is to handle unpredictable disruptions and traffic fluctuations on a road network. Traffic-responsive systems are introduced afterwards which is an online real-time control. Traffic-responsive systems differ in control structure and can be classified into centralised and decentralised control systems. Majority of the systems using in cities (e.g. SCOOT and SCATS) have a centralised control structure where the signal plans are derived from a central computer or regional computer and each of them can control more than a hundred traffic signals. In contrast to the centralised control structure, the decentralised systems are operated independently at each intersection. It is not common to see a fully decentralised system operate on a urban network, and the decentralised system may require a certain degree of centralised coordination.

In this study, the centralised and decentralised systems are going to be compared in performance. A fully decentralised system is relatively new in the field and still under development. Chapter 3 analyses the centralised and decentralised control systems which will be used in the experiment, and explains the differences between the two at the operational level. The next section focuses on optimisation technique, which used to derive an optimal signal plan for a centralised traffic signal control system.

2.4 Optimisation methods for signal control

In centralised traffic control systems, optimisation techniques are implemented to derive traffic signal plans with associated traffic demands. There exist many optimisation methods and choosing the right method needs to consider the control problem feature, computational time and any other factors.

2.4.1 Formulation of the traffic signal control problem

In order to search for an optimal signal plan for a traffic signal control problem, it is generally formulated in an optimisation problem format. An optimisation problem consists three components: an objective function, constraints and decision variables. The objective function usually minimises or maximises a system performance measure. The operational objective of a traffic control system is to improve traffic performance on a road network. Various performance measures have been used to evaluate the traffic signal settings of a traffic control system, such as delay and queue length. Delay is the number of vehicle-hour where traffic waited during the red light signal. Queue length is another performance measure where it is the number of vehicles cannot be clear by the end of a green signal. Other performance measures such as phase utilisation and green bandwidth also reflect the performance of signal settings at the signalised intersections. The constraints of an optimisation problem define the range of feasible solutions. The constraints for a signal control problem can be traffic dynamics and traffic signal settings. Traffic dynamics' constraints describe how traffic could propagate in a road network. For example, a road could have a 30 mph speed limit and the capacity of the road could be 230 vehicles per mile. Both of the road properties can be defined in the optimisation problem by constraints. In terms of the traffic signal settings, a signal controller could have a cycle time which equals to 100 seconds. In this case, the traffic signal plan should repeat every 100 seconds. This need to be defined in the optimisation problem by constraints as well. Decision variables form the solution of an optimisation problem. When the optimisation problem minimises the network delay through traffic signal plans, the signal plans are the decision variables. Both of the objective function and constraints are functions of the decision variables.

Delay is one of the most popular performance measure used as the objective function for a traffic signal control problem. It describes the loss of efficiency in the traffic control system under both undersaturated and oversaturated cases. Delay is calculated as the difference between actual vehicle hour travelled (VHT) and vehicle distance travelled (VDT) under free flow speed υ_{f}. The VHT is the number of vehicles on a link i at a time step t:

$$VHT_i(t) = \rho_i(t) l^{\mathrm{link}} \Delta t \tag{2.19}$$

where ρ is the traffic density on the link i, l is the length of the road link and Δt is the interval of a time step. The VDT is the number of vehicle flow through the link i and formulated as:

$$VDT_i(t) = q_i(t) l^{\text{link}} \Delta t \tag{2.20}$$

The expression of the delay on a link i at a time step t is:

$$TND(t) = \sum_{i=1}^{\mathbf{I}} VHT_i(t) - VDT_i(t)/\upsilon_{\text{f}} \tag{2.21}$$

The traffic flow model CTM could be converted into constraints of an optimisation problem. It is a macroscopic flow model and capsules flow dynamics such as formation and dissipation of traffic queues (see Section 2.2.2). CTM splits a road into sections (cells), and the traffic density of a cell c at time step t is defined as follow:

$$\rho_c(t+1) = \rho_c(t) + \frac{\Delta t}{l_c^{\text{cell}}} \left[q_{c-1}(t) - q_c(t) \right] \tag{2.22}$$

where the traffic flow q of cell c at time t is:

$$q_c(t) = \min \left\{ \upsilon_c \rho_c(t), Q_c, Q_{c+1}, w_{c+1} \left[\rho_{\text{jam},c+1} - \rho_{c+1}(t) \right] \right\} \tag{2.23}$$

In order to convert the traffic dynamics of CTM into an optimisation problem, the nonlinear equation 2.23 are modified into four linear inequality constraints [63] [64]:

$$
\begin{aligned}
& q_c(t) \leq \upsilon_c \rho_c(t) \\
& q_c(t) \leq Q_c \\
& q_c(t) \leq Q_{c+1} \\
& q_c(t) \leq w_{c+1} \left[\rho_{\text{jam},c+1} - \rho_{c+1}(t)\right]
\end{aligned}
\tag{2.24}
$$

The traffic signal plans are the decision variables for a traffic signal control problems. When operating traffic signals, time unit usually is second which means all the decision variables are positive integers. In this case, additional integer constraints are added to the traffic signal control problem and it is known as a mixed-integer optimisation problem. In Lo's study [63], the network signal control problem is formulated as a mixed-integer programming model with the traffic flow model CTM (see Section 2.2.2). The traffic signals are simulated by the binary variables at the last cells of incoming links to a signalised intersection. Assuming the traffic signal has two stages, $\theta(t) = 1$ for stage one and $\theta(t) = 0$ for stage two. The maximum flow rate of the last cells of two incoming links c_1 and c_2 at an intersection can be formulated as follows:

$$
\begin{aligned}
Q_{c_1}(t) &= \theta(t) Q_{c_1} \\
Q_{c_2}(t) &= [1 - \theta(t)] Q_{c_2} \\
\theta(t) &\in [0,1]
\end{aligned}
\tag{2.25}
$$

When the stage index $\theta = 1$, the maximum flow rate for stage 2 traffic will be zero and verse vice. Another variable $\imath$ is used to indicate the change of stages [66] and have:

$$\imath(t) = |\theta(t) - \theta(t-1)| \tag{2.26}$$

where the equation is equivalent to inequality equations as follows:

$$\begin{aligned} \theta(t) - \theta(t-1) \leq \imath(t) \leq \theta(t) + \theta(t-1) \\ -\theta(t) + \theta(t-1) \leq \imath(t) \leq 2 - \theta(t) - \theta(t-1) \end{aligned} \tag{2.27}$$

When there is a change of stage at time step t, $\imath(t) = 1$. A signal plan with green split g can be formulated as:

$$g(k) = \sum_{(k-1)C+1}^{kC} \theta(t) \tag{2.28}$$

The green split needs to be in its feasible range, so that it has the constraint:

$$g_{\min} \leq g \leq g_{\max} \tag{2.29}$$

In terms of the offset o, it can started at anytime from the first time step to the last one within a signal cycle. Since the traffic signal is assumed only have two stages, the offset o is always the start time step of stage 1. When $t = o$, it will have $\theta(t) = 1$ and $\imath(t) = 1$. With offset control, there are four cases for a cycle signal plan (see Figure 2.8), the following constraint is held to capture the signal plan with offset control:

$$0 \leq \sum_{(k-1)C+1}^{kC} \imath(t) - 1 \leq 1 \quad \text{where} \quad \imath(t) \in [1,2] \tag{2.30}$$

The final formulation of the traffic signal control problem is:

$$\min \sum_{t=1}^{t=T} \sum_{c \in \mathbf{C}} (\rho_c(t) - q_c(t)/\upsilon_{\mathrm{f}}) l^{\mathrm{cell}} \Delta t$$

subject to

$$\rho_c(t+1) = \rho_c(t) + \frac{\Delta t}{l_c^{\mathrm{cell}}} \left[q_{c-1}(t) - q_c(t) \right]$$

$$Q_{c_{j,1}^{\mathrm{last}}}(t) = \theta_j(t) Q_{c_{j,1}^{\mathrm{last}}}$$

$$Q_{c_{j,2}^{\mathrm{last}}}(t) = [1 - \theta_j(t)] Q_{c_{j,2}^{\mathrm{last}}}$$

$$g_{j,1}(k) = \sum_{(k-1)C+1}^{kC} \theta_j(t)$$

$$q_c(t) \leq \upsilon_c \rho_c(t)$$

$$q_c(t) \leq Q_c$$

$$q_c(t) \leq Q_{c+1}$$

$$q_c(t) \leq w_{c+1} \left[\rho_{\mathrm{jam},c+1} - \rho_{c+1}(t) \right]$$

$$\theta_j(t) - \theta_j(t-1) \leq \iota_j(t) \leq \theta_j(t) + \theta_j(t-1)$$

$$-\theta_j(t) + \theta_j(t-1) \leq \iota_j(t) \leq 2 - \theta_j(t) - \theta_j(t-1)$$

$$g_{\min} \leq g_{j,1} \leq g_{\max}$$

$$0 \leq \sum_{(k-1)C+1}^{kC} \iota_j(t) - 1 \leq 1$$

$$\theta_j(t) \in [0,1]$$

$$\iota_j(t) \in [1,2]$$

Apart from the mixed integer optimisation problem, there are other examples where a traffic signal control problem is formulated in the continuous model instead of a discrete one. TUC system [54] uses a Store-and-Forward model which models the signal controlled traffic as a continuous flow and a time step equals to a signal cycle time. The flow model does simplify the formulation of the signal control problem and avoided the integer constraints. However, it is not an accurate description traffic queues formed by traffic signal [65].

Since the traffic signal control problem is formulated in the optimisation format, the following two sections (Section 2.4.2 and Section 2.4.3) present groups of searching methods which can solve this optimisation problem.

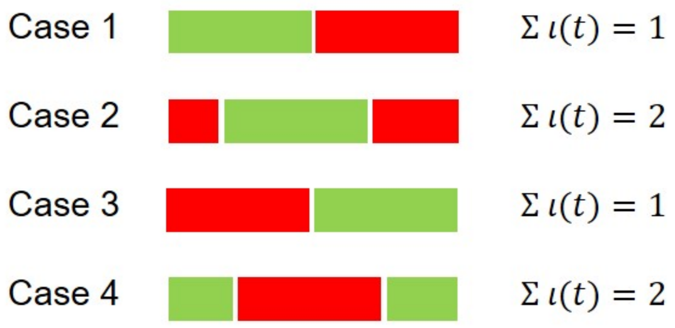

Figure 2.8: Four signal plans with different offset settings

2.4.2 Exact methods

Exact methods are classic optimisation methods where they are guaranteed to find the optimal solutions. The exact methods explore the entire range of the feasible solutions, and this process is also known as Brute Force search or exhaustive search.

Examples of two exact methods are branch and bound and cutting plane method. The branch and bound searches for the global optimal solution of an optimisation problem. It keeps calculating the upper and lower bounds of the optimal solution until the values of the two bounds are close enough. By using the upper and lower bounds, the number of solutions to be examined can be reduced. In term of the cutting plane method, it is designed for integer programming (IP). When the decision variables of an optimisation problem are fully or partially integers, the optimisation is an integer programming problem. The method starts to solve the integer programming problem by treating decision variables as continuous variables. A cut (a constraint) will be generated to separate the non-integer optimal with all feasible integer solutions. This process will repeat until the integer optimal is found.

The advantages of the exact methods come from their simplicity for implementation and its accuracy in solution. However, the simplicity and the accuracy lead the searching process to be time-consuming and resource intensive. An exact method is suitable when the optimisation problem has a smaller number of feasible solutions. It is not popular in real-world problems which are complex and has large dimensions. This is also a reason why it has not been widely implemented for traffic signal operations. Gartner [67] [68] has formulated a traffic signal (offset) control problem in an mixed-integer linear programming model. The objective function is to maximise the bandwidth (green wave) between coordinated traffic signals. Both exact method and heuristic method are used where the heuristic is around 100-300 times faster in running time without significantly compromising the quality of its solution.

2.4.3 Heuristic methods

In contrast with the exact methods, heuristic methods are used to solve a complex problem within a limited time. The heuristic methods do not search for the global optimal but near-optimal solutions. The heuristic methods sacrifice the quality of the solution to save the running time, and they have less restrictions when modelling a optimisation problem. Some examples of the popular heuristic methods used to solve traffic control problems are Genetic Algorithm, Ant Colony Optimisation, Tabu Search and Simulated Annealing.

Genetic Algorithm

Genetic Algorithm (GA) [69] is a heuristic search, which mimics the natural selection process. It uses existing 'good' solutions to regenerate new solutions iteratively until a near optimal solution is achieved. GA is a population-based approach, where a group of solutions are evaluated all together for each time of regeneration. The regeneration process includes: reproduction, crossover and mutation. They ensure the characters of the better solutions can be passed on to the next generation of solutions. The regeneration process will run iteratively until meeting the termination criterion (e.g. maximum number of iterations or only limited improvement can be made in solutions). A flowchart of GA is shown in Figure 2.9. Lo and Chow [70] implemented GA to derive signal timing plans which minimised the total delay of an urban arterial network. BALANCE [71] is an existing traffic control system using GA to optimise signal plans. It operates in Hamburg, Ingolstadt and other cities in Germany.

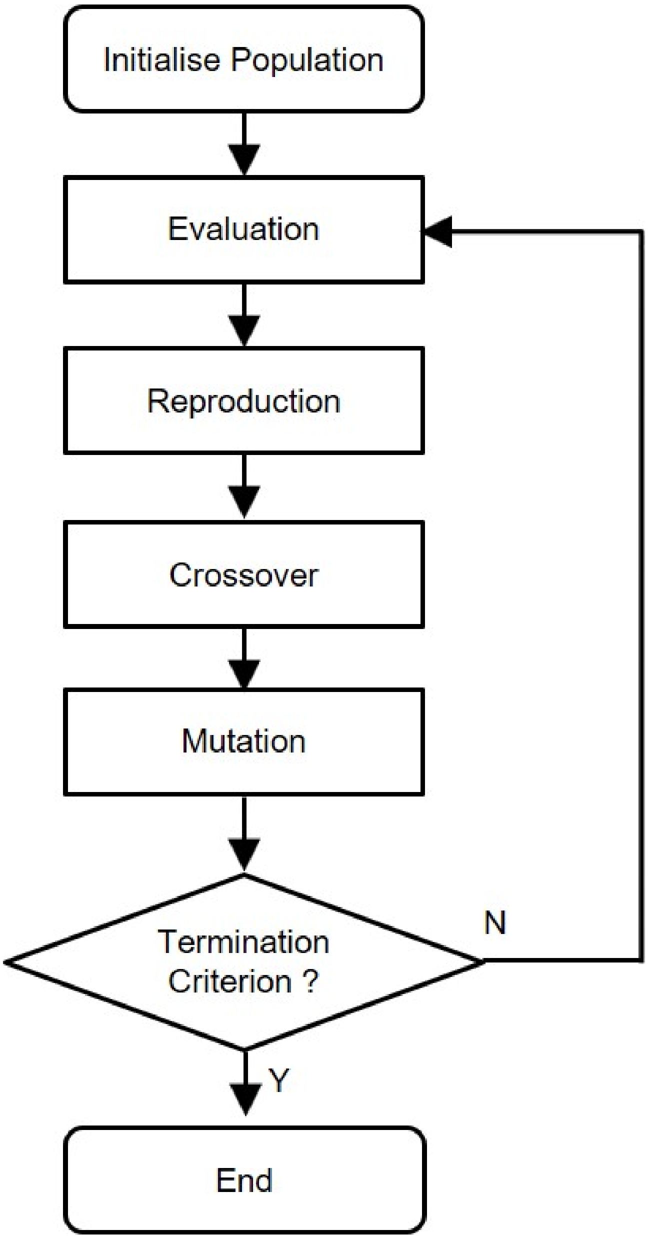

Figure 2.9: A flowchart of Genetic Algorithm

Ant Colony Optimisation

Ant Colony Optimisation (ACO) [72] is basing on the behaviour of ants when they searching for a path between their colony and food. At the beginning of the searching process, ants may tend to randomly choose the paths to search for food. They deposit pheromone on their path to the food, and the path with a higher concentration of pheromone will attract more ants to follow. In this case, a path with shorter distance will have more pheromone since it takes less time to travel. The pheromone will evaporate along the time so that it will help to enforce the path with the shortest distance. ACO is a population-based heuristic search, where each path of an ant is a solution. A flowchart of ACO is shown in Figure 2.10. The ACO has been compared with GA for a traffic signal control problem with oversaturated traffic condition [73]. The results show the ACO could outperform GA when the computational time is sufficient. In other words, GA may be more suitable when the computational time is limited. The ant colony method has also been used to control autonomous intersections in [74] and to solve dynamic traffic routing problem in [75].

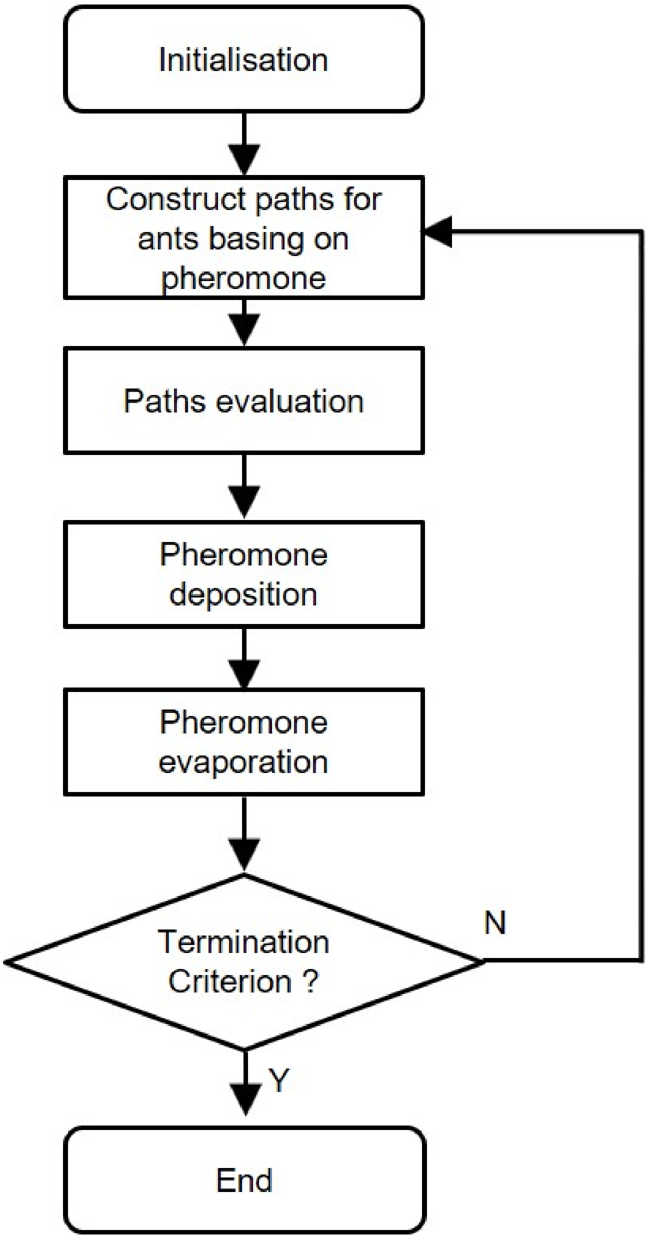

Figure 2.10: A flowchart of Ant Colony Optimisation

Tabu Search

Tabu search [76] [77] is a memory based heuristic search for a single solution. The searching process of Tabu is to explore the neighbour solutions of the existing solution. A Tabu list is a short-term memory, and it saves previously visited solutions. When deciding the next solution to visit, solutions on Tabu list will be avoided. This is forces Tabu explore more feasible spaces and prevents the searching process trapped into a local optimal. The best solution founded by Tabu will be saved as Aspiration criteria. The Aspiration criteria allow Tabu to revisit the same solution, even if it is on the Tabu list. The flowchart of Tabu is showed in Figure 2.11. Tabu search has been used to derive traffic signal plans in [78].

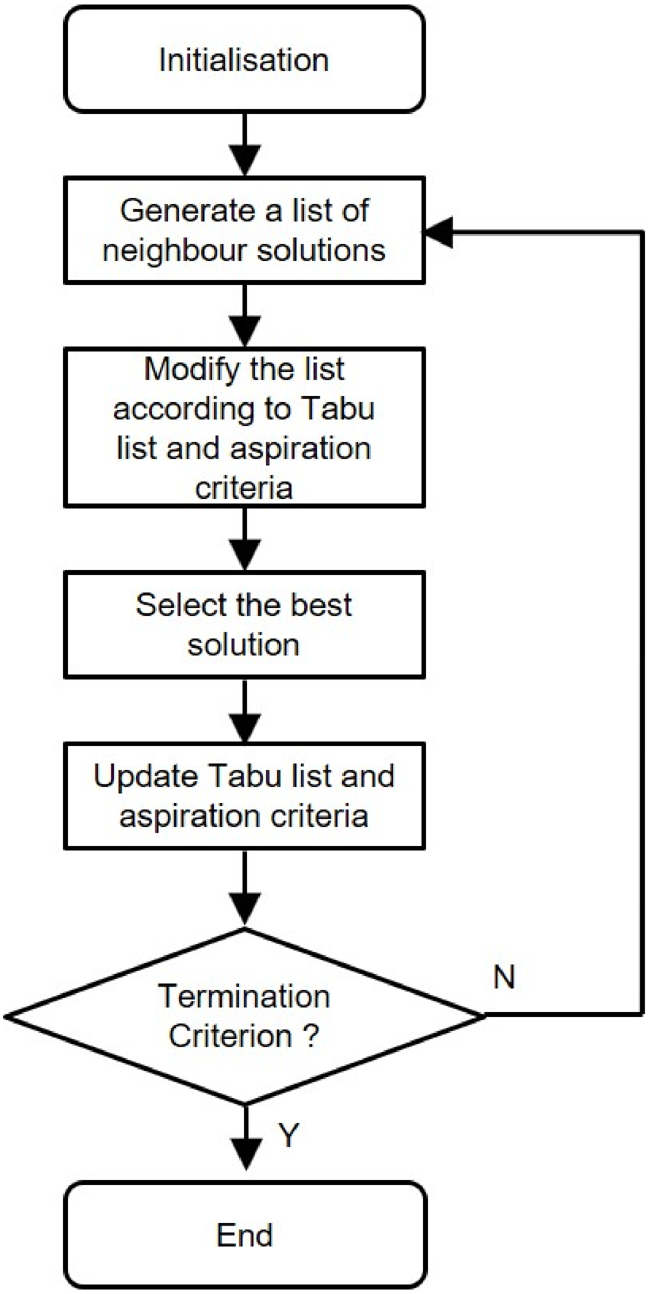
Initialisation
Generate a list of neighbour solutions
Modify the list according to Tabu list and aspiration criteria
Select the best solution
Update Tabu list and aspiration criteria
Termination Criterion ?
N
Y
End

Figure 2.11: A flowchart of Tabu Search

Simulated Annealing

Simulated annealing [79] is a heuristic searching method which inspired by the heating and cooling method to increase a material's crystal size. A higher crystal size corresponds to a lower energy level. The material first heats up to its melting point and the cooling process will start. During the cooling process, a longer cooling time leads to a better result. In terms of an optimisation problem, the various states refer to feasible solutions, the energy level is the cost of a feasible solution. At a temperature, the simulated annealing algorithm explores different states to look for the one with the lowest cost. If the new state has a lower energy level, the new state will be accepted as the current state. If the new state has a higher energy level than the current state, it may be accepted but depends on a probability. The simulated annealing accepts the worse solution which avoids the searching traps at a local optimum. After the minimum global energy is achieved for the current temperature, the temperature will be lowered and the searching process repeats. A flowchart of simulated annealing is in Figure 2.12. The simulated annealing has been used to solve a traffic signal control problem recently [80], which considers the following control parameters: stage sequence, stage duration and offset.

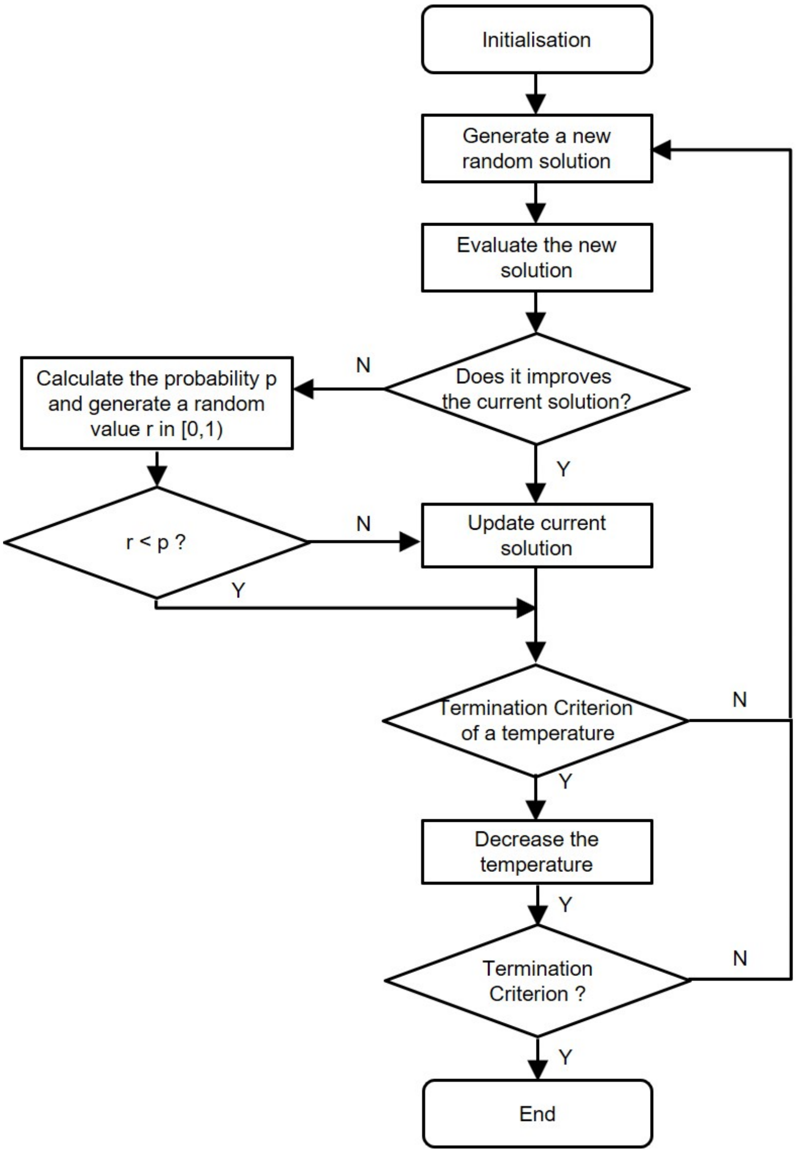
Initialisation
Generate a new random solution
Evaluate the new solution
Does it improves the current solution?
N
Calculate the probability p and generate a random value r in [0,1)
Y
r < p ?
N
Update current solution
Y
Termination Criterion of a temperature
N
Y
Decrease the temperature
Y
Termination Criterion ?
N
Y
End

Figure 2.12: A flowchart of Simulated Annealing

2.4.4 Discussion

The Section 2.4.2 and Section 2.4.3 explain various optimisation algorithms which used in centralised traffic control systems for deriving optimal signal plans. The exact method and heuristic method are two main types of the algorithms. An exact method looks for a global optimal solution and explores all feasible solutions. However, it generally requires long computational time and difficult to implement in real life problems. A heuristic method looks for local optimal solutions. It requires less execution time and can be applied to a wider range of optimisation problems. The heuristic method is more practical to use when the time is limited and global optimal solution is not necessary.

In this study, both of the exact method and heuristic method are going to be used which derive global optimal and local optimal solutions. A brute force approach is a simulation-based exact method. It is easy to implement and guarantees to find the best solution. It is not a practical method but gives a benchmark to compare the centralised control solution with other decentralised ones. In terms of the heuristic method, several modern techniques have been reviewed and all have been used to solve traffic signal control problems (see Section 2.4.3). Table 2.1 summarises the characteristics of all the heuristic method mentioned in the previous section and it is based on the classification in [81]. The first criterion in the table is the use of memory. The memoryless method indicates that the use of memory in heuristic methods do not have an impact on the searching process. Heuristic methods like Tabu search require memory from the computer to record a list of solutions where they have visited. The list will keep growing during the searching process, since the Tabu list tracks the solutions with bad performance or visited solutions. This is also the reason why Tabu search is not considered to use in this study. The next criterion on the table is neighbourhood exploration type. The trajectory method chooses adjacent solutions where the discontinuous method chooses any locations in the feasible range. Comparing to the trajectory method, the discontinuous method involves more randomness and could explore the full range of the feasible solutions faster. Following the neighbourhood exploration, the heuristic methods are different in the types of their solutions. As the name suggests, the population-based solution means a searching method handles a group of solutions at the same time. The single point search visits only one solution each time. The simulated annealing method uses single point search. Due to the size of a traffic signal control problem, simulated annealing may be too slow to explore a large solution space. Therefore, simulated annealing is not in use for this study as well. Modern computers all have multi-core processors which can carry out multiple calculation tasks at the same time. This kind of computation is known as parallel computing. For example, an eight-core computer comparing to a single-core computer, it can reduce the computational time from T to $T/8$ by parallel computing. GA evaluates the performance of all solutions in a population before generating a new population. The evaluation can be performed at the same time by parallel computing, as the solutions are independent of each other. ACO creates paths of ants basing on pheromone level. This process can also use paralleling computing to calculate the paths simultaneously. The last column in the table explains the inspiration of each heuristic method. Comparing GA and ACO, they have similar characters and both could use parallel computing to save running time. GA has been chosen for this study, due to the fact that it has been widely used in traffic signal control problems, and could derive a better solution quicker than ACO in limited time [73].

Heuristic methods	**Use of memory**	**Neighbourhood exploration**	**Solution type**	**Inspiration**
Ant Colony Optimisation	Memoryless method	Discontinues method	Population based	Nature-inspired
Genetic Algorithm	Memoryless method	Discontinues method	Population based	Nature-inspired
Simulated Annealing	Memoryless method	Trajectory method	Single point search	Nature-inspired
Tabu search	Memory usage	Trajectory method	Single point search	Non-nature

Table 2.1: Classification of review heuristic methods

Chapter 3

Analysis of urban traffic control systems

3.1 Introduction

This chapter analyses the urban traffic control systems to be investigated in this study in the following sections. Section 3.2 starts with two distinctive centralised control systems, the brute force approach and the genetic algorithm. Section 3.3 presents two semi-decentralised control systems: Traffic-responsive Urban Control (TUC) system and its variant a Hybrid system. They are classified as semi-decentralised systems, because two of the split and cycle time controls are optimised in a centralised way and the offset control is decentralised. In Section 3.4, max-pressure is introduced as a fully decentralised control system. At the end, Section 3.5 is a summary of the chapter.

3.2 Centralised control

3.2.1 Brute Force Approach

In a centralised system, all traffic information is sent to a central controller or agent that is responsible for deriving and implementing all control actions. To derive an optimal signal plan for such centralised systems, a straightforward way is by a 'brute force' approach (BF) which calculates the performances of all feasible signal plans and picks the signal plan that gives the best performance. Despite its ability to identify the true global optimal solution, this brute force approach could take an enormous computational time and the amount of computation grows exponentially as the network size and number of decision variables increase [82]. The brute force approach therefore is rarely used in general applications. In this study, the Brute force is implemented on Matlab 2013b, and used parallel computing tool 'parfor' to running evaluation of multiple solutions at the same time.

The brute force approach searches for optimal values of a signal plan. A signal plan consists of three control parameters: cycle time, offset and green split. The time step duration Δt of the traffic flow model to be used is 1 second, so that all the control parameters will be integers. The cycle time and offset are bounded by their feasible ranges. There are two stages in one signal cycle, where the green splits for each stage need to satisfy a lower bound and a cycle time constraint:

$$\begin{aligned} g_{\min} &\leq g_1, g_2 \\ g_1 + g_2 &= C - LT \end{aligned} \tag{3.1}$$

where the g_1 and g_2 stand for the green splits of the two stages. The sum of the green splits always equals to the cycle time C (excluding the lost time LT). An illustration of the feasible green splits is shown in Figure 3.1. The feasible green splits are the integers located along the cycle time constraint and bounded by a minimum green split value. Figure 3.2 demonstrates a signal plan used for the brute force approach. A common cycle time C is used for all controllers, and each controller has a green split g and an offset o for every cycle. The $g_{1,1}$ stands for the green split for stage 1, and the corresponding green split for stage 2 can be calculated from $C - LT - g_{1,1}$. It can be seen that the number of possible signal plans increase dramatically with the controlled network size (number of controllers) and controlling period (number of cycles).

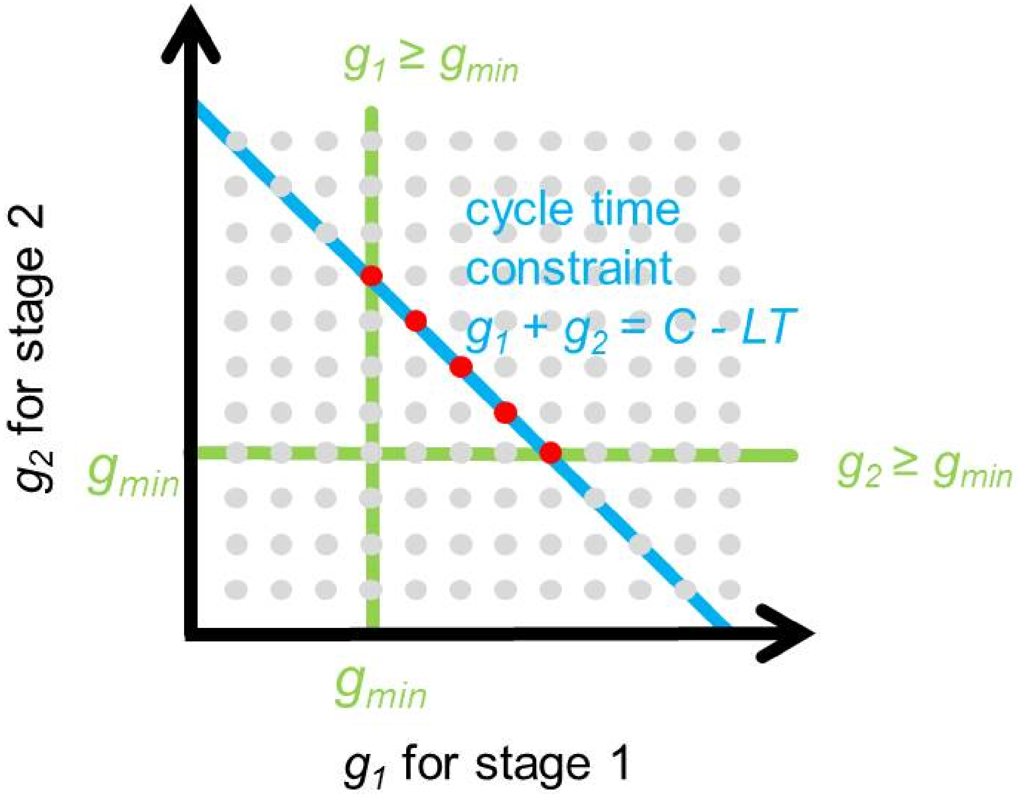

Figure 3.1: An example of feasible values of the green splits

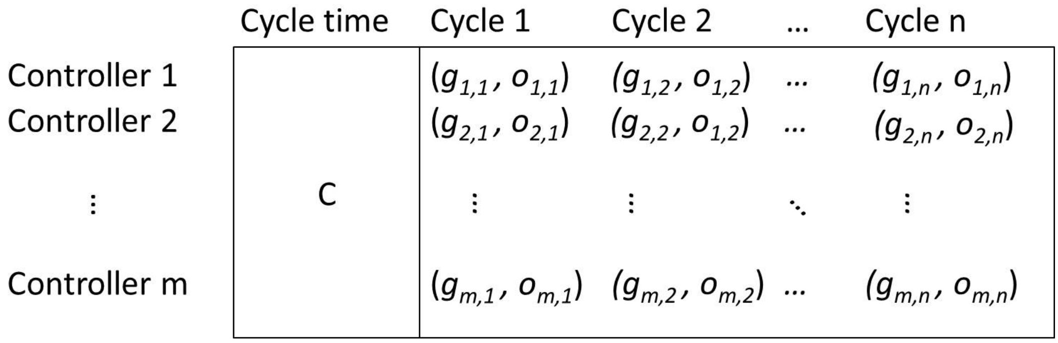

	Cycle time	Cycle 1	Cycle 2	...	Cycle n
Controller 1	C	$(g_{1,1}, o_{1,1})$	$(g_{1,2}, o_{1,2})$	...	$(g_{1,n}, o_{1,n})$
Controller 2		$(g_{2,1}, o_{2,1})$	$(g_{2,2}, o_{1,2})$	...	$(g_{2,n}, o_{2,n})$
⋮		⋮	⋮	⋱	⋮
Controller m		$(g_{m,1}, o_{m,1})$	$(g_{m,2}, o_{m,2})$	...	$(g_{m,n}, o_{m,n})$

Figure 3.2: A set of network signal plans for the brute force approach

3.2.2 Genetic Algorithm

A genetic algorithm (GA) is a heuristic search technique that inspired by natural selection. It provides a solution that can meet practical needs, and requires less computational time compared to an exact searching method. Nevertheless, GA is not designed to find a global optimum, and its result has a certain randomness.

GA initalises the searching process through generating a population (e.g. 500 -1000 chromosomes, 1000 is used for this study) of randomly generated solutions (also called ‘chromosomes’). A solution here is a network signal plan which consists of cycle time, offset and green split. Each component of the signal plan needs to be converted into binary strings (see Figure 3.3, an example of the network signal plan in binary form). It can be seen that the number of feasible signal plans increase exponentially with the number of controllers, the number of control stages and the control period. Similar to the brute force approach, this ‘curse of dimensionality’ [83] is a critical obstacle for applying a centralised system in real-time and in large-scale. In this study, GA is also implemented on Matlab 2013b, and used parallel computing tool ‘parfor’ to evaluate the performance of multiple ‘chromosomes’ simultaneously.

GA has three main operation processes when searching for traffic signal plans: reproduction, crossover and mutation. The reproduction process evaluates the ‘fitness’ of each chromosome i. The ‘fitness’ of a chromosome is the network delay TND in this study and is defined as:

$$FIT_i = \frac{A_i}{\sum A_i} \tag{3.2}$$

$$A_i = \exp[(\frac{TND_{\max} - TND_i}{TND_{\max} - TND_{\min}})c_s] \tag{3.3}$$

where the parameter c_s magnifies the differences between the performances of the chromosomes. $TND_{\max}$ and $TND_{\min}$ are the maximum and minimum total network delays of the current generation of chromosomes. A higher fitness value will be assigned to a chromosome that achieves lower total network delay. The chromosomes are 'reproduced' in proportion to their relative fitness, so that the chromosomes with higher fitness are more likely to be passed onto the other operation processes. Following the reproduction, the crossover process is to 'mate' two chromosomes (regarded as 'parents' chromosomes). Each 'parent' chromosome is separated into two parts, and the second half part swaps with its pair (see Figure 3.4). The newly formed pair of chromosomes are regarded as 'children' chromosomes. This crossover process generates a new set of population with respect to the previous population's characteristics. In terms of the 'mutation' process, it selects some bits in the population randomly with a predefined probability (typically 0.005 - 0.01, and 0.005 is used for this study) and 'mutate' them (i.e. a '0' bit will be changed to '1', and a '1' bit will be changed to '0'). This is to prevent the searching being trapped in a local optimum. After the mutation process, all the new chromosomes will be evaluated for their performance. The three main operation processes will be repeated until reach-

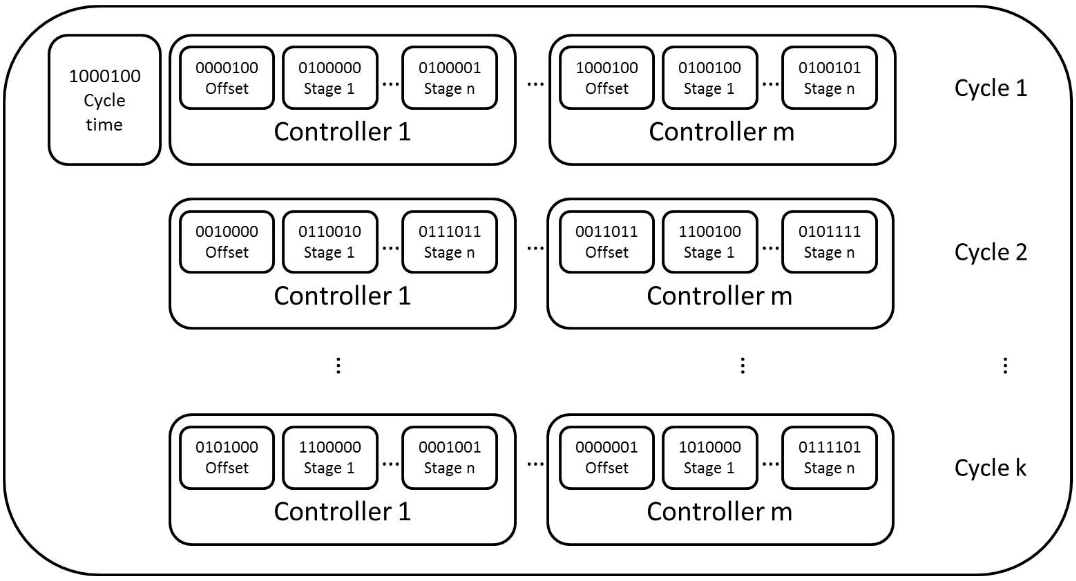

Figure 3.3: A chromosome structure of a network signal plan

ing a predefined maximum iteration (e.g. 20 to 30, 30 is used for this study).

In practice, GA needs to take different kinds of engineering constraints into consideration. Decoding is a process here to convert the GA solutions (chromosomes) into feasible signal plans. For example, when the maximum cycle time C_{max} is set equal to be 120 seconds, the offset can have a range from 0 to 120 seconds. The corresponding binary string needs be sufficient to represent all of the possible values for the feasible cycle time, offset and green split. A binary string with seven bits can create $2^7 = 128$ different integers from 0 to 127 to cover the possible values. A value *CI* from a cycle time binary string can be ‘decoded’ as:

$$C = (\frac{CI}{127})(C_{\max} - C_{\min}) + C_{\min} \tag{3.4}$$

where $C_{\max}$ and $C_{\min}$ are the maximum and minimum values for feasible cycle time.

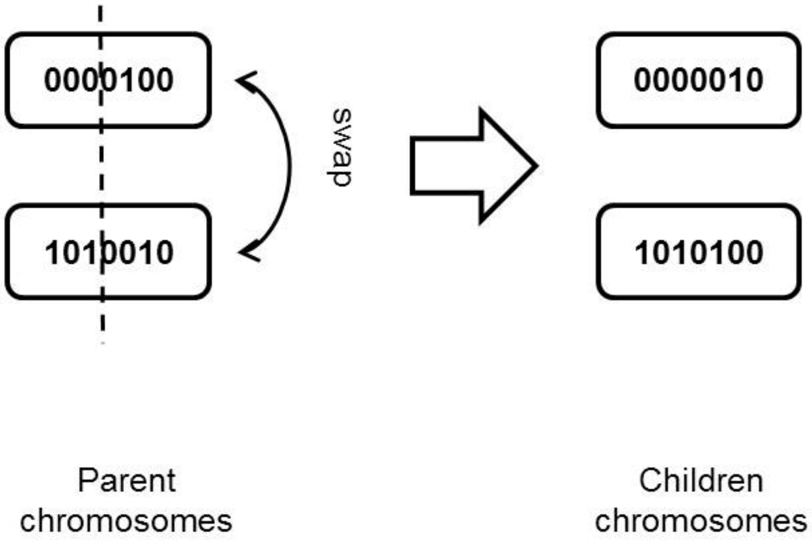

Figure 3.4: GA's crossover process

The green split value GI_θ of stage θ can be 'decoded' as:

$$g_\theta = (\frac{GI_\theta}{\sum GI})(C - LT - \sum g_{\min}) + g_{\min} \tag{3.5}$$

where $g_{\min}$ is the minimum green split of one stage.

3.3 Semi-decentralised control

3.3.1 TUC system

The ‘semi-decentralised’ system is represented by a TUC [54] system and a hybrid system (a variant of the TUC system). TUC system uses three control parameters: green splits, offsets, and cycle time. The TUC is considered as a ‘semi-decentralised’ system in this study, since the cycle time is optimised in a centralised way, while the green splits and offset controllers are decentralised.

Split Control

TUC adjusts green splits to minimise network queues. The green splits $\mathbf{g} = [g_i]$ for each road i is calculated from a centralised linear quadratic regulator (LQR) [54]. The LQR uses a store-and-forward model with a time interval Δt set to be the cycle time C. The LQR optimal control problem is formulated as:

$$\begin{aligned} &\min_{\Delta\mathbf{g}(k)} Z_n = \frac{1}{2}\sum_{k=0}^{\infty}(\mathbf{x}(k)^T\mathbf{S}\mathbf{x}(k) + \Delta\mathbf{g}(k)^T\mathbf{R}\Delta\mathbf{g}(k)) \\ &\text{subject to} \quad \mathbf{x}(k+1) = \mathbf{x}(k) + \mathbf{B}\Delta\mathbf{g}(k) \end{aligned} \tag{3.6}$$

where $\mathbf{x}(k)$ is a vector of residual queue lengths $\mathbf{x}(k) = [x_i(k)]$ for each road i by the end of green light of cycle k. $\Delta\mathbf{g}(k)$ is a vector of change in green splits. Regulating the $\Delta\mathbf{g}(k)$ instead of $\mathbf{g}(k)$ in Equation 3.6 can avoid over fluctuation in the green splits. $\Delta g_i(k) = g_i(k) - g_i^N$ where g_i^N is the associated nominal green split.

The **S** and **R** are both diagonal weighting matrices and they determine the trade-off between minimising queues and adjusting the signal plan[54]. The diagonal elements of $S(y,z)(y=z=i)$ are the reciprocals of road capacity $\frac{1}{x_{i,\max}}$ for road i, and $S(y,z)=0$ otherwise. $\mathbf{R}=r\mathbf{I}$ where I is a identity matrix. The choice of r in **R** nevertheless will be a trial-and-error process so as to achieve the most satisfactory control performance. It is noted that the original green split regulator is a centralised optimisation model as it considers all roads i in (3.6) while recently there have been studies (e.g. [11]) aiming to decompose (3.6) and hence operate it in a decentralised manner.

The optimality condition of (3.6) can be derived in the form of the following feedback control law [53] on green split $\mathbf{g}(k)$ allocated to each road i over each cycle k as:

$$\mathbf{g}(k)=\mathbf{g}^N-\mathbf{L}\mathbf{x}(k) \tag{3.7}$$

where **L** is the corresponding control gain associated with each road i. The control gain **L**, which will be dependent on **S**, **R**, and **B** where **B** is a diagonal matrix of 'minus' saturation flows in which $B(y,z)=-Q_i$ if $y=z=i$, and $B(y,z)=0$ otherwise. To determine **L**, the matrix can be derived from the Hamilton-Jacobi-Bellman (HJB) equation. Suppose that $Z^*(\mathbf{x}_k)$ is the optimal 'cost-to-go' function at cycle k with state $\mathbf{x}_k$, the HJB equation can be written as:

$$\begin{aligned} Z^*(\mathbf{x}_k) &= \min_{\Delta\mathbf{g}(k)}[(\mathbf{x}_k^T\mathbf{S}\mathbf{x}_k+\Delta\mathbf{g}_k^T\mathbf{R}\Delta\mathbf{g}_k)+Z^*(\mathbf{x}_{k+1})] \\ &= \min_{\Delta\mathbf{g}(k)}[(\mathbf{x}_k^T\mathbf{S}\mathbf{x}_k+\Delta\mathbf{g}_k^T\mathbf{R}\Delta\mathbf{g}_k)+Z^*(\mathbf{x}_k+\mathbf{B}\Delta\mathbf{g}_k)] \end{aligned} \tag{3.8}$$

It is known that the optimal cost-to-go function Z^* is quadratic in $\mathbf{x}$, i.e. $Z^*(\mathbf{x}_k) = \mathbf{x}_k^T\mathbf{P}\mathbf{x}_k$, for some matrix $\mathbf{P} = \mathbf{P}^T \geq 0$ and all k. Hence, the HJB equation can be rewritten as:

$$\mathbf{x}_k^T\mathbf{P}\mathbf{x}_k = \min_{\Delta\mathbf{g}(k)}[(\mathbf{x}_k^T\mathbf{S}\mathbf{x}_k + \Delta\mathbf{g}_k^T\mathbf{R}\Delta\mathbf{g}_k) + (\mathbf{x}_k + \mathbf{S}\Delta\mathbf{g}_k)^T\mathbf{P}(\mathbf{x}_k + \mathbf{S}\Delta\mathbf{g}_k)] \tag{3.9}$$

Differentiating the right-hand side with respect to $\Delta\mathbf{g}_k$ gives the corresponding derivative: $2\mathbf{R}\Delta\mathbf{g}_k + 2\mathbf{B}\mathbf{P}(\mathbf{x}_k + \mathbf{B}\Delta\mathbf{g}_k)$. Setting this derivative to zero, the optimal $\Delta\mathbf{g}_k$ can be obtained as:

$$\begin{aligned}
&2\mathbf{R}\Delta\mathbf{g}_k + 2\mathbf{B}^T\mathbf{P}(\mathbf{x}_k + \mathbf{B}\Delta\mathbf{g}_k) = \mathbf{0}\\
&\Rightarrow \Delta\mathbf{g}_k = -(\mathbf{R} + \mathbf{B}^T\mathbf{P}\mathbf{B})^{-1}\mathbf{B}^T\mathbf{P}\mathbf{x}_k\\
&\Rightarrow \Delta\mathbf{g}_k = \mathbf{L}\mathbf{x}_k
\end{aligned} \tag{3.10}$$

The matrix $\mathbf{L}$ expressed as:

$$\mathbf{L} = -(\mathbf{R} + \mathbf{B}^T\mathbf{P}\mathbf{B})^{-1}\mathbf{B}^T\mathbf{P} \tag{3.11}$$

By substitute $\Delta\mathbf{g}_k$, $\Delta\mathbf{g}_k = \mathbf{g}_k - \mathbf{g}^N$, into the (3.9), it gives:

$$\begin{aligned}
\mathbf{x}_k^T\mathbf{P}\mathbf{x}_k &= (\mathbf{x}_k^T\mathbf{S}\mathbf{x}_k + \Delta\mathbf{g}_k^T\mathbf{R}\Delta\mathbf{g}_k) + (\mathbf{x}_k + \mathbf{B}\Delta\mathbf{g}_k)^T\mathbf{P}(\mathbf{x}_k + \mathbf{B}\Delta\mathbf{g}_k)\\
&= \mathbf{x}_k^T(\mathbf{S} + \mathbf{P} - \mathbf{P}\mathbf{B}(\mathbf{R} + \mathbf{B}^T\mathbf{P}\mathbf{B})^{-1}\mathbf{B}^T\mathbf{P})\mathbf{x}_k
\end{aligned} \tag{3.12}$$

According to (3.12), the matrix **P** in (3.11) can be determined by solving the following Riccati equation:

$$\mathbf{P} = \mathbf{S} + \mathbf{P} - \mathbf{P}\mathbf{B}(\mathbf{R} + \mathbf{B}^T\mathbf{P}\mathbf{B})^{-1}\mathbf{B}^T\mathbf{P} \tag{3.13}$$

Equation 3.13 can be solved readily by various numerical solution packages , such as the ‘dlqr’ package in MATLAB. An example of how to derive the control gain **L** matrix is in Appendix B. By considering an infinite horizon in time k in (3.6), the control gain **L** can be calculated offline as the steady-state solution to (3.11). Consequently, the control law (3.7) can be operated readily with feeding information of queue lengths **x** in real-time without solving any optimisation problem. This makes TUC a more computationally effective system than other centralised algorithms such as GA for real-time operations. Previous studies show that the setting of nominal green $\mathbf{g}^N$ would play an important role in defining the performance of the TUC. To address this, [54] presents a revised TUC control rule:

$$\mathbf{g}(k) = \mathbf{g}(k-1) - \mathbf{L}[\mathbf{x}(k) - \mathbf{x}(k-1)] \tag{3.14}$$

by subtracting (3.7) for cycle $(k-1)$ from (3.7) for cycle k. The advantage of using (3.14) over (3.7) is that it does not require predefining the nominal green $\mathbf{g}^N$. As shown, the crucial information for operating TUC is the observation of queue lengths **x**. In the CTM, this can be estimated by determining the number of cells (or length of road section) that contain traffic in jam density [84]. In reality, however, these queue lengths could be difficult to observe directly as it requires spatial surveillance, say through overground cameras with appropriate image processing techniques [85]. Nevertheless, there have also been effective algorithms (see e.g. [86]) developed in the literature that can estimate queue lengths from local occupancy or speed measured by standard fixed loop detectors.

In addtion, the green splits **g** obtained here will not satisfy the engineering constraints such as consistency between cycle time and green splits and minimum (maximum) bounds on the control variables. Diakaki [53] proposes the following method to determine 'scaled' green splits $\mathbf{g}^*{}_k$ from $\mathbf{g}_k$ over each cycle k that would satisfy all required engineering constraints:

$$\min_{\mathbf{g}^*} \sum_{i \in \mathbf{I}_n^{\text{in}}} [g_i^*(k) - g_i(k)]^2, \tag{3.15}$$

Minimising (3.15) is subject to:

$$\sum_{i \in \mathbf{I}_n^{\text{in}}} g_i^*(k) + LT = C, \tag{3.16}$$

$$g_{\min} \leq g_i^*(k) \leq g_{\max}. \tag{3.17}$$

where LT is the lost time (i.e. all-red period) within cycle C, $g_{\min}$ and $g_{\max}$ are respectively the predefined lower and upper bounds on the green splits. A solution has also been provided for the above optimisation problem in [53] and implemented in this study (see Appendix B).

Offset control

Following the green split control, the TUC adopts a decentralised approach (known as Gazis offset control) for adjusting the network offsets based upon the concept presented in [87]. Following [87] and [88], the offset o_n between two adjacent intersections $(n, n+1)$ (where traffic is flowing from n to $n+1$) is determined as follows (see Figure 3.5, where the intersections are represented by nodes and the roads are represented by links). If no queue exists between the two nodes, the offset between the two nodes will be taken as the nominal free flow travel time:

$$o_n = \frac{l_i^{\text{link}}}{\upsilon_{f,i}}, \tag{3.18}$$

where l_i^{link} is the length of the link i connecting the two nodes, and $\upsilon_{f,i}$ is the associated link free flow speed. If there is no queue, the offset in (3.18) will be the most efficient setting of offset for discharging traffic with the assumption that all vehicles proceed with the same speed υ_i [87] (see the case 2 in Figure 3.5).

When the queue builds up between the nodes, the offset o_n will need to be adjusted according traffic conditions [87]. Suppose the queue length on link i at this cycle k is $x_i(k)$, and a vehicle released from node n proceeds towards $n+1$ through the link

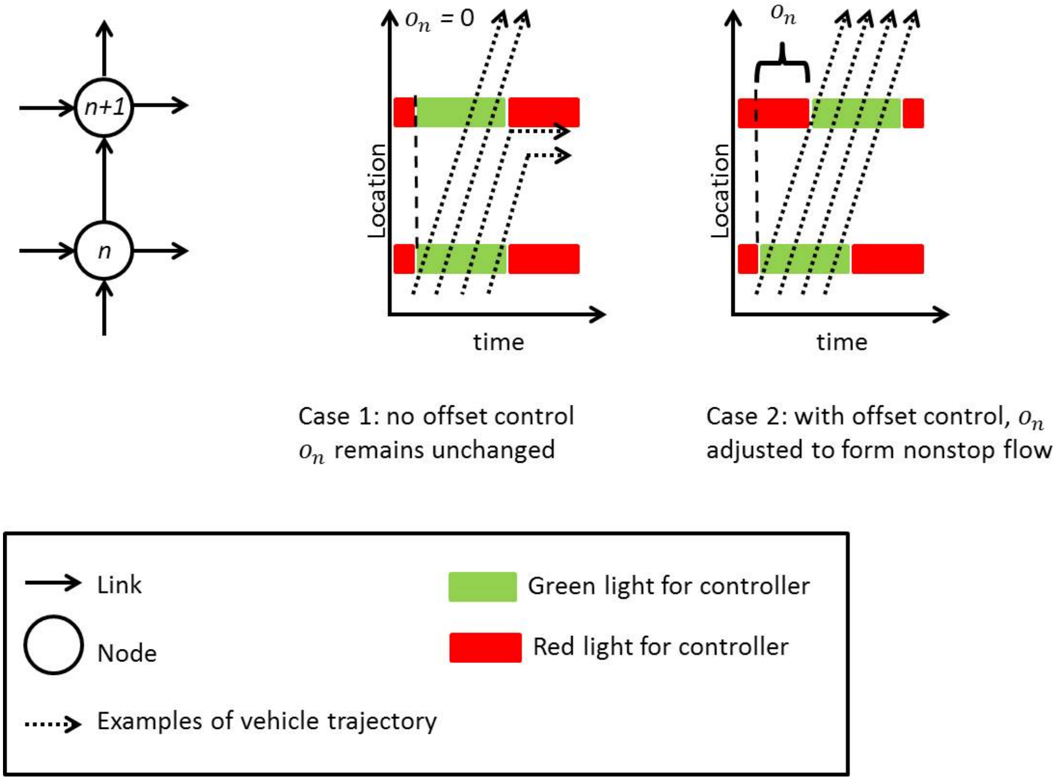

Case 1: no offset control o_n remains unchanged

Case 2: with offset control, o_n adjusted to form nonstop flow

Figure 3.5: An illustration of offset control

i. The time needed for this vehicle to reach the tail of the queue after its release will be $\frac{l_i^{\text{link}}-x_i(k)}{\upsilon_i}$. In terms of the residual queue $x_i(t)$, it also needs an amount of time to discharge. When the flow-density relationship on each link i is characterised by a bi-linear fundamental diagram, it has a constant free flow speed $\upsilon_{f,i}$ for all traffic density less than the critical density value, and a constant shockwave speed w_i for all density higher than the critical density value. A queue dissipating wave will be generated when the traffic signal at node $(n+1)$ turns into green. It propagates toward the upstream (node n) with a speed w_i, so that the time to discharge the queue can be derived as $\frac{x_i(k)}{w_i}$. If $o_n^*(k)$ is an optimal offset for cycle k, then the first vehicle discharged from upstream should reach the end of queue $x_i(k)$ at a time when the queue is just being dissipated. This situation is shown in Figure 3.6 (the intersections are

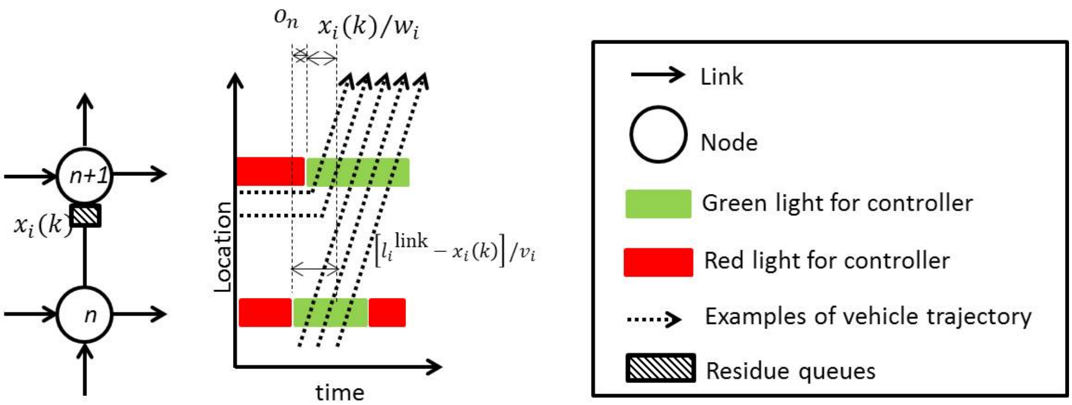
o_n
$x_i(k)/w_i$
n+1
$x_i(k)$
n
Location
time
$[l_i^{\text{link}} - x_i(k)]/v_i$
Link
Node
Green light for controller
Red light for controller
Examples of vehicle trajectory
Residue queues

Figure 3.6: Offset control with residue queues

represented by nodes and the roads are represented by links) and can be written as:

$$\frac{l_i^{\text{link}} - x_i(k)}{\upsilon_i} = o_n^*(k) + \frac{x_i(k)}{w_i}, \tag{3.19}$$

and hence

$$o_n^*(k) = \frac{l_i^{\text{link}} - x_i(k)}{\upsilon_i} - \frac{x_i(k)}{w_i}, \tag{3.20}$$

Equation 3.20 will be reduced to equation 3.18 if the queue length by time k is zero. The extra terms associated with $x_i(k)$ in (3.20) compared with (3.18) can be regarded as adjustments that are there to increase the offset to account for the extra time needed to clear the queue for traffic progression.

According to (3.20), the offset at an intersection will be reduced if there is a queue at that intersection. The rationale for this is to start the green for discharging the local queue at that intersection earlier to create space for the incoming traffic to proceed without hindrance by the present queue and hence pass through the intersection without being held by the local queue or red.

Cycle time control

It is known that the capacity of a signal-controlled network depends on its cycle time. TUC adjusts the cycle times according to the prevailing traffic volume. For example, one may need to increase cycle times for creating extra operational capacity to cope with oversaturated traffic. A P-regulator is proposed in [89] for adjusting network-wide cycle time $C(k)$ over cycle k according to the prevailing traffic:

$$C(k) = C^N + K_c[\xi(k) - \xi^N] \tag{3.21}$$

where C^N is a predefined nominal cycle time, $\xi(k) = \frac{x_i(k)}{x_{i,\max}}$ is the current ratio of queue length at time k to the link queue capacity, ξ^N is a predefined nominal value for $\xi(k)$. The parameter K_c determines the intensity of the cycle time control. The control rule (3.21) is also subject to the maximum and minimum bounds on the cycle times.

3.3.2 Hybrid system

The hybrid system is a variant of the TUC system. As can be seen from (3.7), the TUC system operates based upon the residual queue measured at the end of each signal cycle. When a network is oversaturated, TUC works effectively on balancing and dissipating residual queues, as verified by a number of simulation and field tests (see e.g. [89]). Nevertheless, when the degree of saturation is low, TUC would simply operate close to the nominal plans $\mathbf{g}^N$ as the residual queues $\mathbf{x}$ are close to zero. To remedy this, Kouvelas, *et al.* [90] proposed a hybrid system that runs the TUC under oversaturated conditions; it switches to a demand-based control mode when the demands are low. The demand-based control strategy essentially allocates green splits to the inflow links i according to the corresponding 'demand-saturation flow' ratios. This control strategy can be stated as:

$$g_i(k) = \frac{h_i}{\sum_{i \in \mathbf{I}^{\text{in}}} h_i}(C - LT) \tag{3.22}$$

where $h_i(k) = \frac{q_i(k)}{Q_i}$ is the demand-saturation ratio on link i in cycle k. The objective here is to balance the degree of saturation which is shown to be an effective way of operating an intersection [91]. With the demand-based control rule, the hybrid system operates based upon the measured queue lengths in the following way [90]:

1. if the hybrid controller is in demand-based control mode in cycle $k-1$, it will be switched to the TUC control mode in the next cycle k if the queue length on any one of the inflow links i exceeds a predefined threshold. Otherwise, the hybrid controller will stay in demand-based mode;

2. if the hybrid controller is in the TUC control mode in cycle $k-1$, it will be switched to demand-based mode in the next cycle k if queue lengths on all inflow links return below the predefined threshold. Otherwise, the hybrid controller will stay in the TUC mode.

3.4 Decentralised control

3.4.1 Max-pressure controller

Max-pressure controller (MP) is a purely decentralised method to control traffic signals [8] [92]. It was first used for packets transmission in a wireless network [93]. Different from the TUC, it does not require knowledge of network traffic flow and it operates traffic controllers separately at each intersection. As discussed in [65], [94], a weakness of the TUC system is that it does not consider explicitly the downstream queue constraint and spillover phenomena. The MP controller adjusts local green splits based on the differences between upstream and downstream local queue length of each intersection. Given the traffic flowing from an inflow link i to a set of outflow links $\mathbf{I}_n^{\text{out}}$, where $j \in \mathbf{I}_n^{\text{out}}$, through an intersection n, the 'pressure' $\psi_i(k)$ for this movement over a time period T can be defined as:

$$\psi_i = \sum_{t=1}^{T} Q_i \left[x_i(t) - \sum_{j \in \mathbf{I}_n^{\text{out}}} \zeta_{ij} x_j(t) \right], \tag{3.23}$$

where x_i is the queue length of the link, Q_i is the maximum flow rate of the link. ζ_{ij} is the associated turning ratios for each pair of (i, j). At each signal stage, the inflow link i which has right of way will be associated with their pressure ψ_i. The MP controller assigns green light time to the signal stage with the maximum pressure. The MP is not a cyclic control, so that the controller can allocates more green split to the links with higher pressure in any sequences. The pseudo code of the non-cyclic

Max-pressure controller shows as follows:

Algorithm 1 Max-pressure non-cyclic control

```
for all signal controllers do
    for each stage $iStg$ do
        for each incoming link $i$ with right a way at $iStg$ do
            $\psi_i(t) = Q_i \left[ x_i(t) - \sum_{j \in \mathbf{I}_n^{\text{out}}} \zeta_{ij} x_j(t) \right]$
        end for
        $\psi_{iStg}(t) = \max\{\psi_i(t)\}$
    end for
    if there exist $\psi_{iStg} > \psi_{currentStage}$ then
        if $t - t_{\text{begin of Current Stage}} >= g_{\min}$ then
            green light switch to $iStg$
        end if
    else if $t - t_{\text{begin of Current Stage}} >= g_{\max}$ then
        green light switch to next Stage
    end if
end for
```

Following [8], Le et al[95] presented a cycle-based green allocation rule using a logit function based on the pressure function in Equation 3.23 as:

$$g_i(k) = \frac{\exp\{\eta \psi_i(k)\}}{\sum_{i \in \mathbf{I}_n^{\text{in}}} \exp\{\eta \psi_i(k)\}} (C - LT), \tag{3.24}$$

where $g_i(k)$ is the proportion of cycle time allocated to link i among all inflow links in $\mathbf{I}_n^{\text{in}}$ during cycle k, $\eta \geq 0$ is a model parameter tuning the sensitivity of green proportion with respect to the pressure. As η tends to zero, the green allocation tends to uniform. As η tends to ∞, all green will simply be allocated to the link or traffic movement i with the highest pressure during cycle k [95].

For an intersection that is isolated from any other bottleneck and hence is not subject to any downstream congestion constraint, the downstream queue term '$\sum_{j \in \mathbf{I}_n^{\text{out}}} \zeta_{ij} x_j(t)$' in Equation 3.23 will indeed be zero and hence the MP controller will be reduced to a TUC-like control that operates only based upon local queue and saturation flow measurements. The major difference between MP and TUC rules is that TUC would allocate the green according to the predefined nominal green split $\mathbf{g}^N$ if there is low or even zero queue detected, while the MP controller will simply allocate the green uniformly in the low (or zero) queue circumstance. Moreover, different from the TUC controller, the derivation of the MP control rule does not require any underlying traffic model and hence the frequency of updating the control policy can theoretically be flexible, say can range from once a cycle down to every second. It should be noted that the operation of the MP control does not require any information of network configuration and traffic inflow, and it only requires on-site estimation of queue lengths which can now be available through various technologies (see e.g. [96]). Regarding the frequency of updating the control policy, it may be desirable to only update the MP control once a cycle from a practical perspective. Nevertheless, as [8] points out, updating the control policy only once a cycle may have undesirable outcomes, say uneven distribution of queues in favour of links with significantly higher demand [8]. Finally, [8] proves that the MP controller is stabilising (i.e. all queue lengths are bounded over time) as long as the traffic inflow to each intersection is within the oversaturation capacity.

The control law (Equation 3.24) determines the green splits at each junction over cycles. Given the green splits, the MP controller can further regulates the offsets and network cycle time using the methods described in Sections 3.3.1.

3.5 Summary

This chapter analysed a set of different urban traffic systems, starting from centralised, semi-decentralised, to decentralised. To evaluate their performances, the systems will be implemented and tested over different network settings in the next chapter.

One of the chosen centralised control systems is the brute force approach, which guarantees to find the best solution for the traffic control problem. The optimal solution is an important benchmark, especially for comparing with solutions of the other systems in this study. However, the brute force approach is not commonly used in practice, since the computational time increases exponentially in respect to the dimensions of the problem and finding the optimal solution can be difficult or not applicable at all. The other centralised system is the GA, which is a heuristic search algorithm. Generally, the solution provided by the heuristic algorithm can meet the practical needs and the algorithm requires less computational time. Nevertheless, the solution obtained from GA is not a global optimum, and the search in feasible solutions is randomised.

In terms of the semi-decentralised systems, the TUC system and its modified version the Hybrid system are presented. TUC is an existing system implemented in real life, and it is selected in this study to represent a modern urban control system. The TUC system optimises the green splits and cycle time in a centralised way, while offset control is decentralised. The Hybrid system operates in TUC mode when network is oversaturated, and switches to a demand-based mode when undersaturated.

Finally, the max-pressure is a decentralised control system proposed in recent years. It regulates the local green splits according to the local queue lengths at each intersection. Different from the centralised and semi-decentralised systems, the max-pressure does not require global traffic information and each controller operates separately.

Chapter 4

Comparing centralised and decentralised traffic control under a macroscopic flow model

4.1 Introduction

This chapter implements and tests the control systems presented in Chapter 3 over different networks. This chapter begins with the test of control systems on a one-way arterial network in Section 4.2. The test extends to a two-way arterial network in Section 4.3 and a two-dimensional grid network in Section 4.4. Since, the offset plan is found as a key to bridge the gap between the centralised and the decentralised control systems, a centralised offset controller is proposed and tested in Section 4.5. Finally, Section 4.6 is a summary of this chapter.

4.2 One-way arterial network

4.2.1 Network Configurations

Figure 4.1 shows the one-way arterial network considered in this study. It consists of three intersections and ten roads, where the intersections are represented by nodes and the roads are represented by links. The traffic dynamics are modelled by the CTM, and the flow-density relationship on each link is described by a bi-linear fundamental diagram (see Section 2.2.2). The network is discretised into 120 cells where each cell is 14 metres long. The cell length is calculated from $\upsilon\Delta t$, which is the minimum distance for a vehicle to travel at the free flow speed υ during one time step Δt. For each cell c (the CTM model divides links into cells), the free flow speed υ_c and shockwave speed w_c are set to 50 kph and 16 kph respectively (approximately equivalent to 30 mph and 10 mph). The speed limit of an urban area commonly is 30 mph, such as London and Paris, and the shockwave speed is calculated basing on the defined flow-density relationship. In addition, the distance between two successive nodes for the arterial is set to 160 metres (around 0.1 mile), which is the length of city blocks seen in New York and Barcelona. By knowing the distance between two adjacent nodes on the arterial and the free flow speed of the vehicles, the free flow travel time between the two nodes can be calculated which equals to 12 seconds.

The test scenario is specified by a time horizon, traffic demand profiles and other settings. The time horizon T of the test is set as 1500 time steps, where one time step Δt is one second. The following demand profiles $\Lambda_x(t)$ and $\Lambda_y(t)$ are assigned to the horizontal and vertical (cross) streets accordingly:

$$\Lambda_x(t) = \begin{cases} 0.6\lambda, & 0 \leq t \leq 300 \\ \lambda, & 301 \leq t \leq 600 \\ 0.6\lambda, & 601 \leq t \leq 900 \\ 0, & t > 900 \end{cases} \tag{4.1}$$

$$\Lambda_y(t) = \begin{cases} 0.48\lambda, & 0 \leq t \leq 300 \\ 0.8\lambda, & 301 \leq t \leq 600 \\ 0.48\lambda, & 601 \leq t \leq 900 \\ 0, & t > 900 \end{cases} \tag{4.2}$$

where λ is a parameter (with unit: [veh/hr]) for tuning the magnitude of demand. The period from time step 901 to 1500 is regarded as the cooling period in which no further traffic will be loaded into the network. This cooling period is used to ensure all traffic can be cleared by the end of test and hence a fair comparison of performance (in terms of the network delays) of the control systems over all circumstances can be obtained. The control systems will be tested over different values of the parameter λ which represent different levels of demand. To quantify the degree of congestion, an indicator γ is defined as:

$$\gamma = \frac{1}{n} \sum_{t=1}^{T} \sum_{c=1}^{\mathbf{C}} \frac{q_c(t)}{Q_c(t)}. \tag{4.3}$$

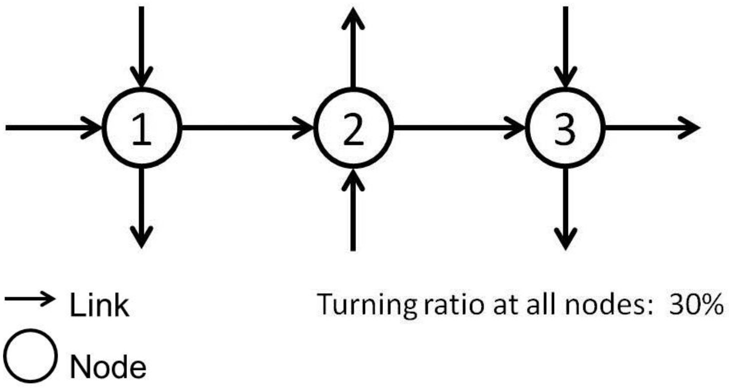

Figure 4.1: Test one-way arterial network

For each cell c and time step t, $q_c(t)$ is the flow and $Q_c(t)$ is the saturation flow which is set to be 1800 vehicles per hour. n represents total number of nodes in the network. Then γ can be regarded as a network-wide demand-capacity ratio which is the space-time average of ratios of flow to saturation flow over each cell c and time t. Regarding the turning ratios along the arterial, it is assumed that 70% of the traffic will proceed straight on, while 30% will make a turn at each node. Given the arterial topology and demand settings, it is then possible to derive the corresponding timing plans for each of the control systems over five levels of γ: 0.5, 0.6, 0.7, 0.8, and 0.9 which represent different degrees of congestion. It is noted that γ is unfeasible to achieve 1 with the cooling period that is adopted, as $\gamma = 1$ implies the network is filled with traffic over the entire time horizon T.

4.2.2 Settings of the test control systems

To derive the centralised timing plans, a ‘brute force’ solution is computed, which minimises the total delay on all links by simulating the arterial network over all possible timing plan settings. The timing plan settings include cycle time, green splits and offsets. To mimic actual operations, a total of 16 seconds lost time is considered in each cycle when deriving the timing plan. The green splits and offsets are allowed to vary every cycle according to the temporal variations in the demand flows. The workstation used for the tests in this chapter has Intel Xeon E5-2630 v3 2.4GHz processor and 16GB RAM. The test program is written in Matlab 2013b. The brute force solution can be regarded as the global optimal plan that minimises the total arterial delay.It takes 12 hours to complete a brute force search. It is known that the brute force is rarely used in practice, however, it is a useful benchmark for evaluating the performance of different control systems. Compared with the brute force solution, another centralised timing plan is also computed by using GA which takes an hour to solve. Additionally, the offset values at one of the nodes (Node 2) in the test network remains unchanged through the test (also applies to the decentralised offset controller); this setting is to make a valid comparison between different offset controls.

To derive the control timing plans of the semi-decentralised and decentralised systems, some control parameters need to be specified before conducting the experiment. The nominal green $\mathbf{g^N}$ in the TUC controller is set according to the estimated demand-saturation flow ratios as shown in Equation 3.22. Since the centralised systems are cyclic control, so the decentralised system max-pressure will be using its cyclic version for comparison. As noted by [95], there is no straightforward way to determine an optimal value for η in the cyclic MP controller. Consequently, the value of η is determined by trial-and-error over different settings for the best performance results. It is found that the best value of η will be 0.91, 0.64, 0.61, 0.55, 0.46 for γ equals to 0.5, 0.6, 0.7, 0.8, 0.9 respectively. The finding is not intuitive, as it implies that the cyclic MP should be made to be less sensitive to the pressure as the degree of congestion increases. For all of the considered semi-decentralised and decentralised systems, the control timing plans are derived instantaneously.

4.2.3 Test results

The total network delays delivered by each of the control system are compared and plotted in Figure 4.2 over different γ. To mimic the effect of imperfect estimation in traffic flow quantities, all controllers are run over a set of 100 Monte Carlo simulations in which all inflows and turning ratios are incorporated with a Gaussian white noise with a standard deviation equalling to 10% of the associated expected flow or split value. Therefore, the delay values plotted in Figure 4.2 are averages produced by each controller over the 100 Monte Carlo runs. The optimal arterial cycle times are determined as 54, 80, 80, 92, and 102 seconds for $\gamma = 0.5, 0.6, 0.7, 0.8$, and 0.9 respectively.

The centralised system, brute force approach, outperforms all other systems in Figure 4.2. This is expected while such a brute force solution would take a much longer time to compute. Interestingly, all semi-decentralised or decentralised systems can outperform the centralised GA at high γ values, due to the adaptive nature of the decentralised systems. Although GA does derive plans that have variable green splits over different cycles (i.e. the Variable-Green-Fixed-Cycle plan as in [70]), its long computing time (1-hr) prevents it from being adaptive to prevailing traffic and hence discounts its effectiveness when subject to the 10% stochastic variations.

In terms of the performance of semi-decentralised and decentralised control systems, Hybrid controller performs slightly better than TUC under a low degree of congestion (e.g. $\gamma = 0.5$ or 0.6). The Hybrid system is structurally the same as TUC except it will operate in a demand-based mode when the network occupancy is low. With the low occupancies, the network may not have residue queues being detected at the end of each cycle and the TUC system behaves similarly to a fixed-time controller (see the control rule in Equation 3.7). With the demand-based mode, the Hybrid system still can adapt to the traffic, since its operation is based on the traffic flow rate. With a high γ value (e.g. 0.8 or 0.9), the arterial is congested and hence the Hybrid system will be operating in TUC mode most of the time. Consequently, the performances of the two systems are almost identical. The cyclic MP performs similarly to TUC and Hybrid. As mentioned, when there is a low (or zero) queue on the downstream links, the cyclic MP reduces to a TUC-like control.

To gain further insight into the control systems, Figure 4.3 shows the profiles of green

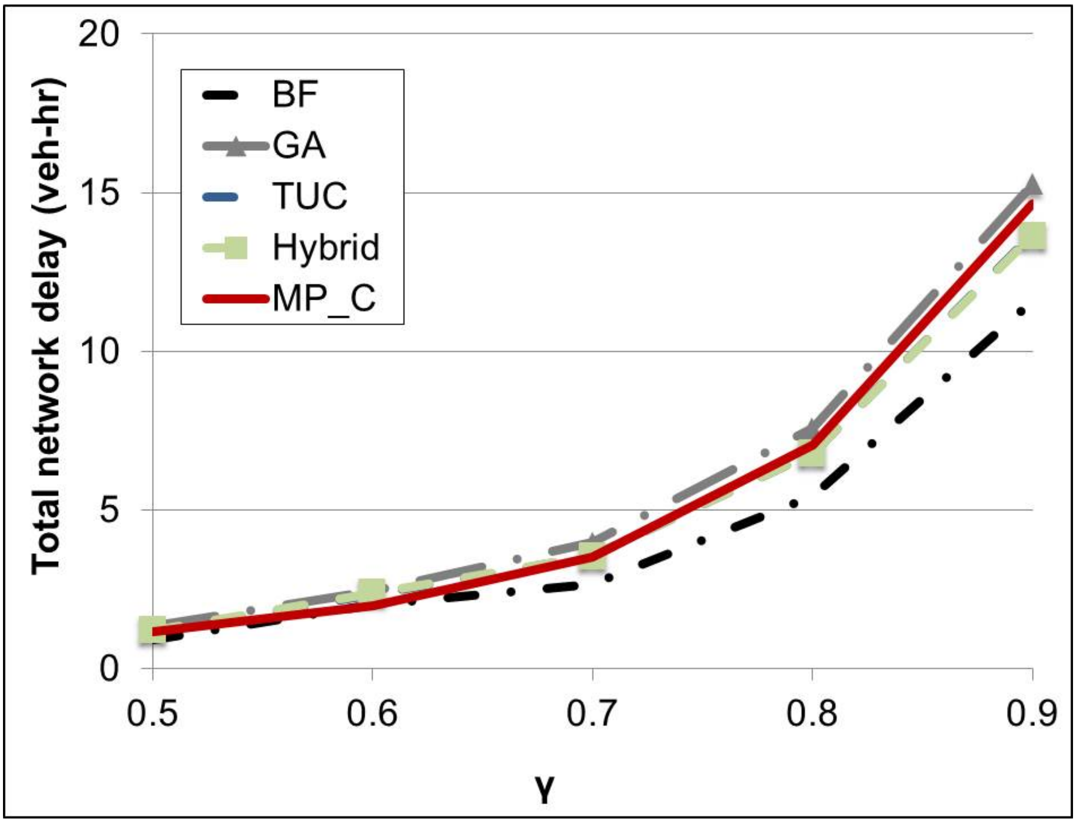

Figure 4.2: Average network delays on the one-way arterial

splits allocated to the horizontal arterial by some of the control systems over the test period. The green splits of brute force (centralised), TUC (semi-decentralised), and cyclic MP (decentralised) at Node 3 under low ($\gamma = 0.5$), medium ($\gamma = 0.7$) and high ($\gamma = 0.9$) degrees of saturation are presented. It is noted that fewer cycles are run within the 1500-second test period under γ = 0.7 and 0.9 due to the longer cycle time. It can be seen that the evolutions of green splits essentially follows a similar trend as all systems under low and medium demands (γ = 0.5 and 0.7) do, with an average green split around 30 seconds when $\gamma = 0.5$, and average green split around 40 seconds when $\gamma = 0.7$. Additionally, the green splits derived by brute force are more dynamic than the semi-decentralised and decentralised systems. However, this can be understood as TUC and cyclic MP are designed as stabilisers for oversatu-

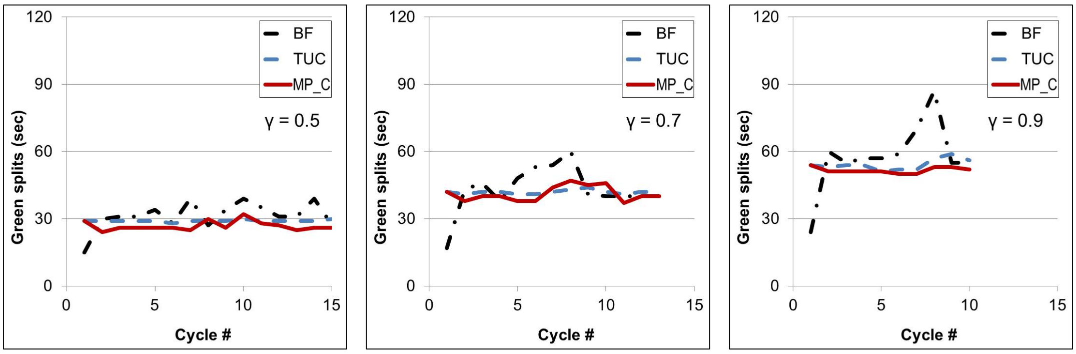

Figure 4.3: Green splits at Node 3 over different γ on the one-way arterial network

rated traffic whose split controller can be ineffective and remain at its nominal value when there is no cycle failure (i.e. cycle with non-zero residual queue) occurring.

At high demand ($\gamma = 0.9$) in Figure 4.3, brute force has different green split plans compared to the plans of the other systems. According to Figure 4.1, the highest demand travels along the horizontal direction and all of the nodes are oversaturated in this scenario. Cyclic MP assigns a lower green to the arterial and facilitates the movement on cross streets, while the TUC controller tends to continue allocating to approaches with higher demand (horizontal streets in this case). TUC does not respond to the downstream blockage or 'de-facto red' [70] under oversaturation, so that allocates a slightly higher green split to the horizontal traffic flows. However, brute force gives far more green splits to the horizontal direction after the 6th cycle, which indicates that brute force controls traffic differently to the semi-decentralised and decentralised systems.

Figure 4.4 shows the profiles of offset at the Node 3 under different systems. While the green split profiles are similar, the offset profiles derived from the decentralised

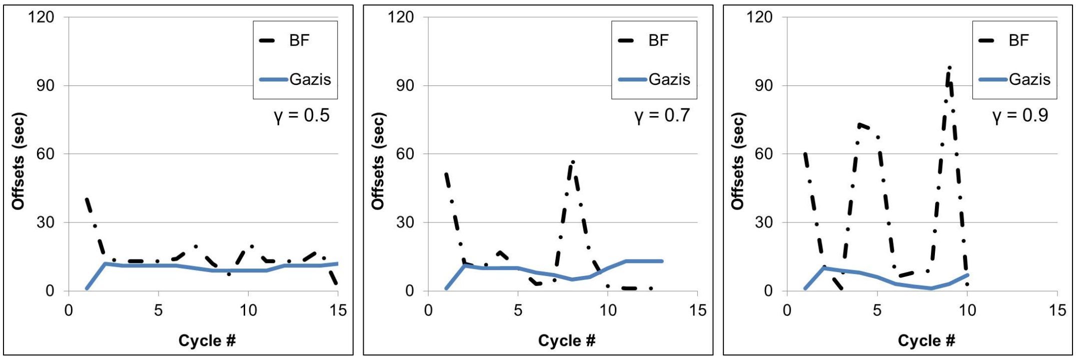

Figure 4.4: Offsets at Node 3 over different γ on the one-way arterial network

systems are quite different from the centralised one. The Gazis's controller keeps the offsets low due to excessive queues, and the brute force controller will maintain or even increase the offset with an objective to maximise the throughput from a system-wide perspective; this probably is the reason why brute force allocates more greens to the horizontal direction whilst the decentralised systems do not.

Figure 4.5 is the traffic density plot of the arterial, where $\gamma = 0.9$ and the signal plan is calculated by brute force. It can be noticed that the upstream node (Node 1) reduces its green split at the 5th cycle, which is to prevent the downstream blockage. At the same time, both Node 1 and Node 3 adjust their offsets to prioritise vertical traffic flows. After the 5th cycle, priority is given back to the horizontal traffic. Hence, the controller at the Node 3 starts to increase the green splits to the horizontal traffic (in Figure 4.3). For the decentralised control systems, cyclic MP can reduce the green splits to prevent the downstream blockage; however, the Gazis offset controller can not incorporate this change in the green split. Therefore, the adjustments of offsets difference between centralised and decentralised systems is a valid reason for their overall performance differences.

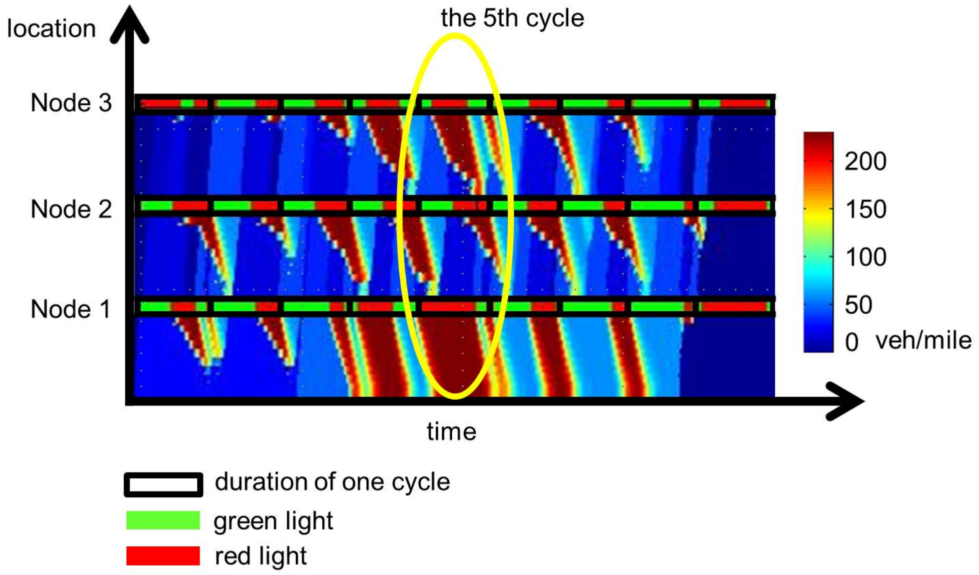

Figure 4.5: Density plot at $\gamma = 0.9$ on the one-way arterial network controlled by the brute force approach

4.3 Two-way arterial network

4.3.1 Network configurations

Control systems are applied to a two-way arterial network, which as seen in Figure 4.6 is more complex. The two-way arterial network has an identical geometry to the one-way arterial network shown in Figure 4.1. It is also discretised into 240 cells with the same set of values assigned to the parameters: υ_c, w_c, Q_c as in the one-way case for all cells c. The test time horizon T and the time step Δt remains the same, also the traffic inflow to all the six vertical cross streets is the same as that specified in (5.11). The inflow to the horizontal main arterial along the 'left-to-right' direction is as that specified in (4.1), while the inflow along the 'right-to-left' direction will be 90% of it in order to create an asymmetric demand on the mainline, i.e.

$$\Lambda_{x2}(t) = \begin{cases} 0.54\lambda, & 0 \leq t \leq 300 \\ 0.9\lambda, & 301 \leq t \leq 600 \\ 0.54\lambda, & 601 \leq t \leq 900 \\ 0, & t > 900 \end{cases} \tag{4.4}$$

The turning ratios in this arterial network are set as follows: 70% of the link traffic proceeds forward, while 30% makes a left turn at each node, no traffic makes right turns irrespective of there being two-way streets. The magnitudes of the inflow profiles are adjusted to match the predefined set of γ ratios: 0.5, 0.6, 0.7, 0.8, and 0.9. The optimal cycle times for the two-way arterial network are determined as 54, 64,

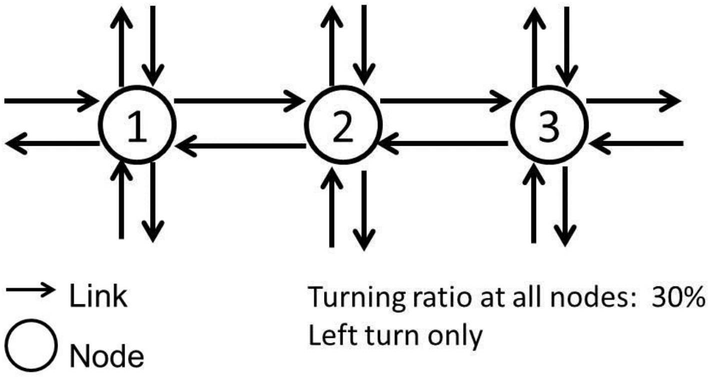

Figure 4.6: Test two-way arterial network

80, 104, and 118 seconds for γ = 0.5, 0.6, 0.7, 0.8, and 0.9. The cycle times are slightly higher than the one-way case due to the heavier and asymmetric demand.

4.3.2 Test results

The performances of the controllers for different values of γ are shown in Figure 4.7. The performance trend indeed is similar to the one-way arterial network case in Section 4.2, where the brute force outperform all of the other considered systems and the decentralised systems outperform the centralised GA. TUC and Hybrid behave similarly at higher demand levels and cyclic MP is similar to the two semi-decentralised systems.

Figures 4.8 and 4.9 show the green splits (to horizontal mainline) and the offsets derived by different control systems at Node 3 in the two-way arterial network, respectively. It can be seen that all control systems can essentially derive a similar green split compared with the brute force solution as found previously in Section 4.2, while the main differences in the timing plans come from the offsets. This

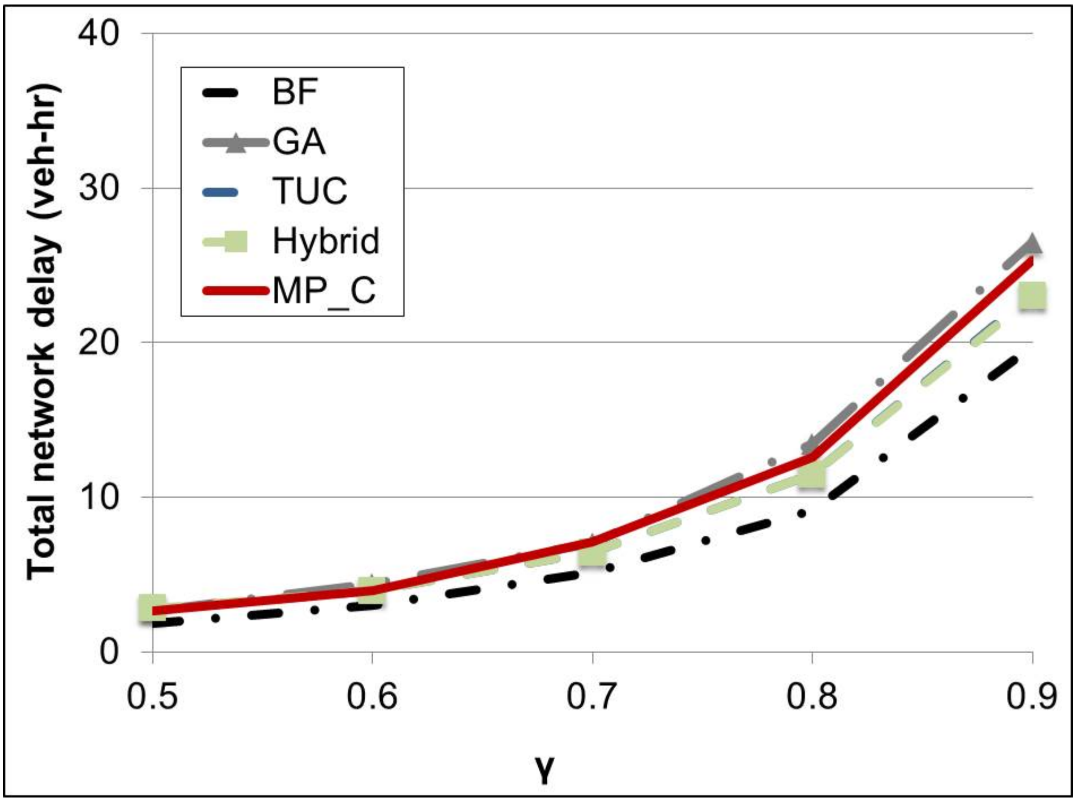

Figure 4.7: Average network delays on the two-way arterial

suggests that an effective offset controller is key in improving the effectiveness of decentralised systems for arterial traffic management.

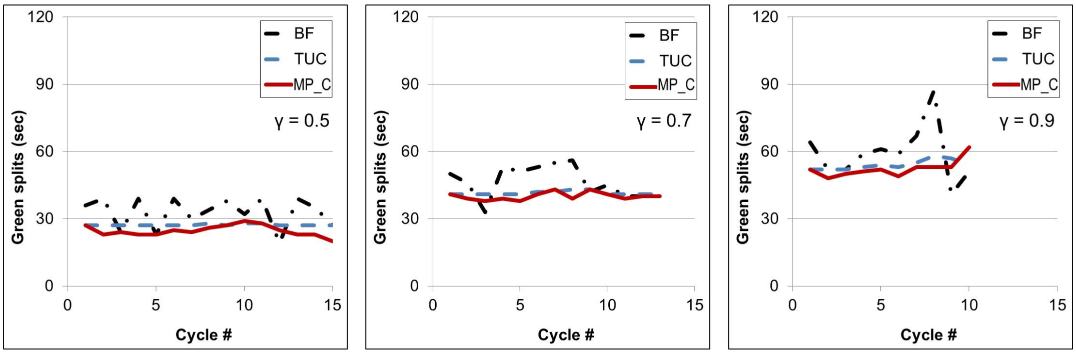

Figure 4.8: Green splits at Node 3 over different γ on the two-way arterial network

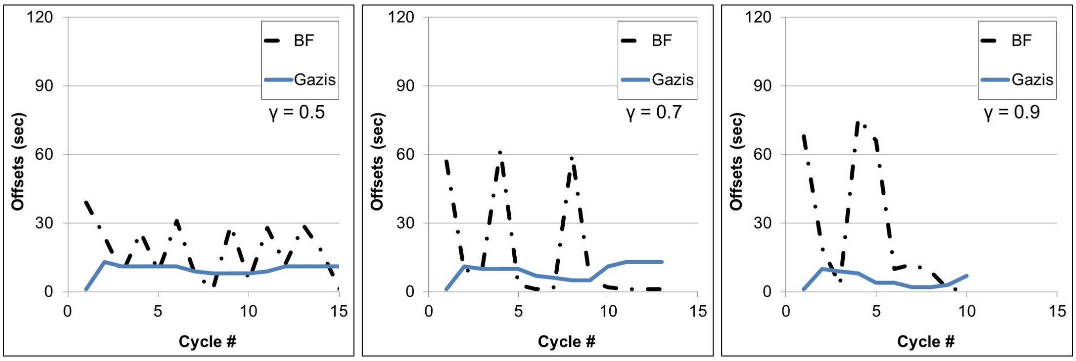

Figure 4.9: Offsets at Node 3 over different γ on the two-way arterial network

4.4 Grid network

4.4.1 Network configurations

The control systems are further applied to a two-dimensional grid network (Figure 4.10). The network is different from the one-dimensional arterial network, and the traffic interaction in the grid network is more complex due to the turning movements occurring over a two-dimensional plane. The grid network is discretised into 576 cells with the same set of values assigned to the parameters: υ_c, w_c, Q_c as in the arterial case for all cells c; the free flow travel time between each pair of nodes is also the same as for the arterial cases. The demand profile $\Lambda_x(t)$ specified in Equation 4.1 is applied to the horizontal links, and $\Lambda_y(t)$ specified in Equation 4.2 is applied to the vertical links in the network. The total test time, time step size as well as the turning ratios are the same as for the cases in Section 4.2 and Section 4.3.

4.4.2 Test results

The performances of different controllers against γ are shown in Figure 4.11. The optimal cycle times determined as 52, 62, 80, 90, and 102 seconds for $\gamma = 0.5$, 0.6, 0.7, 0.8, and 0.9 respectively, which is not significantly different from the one-way arterial network. Because of the size of the grid network and the number of controllers, the brute force approach takes 23 hours to solve. It is noted GA performs notably worse than its decentralised counterparts due to the complexity of the grid network which it encounters. These highlight the challenge of using centralised

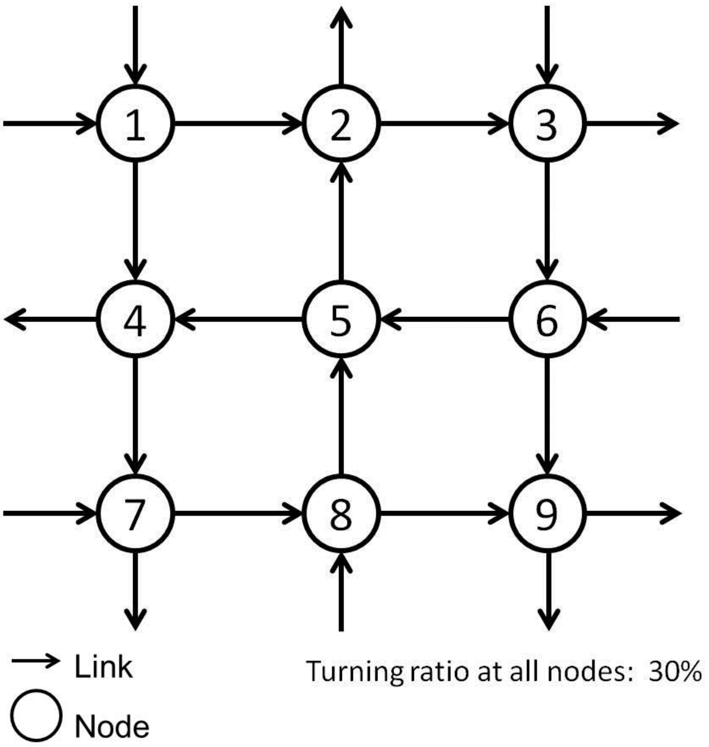

Figure 4.10: Test grid network

optimisation for managing complicated networks and justifies the value of using decentralised systems. As shown in these examples, a properly designed decentralised system may not necessarily perform too much worse than a centralised one considering the complexity involved in the centralised calculations. It is also observed that cyclic MP performs considerably similar with the TUC and Hybrid controllers when demand level is not high. This highlights the effective operation of decentralised systems in complex networks.

Figure 4.12 shows the profiles of green splits allocated to the horizontal street by the controllers at Node 4 under γ = 0.5, 0.7 and 0.9. It is interesting to note that the brute force solution would allocate long green to the horizontal street in the

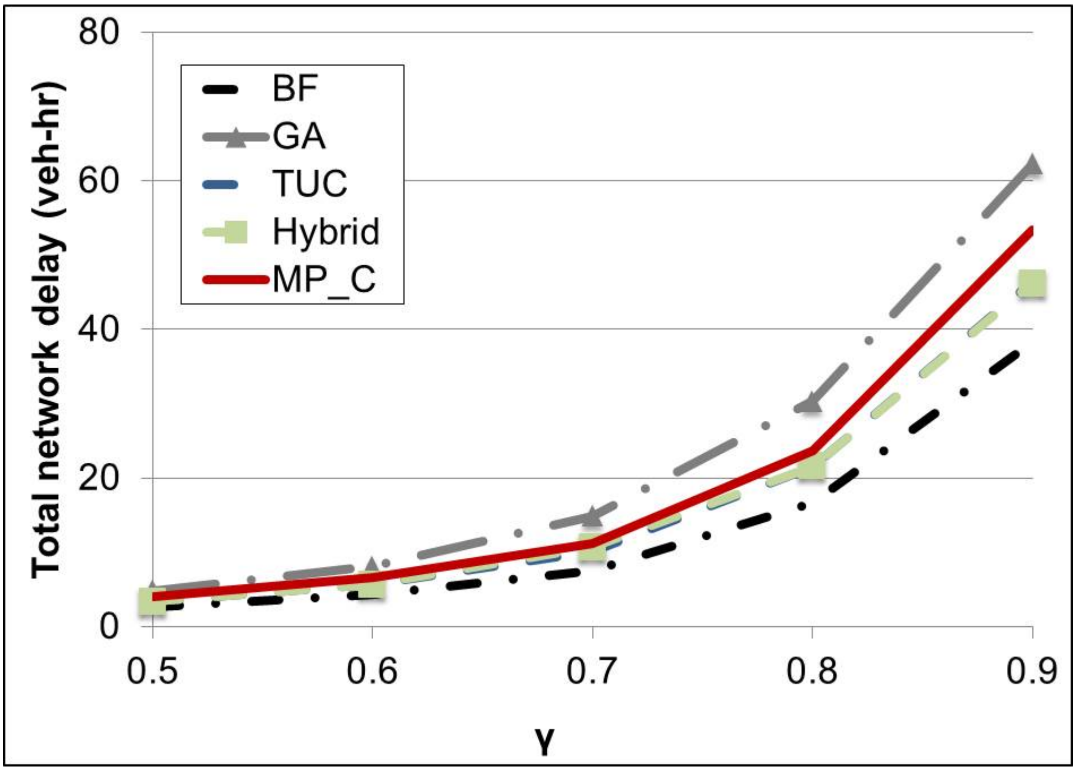

Figure 4.11: Average network delays on the grid network

beginning of the test while it would essentially reach a similar steady state value (30 seconds for $\gamma = 0.5$, 40 seconds for $\gamma = 0.7$ and 60 seconds for $\gamma = 0.9$) as the TUC and cyclic MP. Finally, Figure 4.13 shows the offsets at the node 4; the determination of offsets is more difficult in this two-dimensional grid network than the one-dimensional arterial network as the offset will have to consider progress of traffic in multiple directions. As shown in Figure 4.13, the Gazis's decentralised offset controller fails to mimic the brute force offsets at both low and high degrees of congestion as the global network dynamics are not incorporated in the control rule (Equation 3.20). This again indicates that an effective offset controller is essential for operating the decentralised systems.

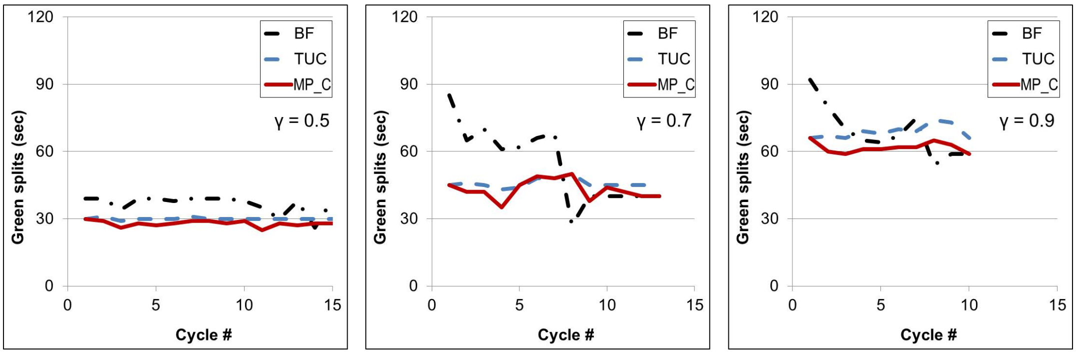

Figure 4.12: Green split at Node 4 over different γ on the grid network

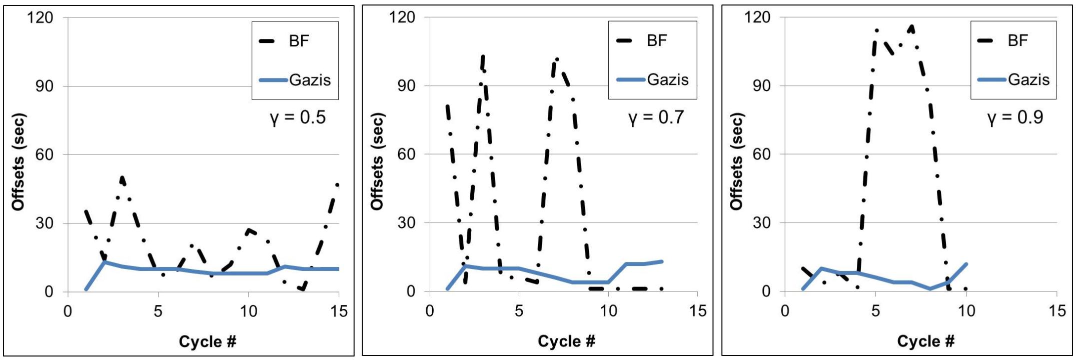

Figure 4.13: Offsets at Node 4 over different γ on the grid network

4.5 Decentralised systems with hill climbing offset controller

As the calculation of offset plans is playing a vital role according to the previous sections, a centralised offset controller is proposed to bridge the gap between the centralised and decentralised control systems. The centralised offset controller proposed here does not have the highest accuracy, however, it is mainly to demonstrate the effectiveness of a centralised offset control. A heuristic local search has been considered as it can converge faster than global searching methods. Decentralised split control is significantly faster than centralised ones. Having a fast centralised offset control will help the whole signal control system to be a practical online control system.

Hill climbing technique is a local searching method. Like the name says, it continuously ‘climbs’ towards to better solutions and terminates at a peak when the objective function needs to be maximised. Hill climbing technique has been implemented in TRANSYT for optimising the traffic signals (see Section 2.3.1). Given the flow measurements and existing green splits, the hill climbing technique refines the intersection offsets in a road network iteratively to minimise the overall network delay in the forthcoming signal cycle (s). To implement the algorithm, the step sizes are needed to be defined. In TRANSYT, a series of searching step sizes are used as follows: 15, 40, 15, 40, 15, 1, 1. The value of the step size means the percentage of the maximum feasible offset. The use of different step sizes is to prevent the searching algorithm from being trapped into a local minimum. With this sequence, the offset value is first increased at a specific node in the road network by '15%' (first entry '15' in the sequence), and then determines the corresponding change in total network delay by re-running the test with this revised offset. If this gives a reduction in the delay, the offset value will continue to be increased, this time by '40%' (second entry '40' in the sequence); otherwise, the offset value will be reduced by 40% and see whether it will bring a reduction in total network delay. The algorithm proceeds with this predefined step size sequence until the sequence is exhausted or if there is no further reduction in total network delay achievable. The algorithm then moves on to the second node in the network, repeating the process until all nodes in the network have been visited. Figure 4.14 shows the procedure of the hill climbing offset control in a flowchart format.

A sensitivity analysis has been carried out for examining the choices of the searching step sizes. The analysis considered the two test networks from the previous sections (Section 4.2 and 4.4): one-way arterial network and 3 by 3 grid network. The tests have carried out with different searching step sizes for offset control. Figure 4.15 shows the average impacts of the step sizes on the network delay. The x-axis is the step size over the searching range, and the y-axis is the scaled performance to the minimum to maximum network delays in the results. For example, when the scaled performance equals 0, it means the performance is the lowest network delay founded in the test. On the other hand, the scaled performance equals to 1 when the result is the highest network delay founded in the test. When the step size larger than 50% of the searching range, there are much less offset values can be visited. This is why the corresponding network delays cannot outperform the results in smaller step sizes. Smaller step sizes lead to better performance, however, will have more offset values need to visit and will take longer time. According to the Figure 4.15, any values less than 20% of the searching range can find better results than any larger step sizes. In this case, the 15% step size looks reasonable and any step size around it gives similar results. Alternatively using the step size 40% and 15% can avoid the algorithm trapped in one local optimal. Leaving the smallest step size (1%) at the end of the searching process is to explore its direct neighbourhood.

Figures 4.16, 4.17 and 4.18 show the performance of the offset controller in the one-way arterial network, the two-way arterial network and the grid network respectively. With the consideration of the performance shown in the previous sections, the focus of this section is on the cyclic MP and replaces the Gazis offset controller with the hill climbing based offset controller. The results show that the offsets determined by the centralised hill climbing algorithm improve the performance of the cyclic MP. Different from the brute force and GA approach, this proposed controller only needs to perform a centralised optimisation to calculate the offsets, while the green splits can be determined through the decentralised MP approach. Consequently, a considerable amount of computational effort can be saved and a similar centralised performance can still be achieved. The saving in computational effort will be even more significant in large networks as it is known that the complexity of the signal optimisation problem grows exponentially with the number of nodes involved. In this specific example, it takes 40 seconds to compute all offsets for the arterial network and 65 seconds for the grid network on a computer (Intel i5-4370 CPU 3.2GHz). The results are promising as they reveal the possibility of using decentralised systems for effective network-wide real-time urban traffic control.

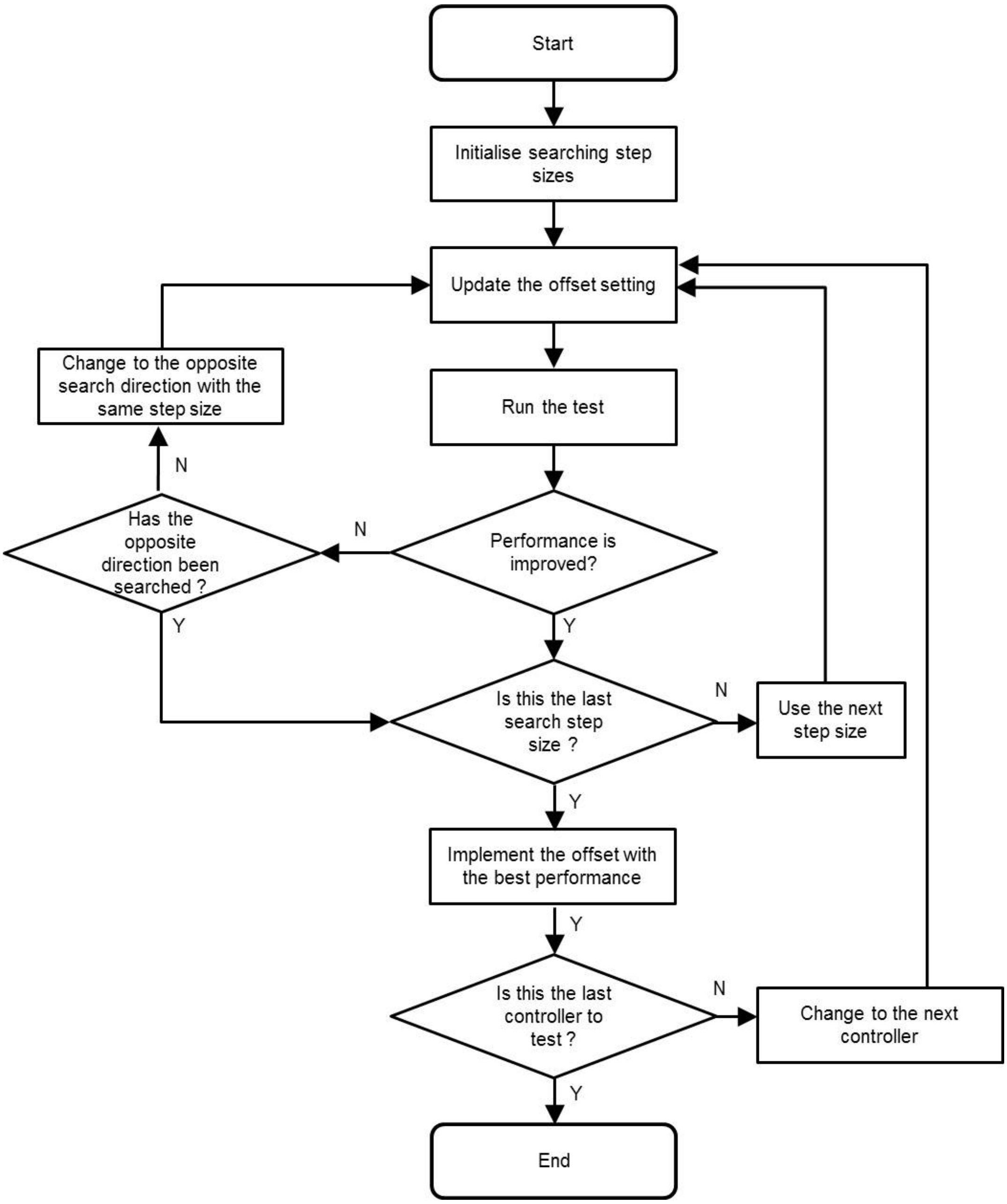
Start
Initialise searching step sizes
Update the offset setting
Change to the opposite search direction with the same step size
Run the test
N
Has the opposite direction been searched ?
N
Performance is improved?
Y
Y
Is this the last search step size ?
N
Use the next step size
Y
Implement the offset with the best performance
Y
Is this the last controller to test ?
N
Change to the next controller
Y
End

Figure 4.14: A flowchart of hill climbing offset control

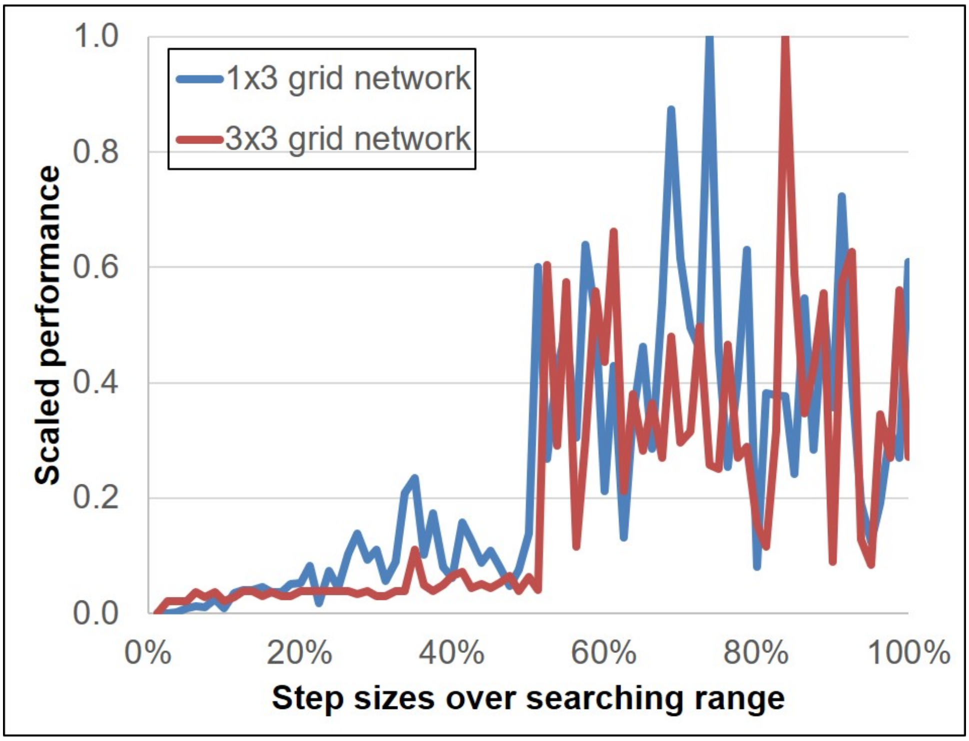

(a) All step sizes

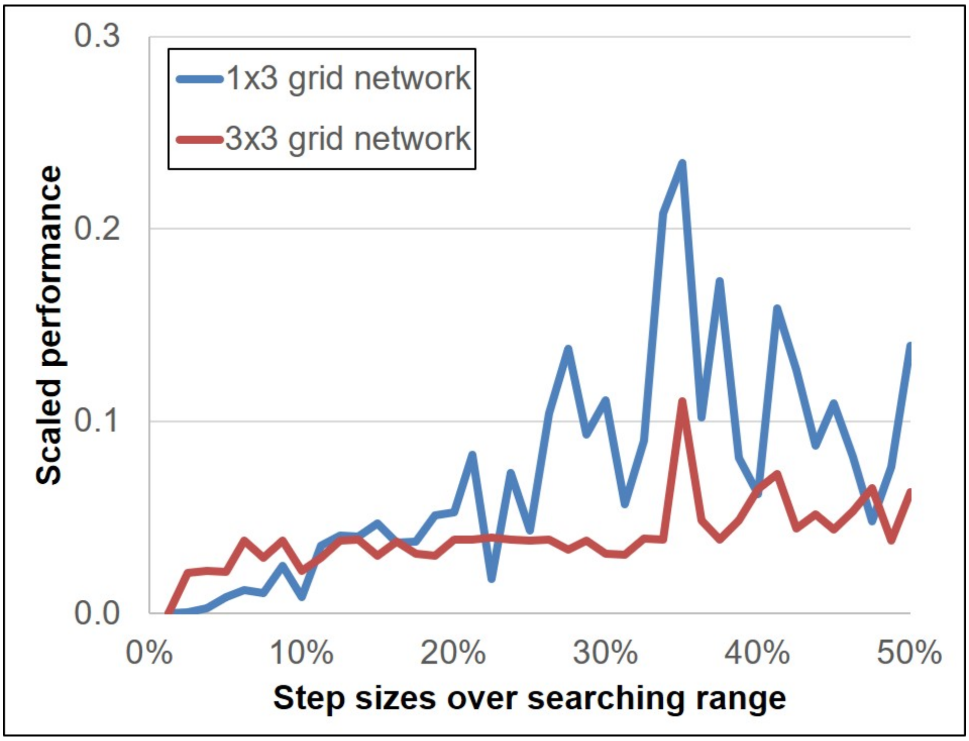

(b) Step sizes upto 50% of the searching range

Figure 4.15: A sensitivity analysis of hill climbing step sizes

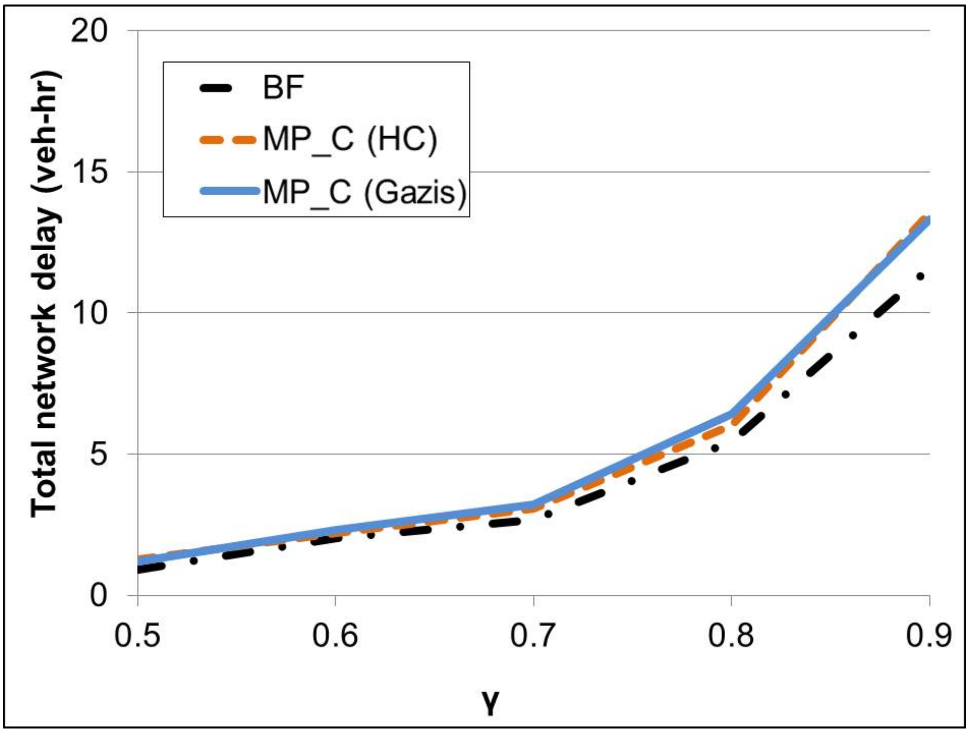

Figure 4.16: Network delays in the one-way arterial network with hill climbing offset controller

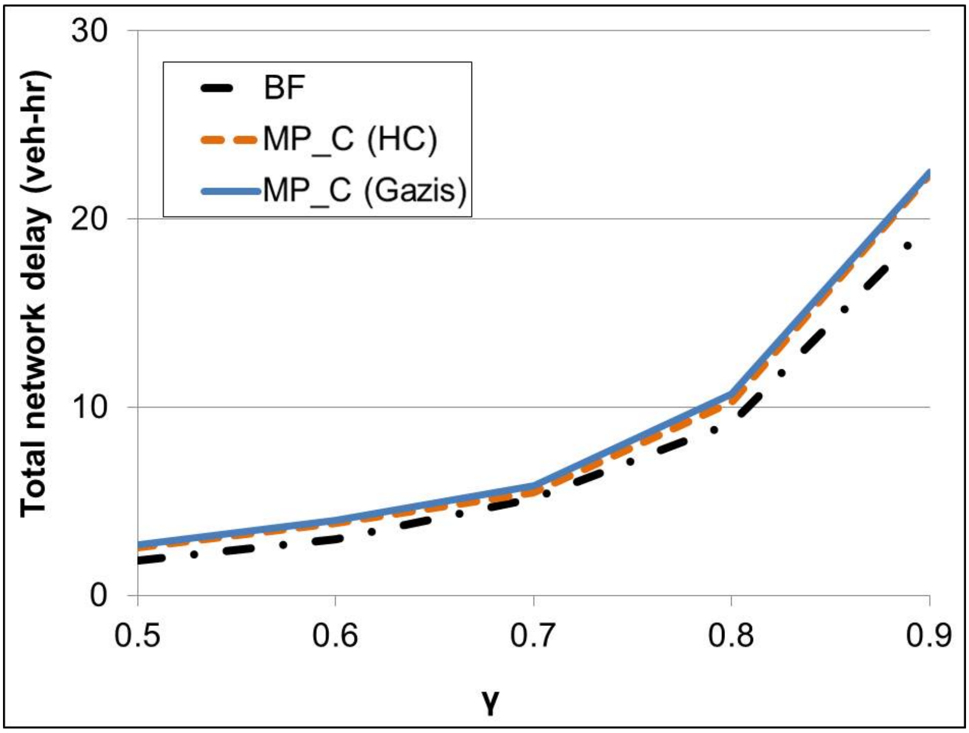

Figure 4.17: Network delays in the two-way arterial network with hill climbing offset controller

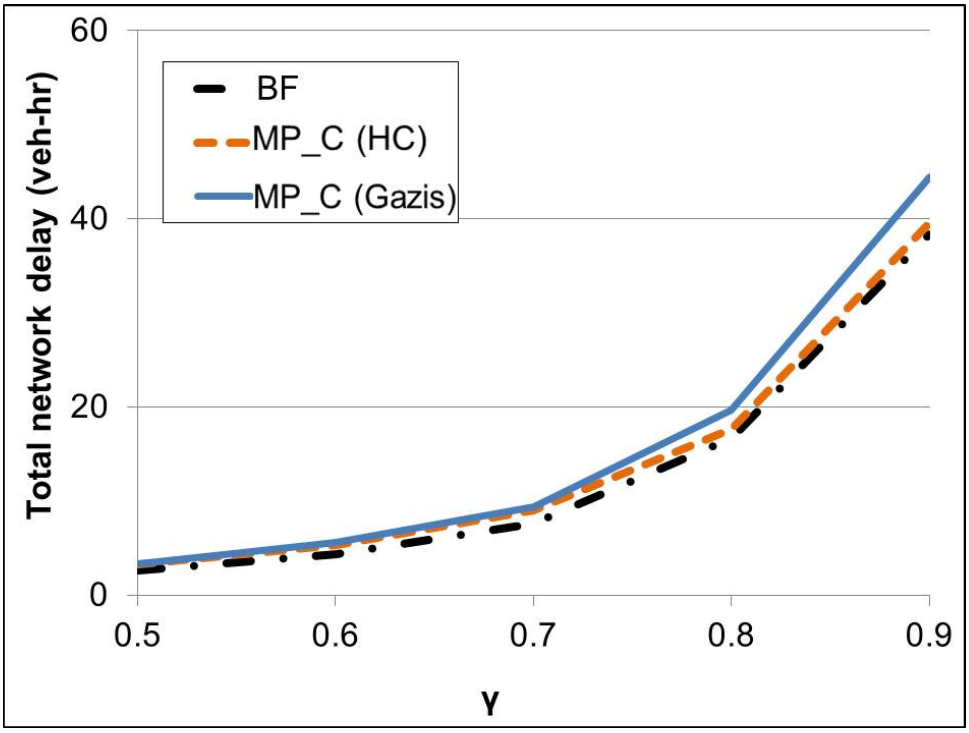

Figure 4.18: Network delays in the grid network with hill climbing offset controller

4.6 Summary

This chapter compared the performances of the control systems: centralised (brute force approach and GA), semi-decentralised (TUC and Hybrid) and decentralised (MP) under one-way arterial, two-way arterial, and grid networks.

In terms of the system performances, the performance differences are not significant before the test networks reach their saturation limits (see Figure 4.2, 4.7 and 4.11). As expected, the brute force approach outperforms all the other control systems. However, the GA is not quite efficient as the control timing plans derived by GA are not adaptive to the stochastic variations in traffic demands. TUC and Hybrid have very close performances. The cyclic MP performs similar with TUC and Hybrid in the arterial networks, but not in the grid network. This shows the advantage of the centralised feature in the TUC system.

To find the insights of the performance differences among the control systems, the derived green splits and offsets by the control systems are presented in the test results of each section. The control timing plans show that the corresponding local green splits determined from centralised, semi-decentralised and decentralised systems are indeed similar. This implies most benefit gained from centralised control comes from the setting of offsets. The major challenge of the decentralised offset control comes when the test network is oversaturated and the controllers are applied to complicated networks, like the grid network adopted in this study. In those cases, offsets have to be adjusted frequently and accurately in order to balance the progression of traffic along different directions through the network. To address the problem, a centralised hill climbing based offset controller is further purposed and integrated with the decentralised control systems. The results suggest that such a centralised offset controller helps to reduce the performance gap between centralised and decentralised systems, and has significantly less computational effort compared to full centralised systems. Therefore, the proposed centralised offset controller can be extended to design an efficient decentralised control system. Moreover, the experiments'result are going to be validated by using a different microscopic traffic flow model SUMO in the next Chapter 5. With the microscopic model, more detailed vehicle's movements (such as acceleration and rerouting behaviours) can be captured.

Chapter 5

Comparing centralised and decentralised traffic control under a microscopic flow model with traffic rerouting

5.1 Introduction

This chapter tests the performance of the centralised and decentralised traffic controls on a microscopic platform with open source SUMO package. Comparing to the macroscopic CTM in previous chapter 4, SUMO can capture more detailed vehicle movements and allows vehicles to reroute according to real-time traffic conditions. The flow model of SUMO is first introduced in Section 5.2 and compared with CTM model. Both centralised and decentralised control systems are tested with SUMO on an arterial network in Section 5.3. Rerouting control is introduced and tested on a grid network in Section 5.4. At the end, Section 5.5 summarises the chapter.

5.2 Simulation of urban mobility - SUMO

Simulation of urban mobility (SUMO) is an open source traffic simulation platform developed by German Aerospace Centre (DLR). It is a tool for transport planning, and can examine the impact of road layout change, new speed limit implementation or other design adjustments of transport facilities. The simulation is done at microscopic level, where the different modes of transport such as vehicles, pedestrian and public transport are modelled together. The open source feature benefits users from spending time to develop their own simulator for test purpose. The results of SUMO have also become comparable between users [97].

The basic usage of SUMO platform can be divided into three parts: network generation, demand modelling and simulation [98]. Network can be created in an application tool NETCOVERT which comes with SUMO, or can be imported from online resources (such as OpenStreetMap) and from other simulation platforms (for instance, VISIM, VISSIM and MATsim). SUMO accepts a wide range of demand types. For example, the traffic demand can be defined by origin and destination data, can be generated by traffic flow and turning ratio and can be defined by the trip routes. In terms of the simulation, the default microscopic flow model of SUMO is a safety-distance model developed by Krauss [99], and a detailed explanation is in Section 5.2.1.

5.2.1 Traffic dynamics

The default flow model of SUMO uses the safe-distance model proposed by Krauss [99]. Krauss' model assumes all vehicles tend to travel at their maximum allowed speed under a safe condition (with no collisions occurring). The safe speed is computed as:

$$v_{\text{safe}}(t) = -\tau\alpha_{\text{max}}^{\text{dec}} + \sqrt{(\tau\alpha_{\text{max}}^{\text{dec}})^2 + v_n(t-1)^2 + 2\alpha_{\text{max}}^{\text{dec}}(\chi_n(t-1) - \chi_{n+1}(t-1))} \tag{5.1}$$

where $\alpha_{\text{max}}^{\text{dec}}$ is the maximum deceleration rate and τ is the follower driver's reaction time. Once the safe speed v_{safe} is known, a desired speed v_{des} can be calculated from the maximum speed v_{max} and acceleration rate α:

$$v_{\text{des}}(t) = \min[v_{\text{max}}, v(t-1) + \alpha, v_{\text{safe}}] \tag{5.2}$$

The desired speed v_{des} is an optimal speed for the Krauss' model, and additional stochastic deceleration rate is used to model drivers' different perspectives to the optimal speed:

$$v(t) = \max[0, v_{\text{des}}(t) - r_{\text{num}}\alpha\varepsilon] \tag{5.3}$$

where the random number r_{num} and drivers' imperfection factor ε are both in a range from 0 to 1. The acceleration rate α is effected by the travelling speed v, where the following relationship holds between α and v:

$$\alpha(v) = \alpha(1 - \frac{v}{v_{\max}}) \tag{5.4}$$

At the end, the effectiveness of drivers' imperfection factor is eliminated when vehicle's speed is low, and the final speed becomes:

$$v_{\text{final}}(t) = \max[0, v_{\text{new}}(t)] \tag{5.5}$$

where

$$v_{\text{new}}(t) = \begin{cases} v_{\text{des}}(t)\varepsilon r_{\text{num}}, & \text{if } v_{\text{des}}(t) < \alpha(v_{\text{des}}(t)) \\ v(t) - \varepsilon r_{\text{num}}\alpha(v_{\text{des}}(t)), & \text{otherwise} \end{cases} \tag{5.6}$$

5.2.2 Dynamic rerouting algorithm

Rerouting algorithms are used to mimic the route changes of drivers with repect to traffic condition[100, 101, 102, 103]. According to real-time traffic condition, it guides each vehicle to travel on the route gives shortest travel time. A real-time feedback rerouting algorithm is implement on SUMO to evaluate traffic controls 'performance with drivers' route change behaviour. Each vehicle is initially assigned with a route which has the shortest distance for its origin and destination. Congestion could build up in the network, and the rerouting algorithm updates the travel time of each link. When a vehicle approach to an intersection, the rerouting algorithm re-evaluates its route for the shortest travel time. $u(r)$ represents the average travel time of a route r over a time interval. If there exist a route r^* and satisfy the following condition:

$$u(r^*) < u(r) \quad \text{and} \quad r^*, r \in R(n, n_{\text{dest}}) \tag{5.7}$$

the vehicle will reroute to route r^*. $R(n, n_{\text{dest}})$ is a set of feasible routes from intersection n (the vehicle's current intersection) to intersection n_{dest} (the vehicle's destination intersection). Due to the dynamic nature of traffic and the relatively short simluation period, there is no guarate to achieve a dynamic user equilibrium for the network [104]. However, the rerouting process is a realistic representation of a short-term travel behaviour and a key feature to investigate the network traffic behaviour with repect to unexpected disruptions [105].

Figure 5.1 is an illustration of rerouting on a grid network, where the intersections are represented by nodes and the roads are represented by links. A vehicle needs to travel from node 1 to node 6 and has an initial route passes node 2 and 3. If traffic congestion occurs between node 2 and 3, the travel time of the initial route will increase. The rerouting algorithm will reroute the vehicle to another route with a shorter travel time.

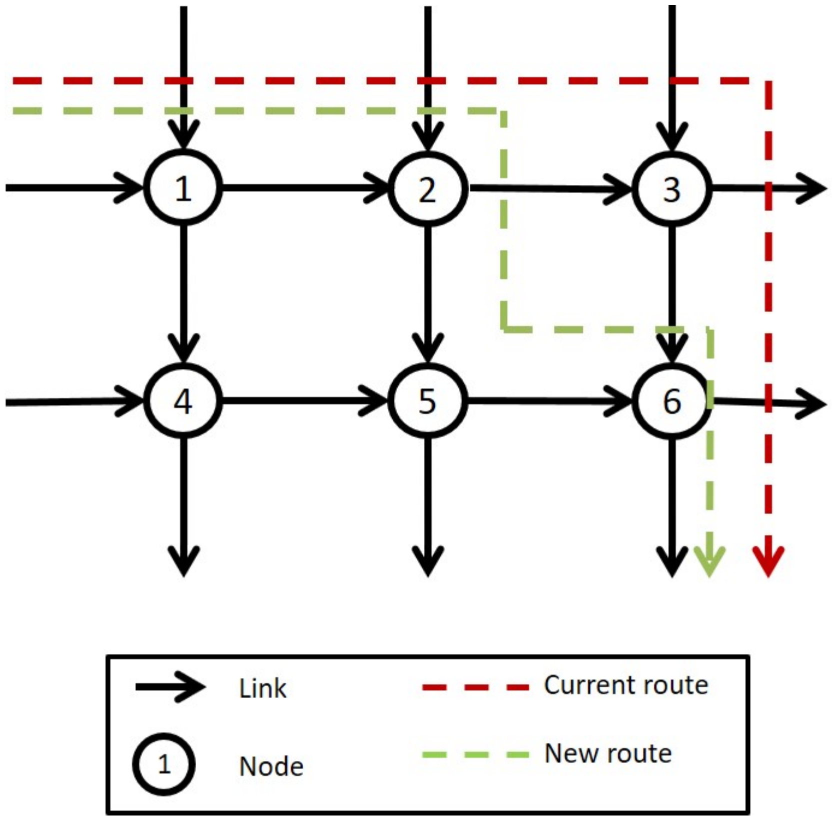

Figure 5.1: An illustration of rerouting on a road network

5.2.3 Converting CTM settings into SUMO

In order to use SUMO under the same settings as in the previous CTM test (chapter 4), parameters used in SUMO's safe-distance model are converted from the CTM. The CTM used free flow speed υ, jam density ρ_{jam} and saturation flow Q to describe traffic flow. The free flow speed υ in CTM is equivalent to vehicles' maximum speed in SUMO. By definition, the jam density ρ_{jam} stands for a maximum number of vehicle in a unit length of a road when traffic is jammed. In SUMO, there exists a minimum physical distance d_{min} between every two vehicles, so that the jam density ρ_{jam} can be expressed as:

$$\rho_{\text{jam}} = \frac{1}{d_{\text{min}} + \bar{l}^{\text{veh}}} \tag{5.8}$$

where $\bar{l}^{\text{veh}}$ is mean vehicle length. In terms of the saturation flow Q, it is the maximum number of vehicle passed a location in a unit of time. If the time for a vehicle to pass a location is $\frac{\bar{l}^{\text{veh}}}{v}$ and the time gap between every two vehicles is driver's reaction time τ, the saturation flow Q can be converted as:

$$Q = \frac{1}{\tau + \frac{\bar{l}^{\text{veh}}}{v}} \tag{5.9}$$

The jam density ρ_{jam}, saturation flow Q and free flow speed υ_{f} were set to be 230 vehicles per mile, 1800 vehicles per hour and 30 mph for CTM tests. Equivalently, the drivers' reaction time, minimum vehicle distance and vehicle length are set to 1.6 seconds, 2 metres and 5 metres. In addition, SUMO captures the individual movements of each vehicle. The acceleration and deceleration of vehicles are considered and are set to be 2.6 m^2/s and 4.5 m^2/s respectively.

In order to visualise the difference between the two flow models, the models are tested on a single intersection network where the network includes one signal controller and a single road. Only SUMO captures vehicles' acceleration and deceleration. In this case, two SUMO models are tested to compare with CTM, where one has acceleration and deceleration constraints (SUMO) and the other one does not have (SUMO (max)). Figure 5.2 and 5.3 show the cumulative arrival and departure

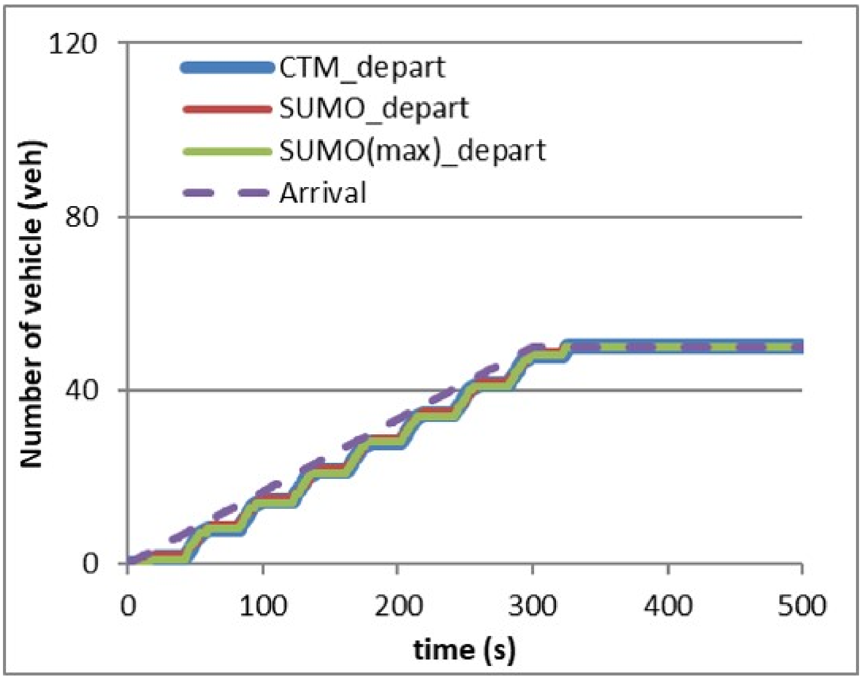

Figure 5.2: Arrival and departure curves of CTM and SUMO when undersaturated

curves of traffic in undersaturated and oversaturated scenarios. It can be seen that all flow models have the similar departure curves when traffic is less saturated. The default SUMO (with consideration of vehicles' acceleration and deceleration) has a steeper departure curve, which means there are less vehicles left the road every cycle. The acceleration constraint affects vehicles' departure. In CTM and SUMO (max), vehicles can accelerate to their maximum speed immediately when the traffic light turns to green. Figure 5.4 and 5.5 are the network delay results of this comparison test. The use of the acceleration constraint also lead to a higher network delay in the default SUMO.

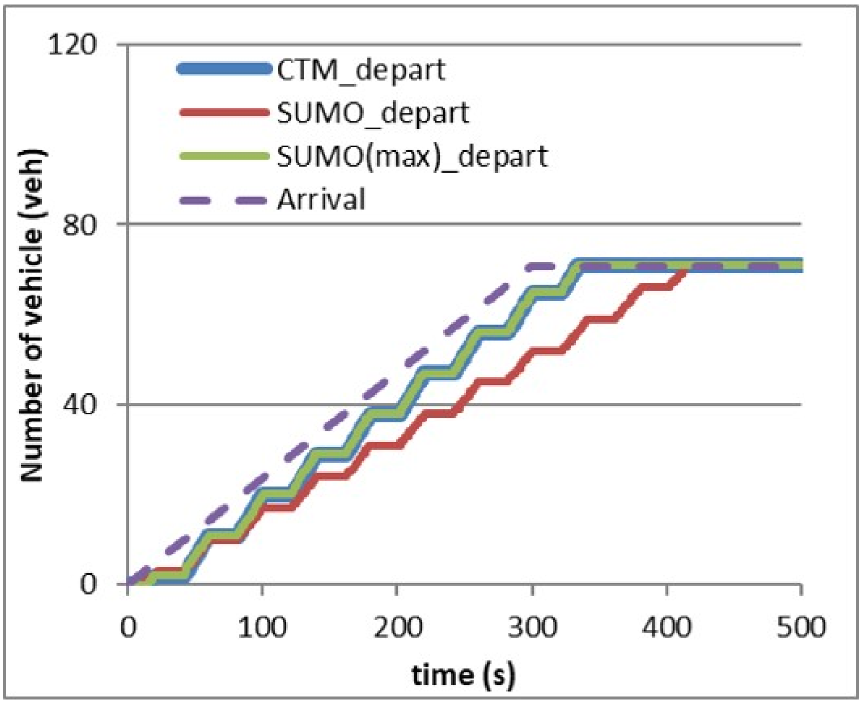

Figure 5.3: Arrival and departure curves of CTM and SUMO when oversaturated

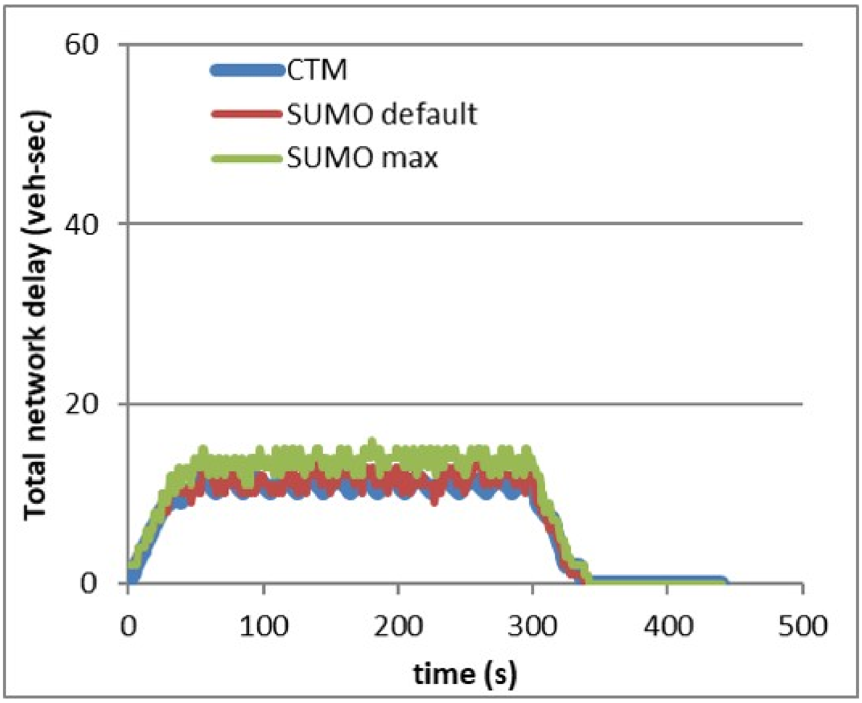

Figure 5.4: Network delay of CTM and SUMO when undersaturated

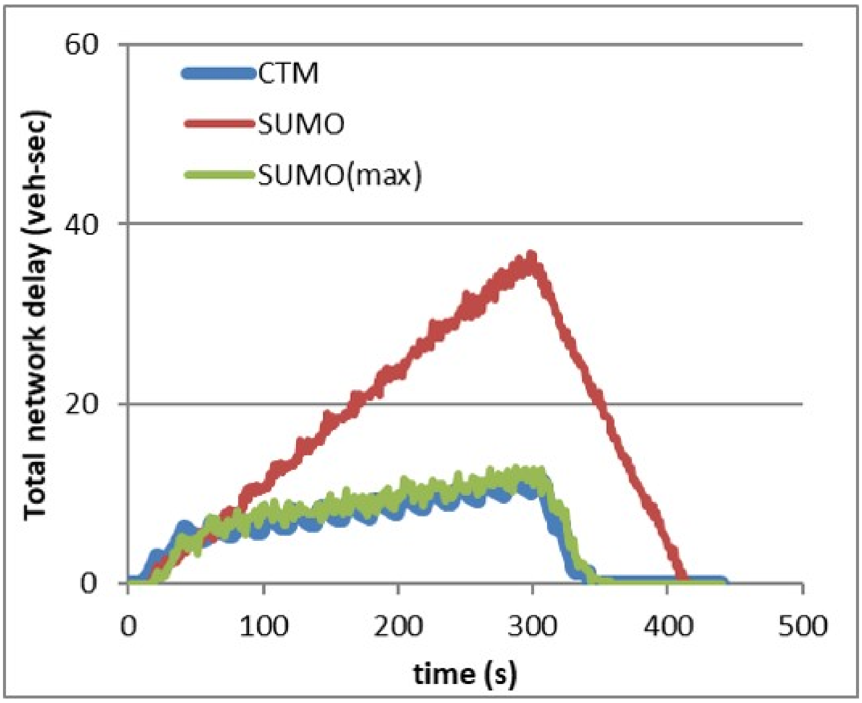

Figure 5.5: Network delay of CTM and SUMO when oversaturated

5.2.4 Implementation of traffic signals

Traffic light settings in SUMO can be initialised by the SUMO tools 'NETGENERATE' and 'NETCONVERT'. The properties of the traffic light consist of type (fixed or actuated), offset, duration of each phase, the status of phases, minimum green and maximum green. Predefined traffic lights are required before the simulation begins. In order to implement external control systems, Traffic Control Interface (TraCI) is used to establish the communication between external controllers and SUMO. TraCI has a client-server structure (see Figure 5.6), which can send the instruction from the controller (client) to SUMO (server) and receive the information back to the client from SUMO. Traffic status (such as mean speed of traffic, traffic count, and vehicle occupancy) from loop detectors in SUMO are available to be used by the external controller. The script of the external traffic controller can be written in many programming languages, such as Python, Matlab, Java and C++.

In this study, the traffic control systems are written in Matlab scripts and the control systems can interact with the signal controllers in SUMO through an interface TraCI4Matlab [106]. To calculate traffic signal plans, traffic status first needs to be taken from SUMO. Matlab commands "traci.edge.getLastStepVehicleNumber(Link(*i*).ID)" and "traci.edge.getLastStepOccupancy(Link(*i*).ID)" allow user to get real-time vehicle number and link occupancy at link *i*. With traffic status, the traffic signal plans are calculated on Matlab. An example of a SUMO signal plan is shown in Figure 5.7. The example is a signal plan of one signal cycle converted into SUMO's signal

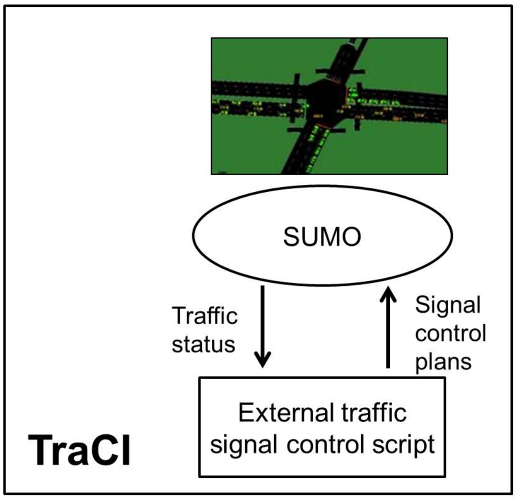

Figure 5.6: Traffic control interface of SUMO

plan. The signal plan has green light times 33 seconds for stage 1 and 37 seconds for stage 2. For each stage, there is a 7-second lost time. The signal plan converts into four phases in the SUMO format. Each phase has a light state, where ‘g’ stands for green light, ‘r’ is red light, ‘y’ means yellow light (vehicles will decelerate if they are approaching the signal, and the vehicle will pass if they are right at the signal’s location), and ‘u’ stands for amber light (vehicles will get ready for an upcoming green light). The traffic light states in the example contain four settings per phase. This is because there are four controlled links at this example intersection. After the signal plans (e.g. green split and offset) are determined on Matlab, the signal plans can be sent to SUMO by using command “traci.trafficlights.setPhase(TrafficLight.ID, Phase.ID)” and “traci.trafficlights.setPhaseDuration(TrafficLight.ID,Duration)”. “traci.trafficlights.setPhase” switches the traffic light to a certain phase of a controller and “traci.trafficlights.setPhaseDuration” sets the duration of the current phase.

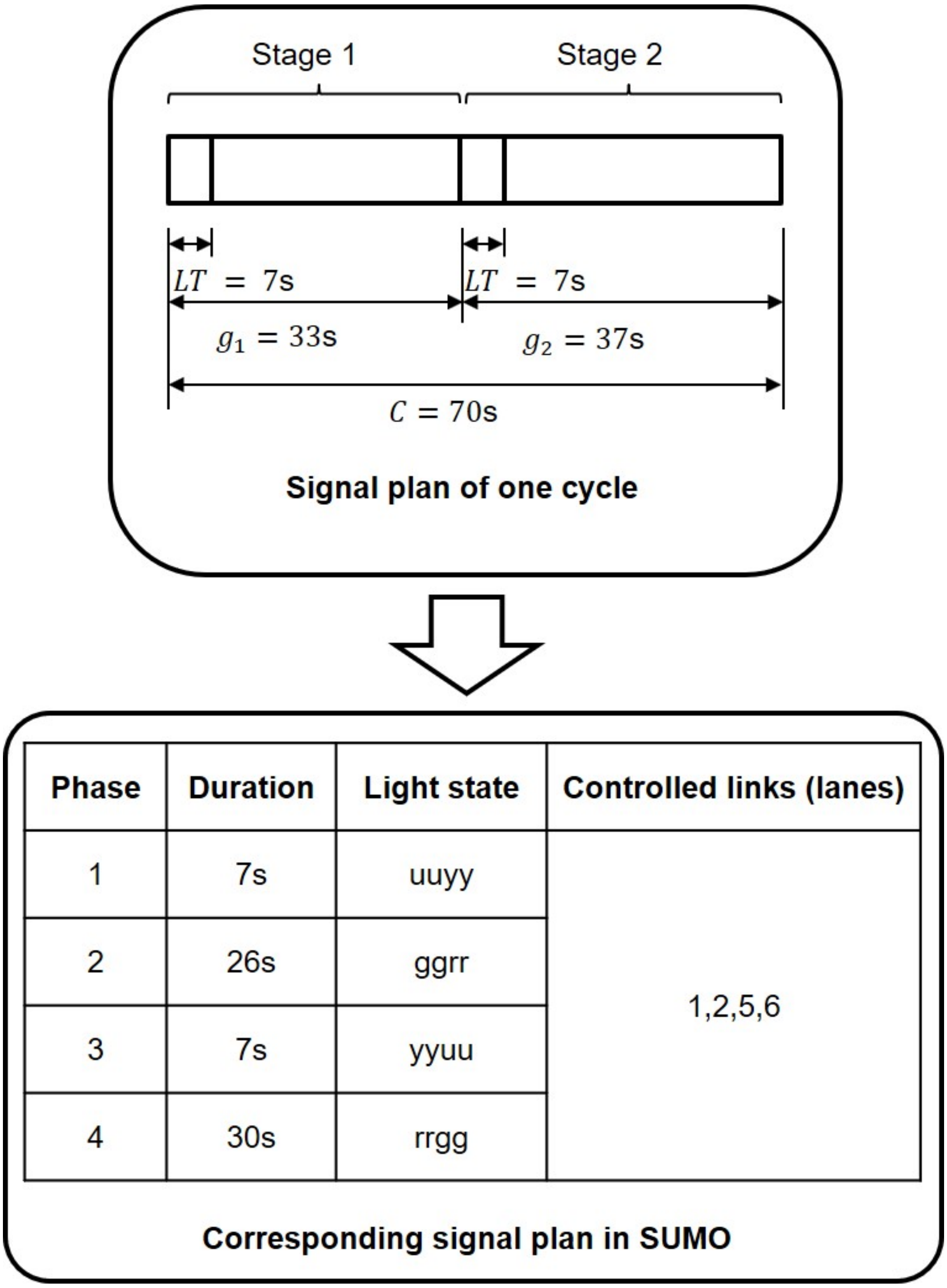

Phase	Duration	Light state	Controlled links (lanes)
1	7s	uuyy	1,2,5,6
2	26s	ggrr	
3	7s	yyuu	
4	30s	rrgg	

Figure 5.7: An example of the signal plan in SUMO

5.3 One-way arterial network

5.3.1 Network configurations

The control systems performance was first evaluated under different traffic saturation levels on a one-way arterial network, as shown in Figure 5.8.The network contained three signalised intersections and ten roads. The distance between each of the two intersections is 0.16 km. The intersections are represented by nodes and the roads are represented by links. The traffic dynamics model used in SUMO is the default Krauss' safe-distance flow model (see Section 5.2.1). The test time horizon T was set to 3600 time steps and a time step Δt was set to 1 second.

To describe saturation level, the parameter γ is used to represent demand-capacity ratio (see the definition in Section 4.2.1). In one-way arterial network, there is one horizontal street and three vertical (cross) streets. The demand on the horizontal street $\Lambda_x(t)$ and the vertical streets $\Lambda_y(t)$ were defined as follows:

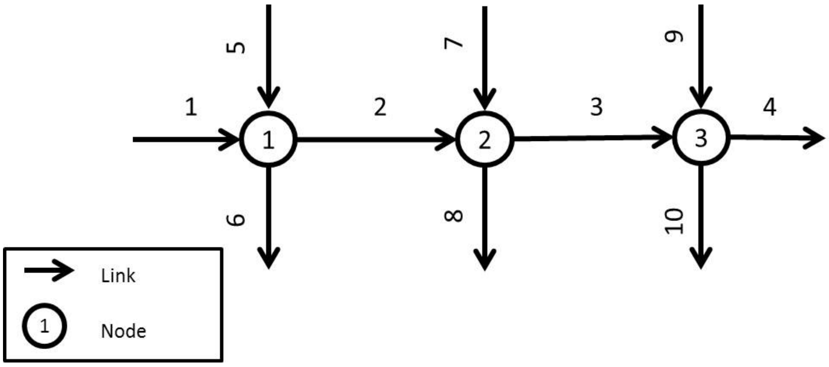

Figure 5.8: Test one-way arterial network used in SUMO

$$\Lambda_x(t) = \begin{cases} 0.6\lambda, & 0 \leq t \leq 720 \\ 0, & t > 720 \end{cases} \tag{5.10}$$

$$\Lambda_y(t) = \begin{cases} 0.4\lambda, & 0 \leq t \leq 720 \\ 0, & t > 720 \end{cases} \tag{5.11}$$

where λ is a parameter (with unit: [veh/hr]) adjusting the traffic saturation level according to γ. The horizontal street is considered as a main street, so it has higher demand than the vertical side streets. The period after time step 720 is a cooling period when no further traffic will be loaded into the network. The cooling period ensures that all vehicles leave the network by the end of the test, so that a fair comparison can be made between different control systems. With the same level of traffic, there exist different traffic spatial distributions.

A parameter σ is introduced here to create the spatial variability that would be seen in the real world. Naturally, traffic is not evenly distributed on a network; the distribution is determined by the origin, destination and route taken by each vehicle. If $\sigma = 0.3$, it means 70% of traffic would go straight through the network, whereas the remaining 30% are randomly assigned to other destinations. For this one-way arterial network test, the random distributed traffic is set to 30% ($\sigma = 0.3$), and 20 Monte Carlo simulations are carried out with different traffic spatial distributions.

5.3.2 Settings of the test control systems

In terms of the traffic control systems, there are some predefined settings for the comparison test. The test chosen four control systems: TUC system (TUC), decentralised TUC system (TUC_D), cyclic max-pressure controller (MP_C) and acyclic max-pressure controller (MP). In previous Chapter 4, offset has been found as a cause to create performance differences between centralised and decentralised systems. For fair comparison in this test, all the cyclic systems are using the same offset control (Gazis offset controller). In this case, the difference between the systems are mainly from the split control, so that the TUC system is a centralised control where the other systems are decentralised. The Hybrid system mentioned in chapter 3 has not been chosen to test on SUMO. The hybrid system only outperform the TUC system when γ is low, otherwise, it has similar performance with the TUC (according to the CTM test results in chapter 4). The TUC system derives centralised green split, where cyclic and acyclic max-pressure derive decentralised green split. The decentralised TUC system is a modified TUC system using as a reference in the test. The green splits of the decentralised TUC are derived separately for each node, so that the decentralised TUC has individual $\mathbf{L}$ matrices for each node. The original TUC only has a single $\mathbf{L}$ matrix for the entire network (see Section 3.3.1). TUC, decentralised TUC and cyclic max-pressure controller are cyclic control, and their signal timing plans consist of cycle time, offset and green split. The three cyclic control systems are using the same decentralised offset controller for comparison purpose, hence, the cycle time used for each node is the same as well. The cycle time was examined over different traffic saturation levels and control systems on the one-way arterial network. The optimal values of cycle time are found as follows: 40s ($\gamma = 0.3$), 50s ($\gamma = 0.5$), 70s ($\gamma = 0.7$), 90s ($\gamma = 0.9$). Conversely, the acyclic MP does not use cycle time, but it has a minimum stage constraint (25 seconds) and a maximum stage constraint (120 seconds). This is to ensure traffic in all directions will be served and to not create an unreasonable long waiting time for drivers. In addition, 5 seconds lost time is considered for both cyclic and acyclic control systems to mimic switching signals in real life operation. The computer used for the test in this chapter has Intel i5-4370 CPU 3.2GHz and 8 GB RAM.The software used to program the test is Matlab 2013b.

5.3.3 Performance criteria

Network delay is the criterion used to examine the performance of the different control systems on SUMO. In the previous CTM tests (in chapter 4), the network delay is the difference between actual vehicle hours travelled and the vehicle hours travelled under free flow speed. SUMO models the movements of each individual vehicle instead of the flow of a group of vehicles in CTM. The network delay at one time step t is calculated as:

$$TND(t) = \begin{cases} \sum_{i \in \mathbf{I}} 1 - v_i(t)/v_{\max}(t), & d < d_{\text{crit}} \\ \\ 0, & d \geq d_{\text{crit}} \end{cases} \tag{5.12}$$

where $v_i(t)$ is the travel speed of vehicle i at time step t. d_{crit} is the critical distance between two continuous vehicles, and its value is converted from the critical density ρ_{crit} used in CTM.

Bandwidth is another criteria to see how traffic control systems are performed. Efficient coordination between signal controllers can help a platoon of vehicles to travel through them without stopping. The movement of this platoon of vehicles under a time-space diagram will be visualised as a pair of speed lines (see Figure 5.9), the band formed by these two speed lines is called green band. The width of the green band is bandwidth, and it indicates the portion of a time period over a signal cycle that the traffic can travel within the green band. When calculating the bandwidth of a route, the signal plans of controllers along the route are compared against the speed lines (see Figure 5.9). The speed lines can also be understood as vehicles' trajectory under free flow speed. However, the part of a bandwidth is excluded when there exists residual queues along the route.

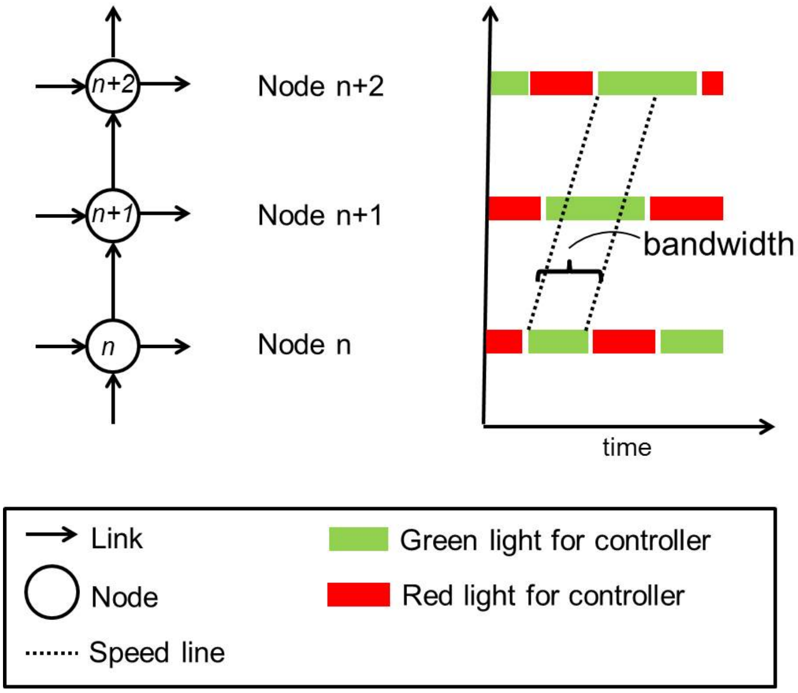

Figure 5.9: An example of a green band formed on an arterial network

5.3.4 Test results

The average network delay of the 20 different traffic distributions are plotted against demand levels γ in Figure 5.10. Both traffic modelling and signal optimisation are carried out on a standard quad-core Windows 7 (64-bit) computer. Centralised TUC outperforms all the decentralised control systems over different γ, which is the same as the results in Chapter 4. This is expected since the centralised TUC has taken the demand distribution (through turning ratio ζ) and the network topology into consideration when calculate the green split. With these network-wide information, the TUC system can recognise the links and nodes which are likely to be congested, and can derive a timing plan which minimise the total network delay. In terms of decentralised control systems, the TUC_D and MP_C perform similarly since they both are queue-based control systems and use the same external offset controller. The perfromances of the two control systems can differ in a spill over scenario, however, this one-dimensional network has not observed a significant spill over in traffic queues. The acyclic MP performs the worst in the decentralised systems. According to [8] and [6], MP has been proved that can stabilise the queue length when demand is in a feasible range. Meanwhile, the MP control is not designed for minimising the network delay.

In this one-way arterial network, the average bandwidth of the horizontal main street is calculated and the results are in Figure 5.11. The centralised TUC creates widest bandwidth on the main street. This is not only an intuitive observation, but the TUC 's centralised green split did helped the offset control in previous study [107]. When calculating the green split, TUC priorities the routes which have more traffic and allocates longer green split. With the longer green split on a route, it will form a wider bandwidth. The bandwidth created by the TUC_D and cyclic MP are similar. Both TUC_D and MP_C are operated under the same offset controller and cyclic feature. Comparing to the cyclic systems, the acyclic MP has the narrowest bandwidth. Different from the control systems which tended to group vehicles together and maximise traffic flow, acyclic MP aims to stabilise the queue distribution instead of minimise the network delay. The narrow bandwidth formed in acyclic MP also explained why it is not performed well on the network delay.

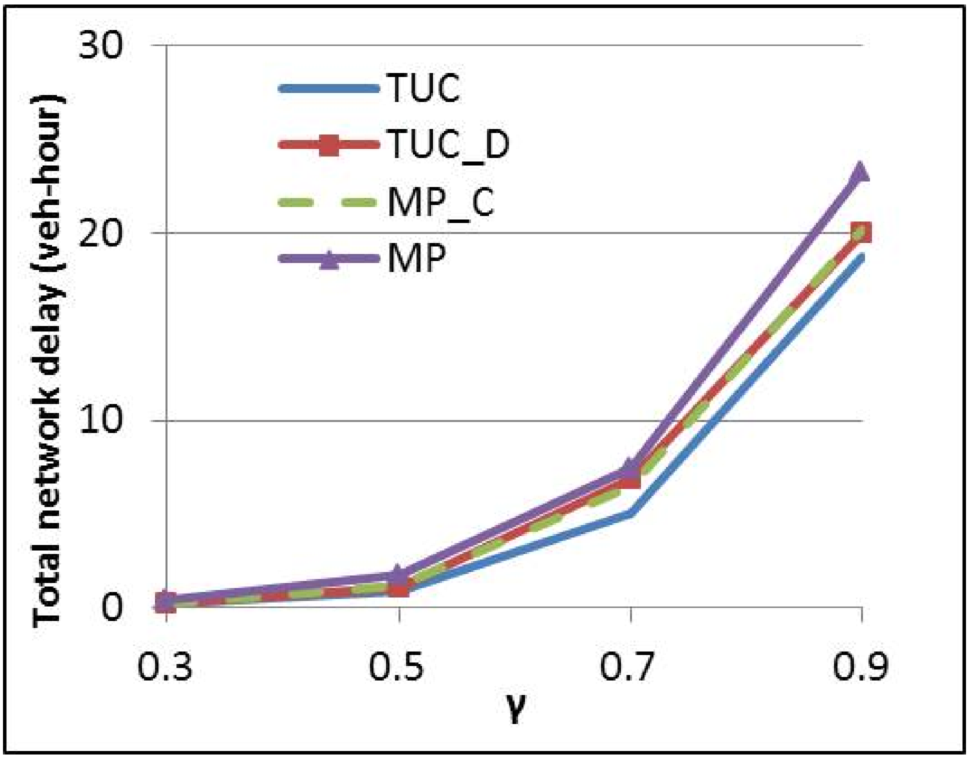

Figure 5.10: Average network delay of the one-way arterial network over γ

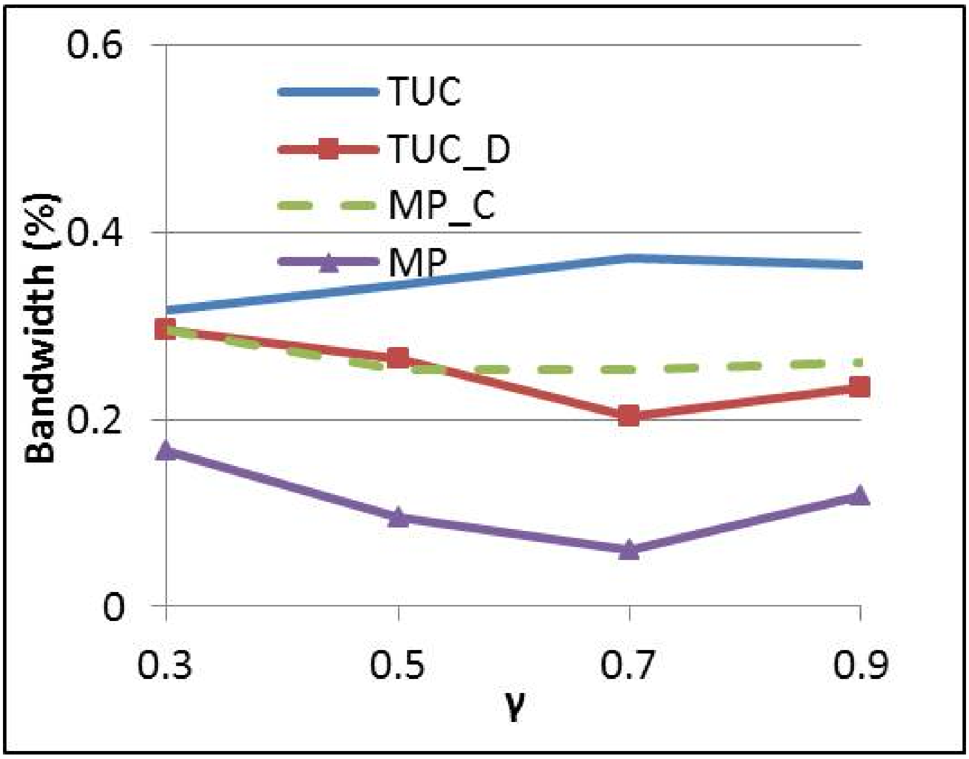

Figure 5.11: Average green bandwidth of the one-way arterial network over γ

5.4 Grid network

5.4.1 Test under different traffic saturation levels

The control systems are further tested on a two-dimensional network: three by three grid network (see Figure 5.12). With the two-dimensional network, signal control at nodes becomes more complex and traffic route choice becomes more flexible. The length of each link is 0.16 km, which is as same as the previous one-way arterial network. Under the same traffic demand on horizontal and vertical roads as in Equation 5.10 and 5.11, the control systems are tested against four saturation levels: $\gamma =$ 0.3, 0.5, 0.7 and 0.9. Figure 5.13 shows the average network delay of each control system under different γ without rerouting. The average network delay is the result from Monte Carlos simulations with $\sigma = 0.3$. The derived optimal cycle times are: 40 ($\gamma = 0.3$), 50 ($\gamma = 0.5$), 70 ($\gamma = 0.7$), 120 ($\gamma = 0.9$).

Similar to the results of one-way arterial network, the centralised TUC outperforms all of the decentralised control systems over different γ. The difference between centralised and decentralised systems becomes obvious when traffic becomes more saturated ($\gamma = 0.7$ and 0.9). Comparing the performance between decentralised control systems, acyclic MP does not perform as well as the cyclic ones. These are similar to what was shown in the one-way arterial network's result. In terms of the average bandwidth, the bandwidth is the average of the three horizontal and vertical roads of the network. Figure 5.14 shows the average bandwidth of the control systems formed in the test. Apart from the centralised TUC achieving the widest bandwidth, the bandwidth formed in all cyclic control systems reached 30% when network is fully saturated ($\gamma = 0.9$). In this case, the performance difference between centralised and decentralised control systems is not clear to see from the average bandwidth. Figure 5.15 is further plotted to show the average queue length formed at each node when $\gamma = 0.9$ over the test period. The centralised TUC has less of a queue at node 1 and 4, but a longer queue at node 2 and 3. This means centralised TUC allowed more traffic to travel through the node 1 to its downstream compared to the decentralised systems. The nodes 1,4,7 are the boundary nodes, where traffic flows into the network. Controlling traffic properly at those boundary nodes directly affects how the downstream nodes perform. So the performance difference between centralised and decentralised control systems is due to the same reason as in the one-dimensional network test. The centralised control can minimise the entire network delay, when it holds accurate traffic information through the network.

In order to capture drivers' response to the real-time traffic condition, a dynamic rerouting algorithm (see Section 5.2.2) is implemented on the three by three grid network. Figure 5.16 is the network delay of different control systems over γ where rerouting is allowed. The results are the average of 20 Monte Carlo simulations when $\sigma = 0.3$. The traffic saturation levels and distributions are the same as the test without rerouting. All decentralised control systems have significant reduction in network delays, but not the centralised TUC. The centralised TUC has predefined settings ($\mathbf{L}$ matrix and nominal green split $\mathbf{g}^N$). They prioritise some more congested routes and remain unchanged through the test. This could be one reason that the centralised TUC has not improved much after rerouting. Decentralised systems can not prioritise any routes but only links at each node. Therefore, they are more adaptive to the changes in traffic distribution caused by rerouting. Comparing the decentralised systems, acyclic MP has the highest improvement in delay. It outperforms the centralised TUC at $\gamma = 0.5$ and 0.7. Decentralised TUC and cyclic MP are slightly worse than centralised TUC in performance, but both are more efficient than the case without rerouting. Figure 5.17 is the average bandwidth measured from the three horizontal roads and vertical roads. The centralised TUC still has the widest bandwidth and acyclic MP has the narrowest. However, acyclic MP's bandwidth slightly increased compared to the result without rerouting. The average queue length of each control system is plotted in Figure 5.18 for $\gamma = 0.9$. Clearly, the decentralised control system reduced queue at boundary nodes, where the centralised control system has a similar queue length as before. The rerouting results here show that there can be a great impact on the performance of decentralised control system by allowing traffic to reroute.

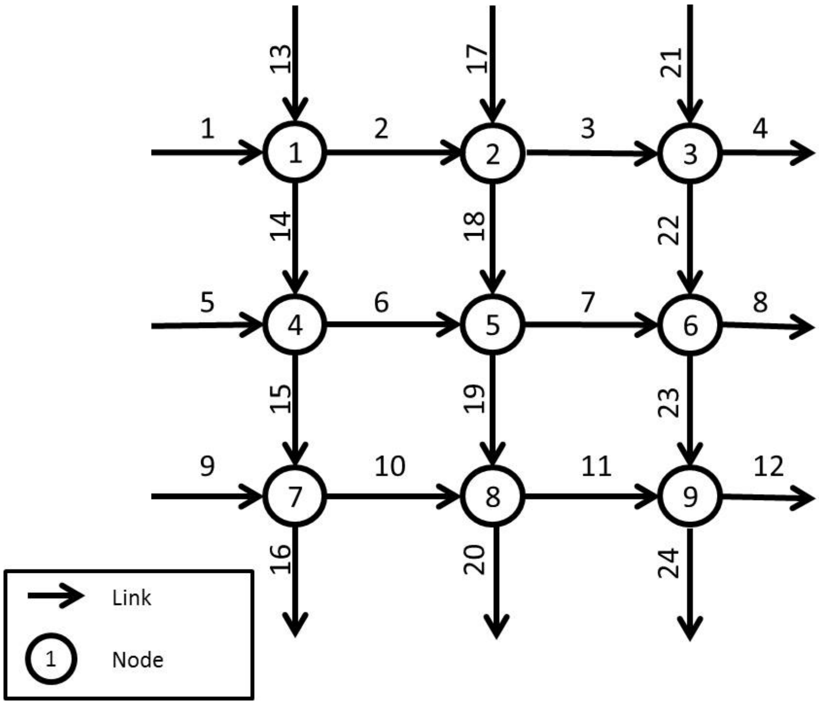

Figure 5.12: Test three by three grid network used in SUMO

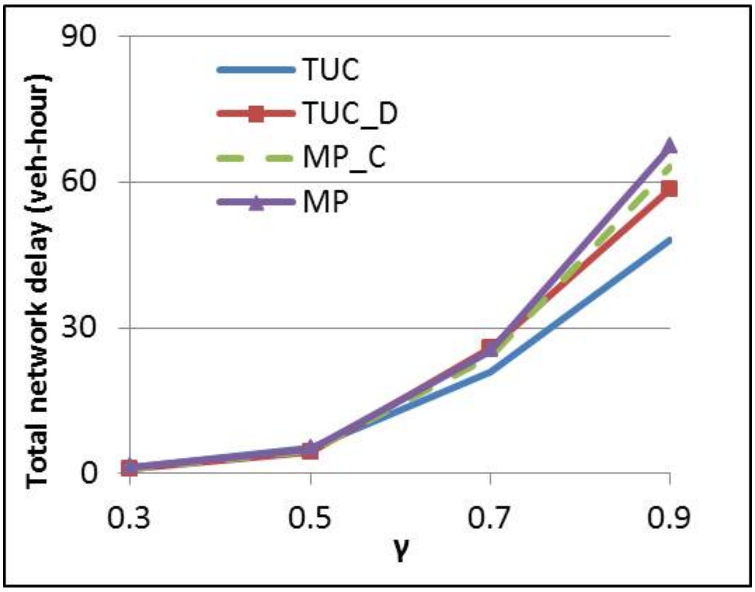

Figure 5.13: Average network delay of the three by three grid network over γ without rerouting

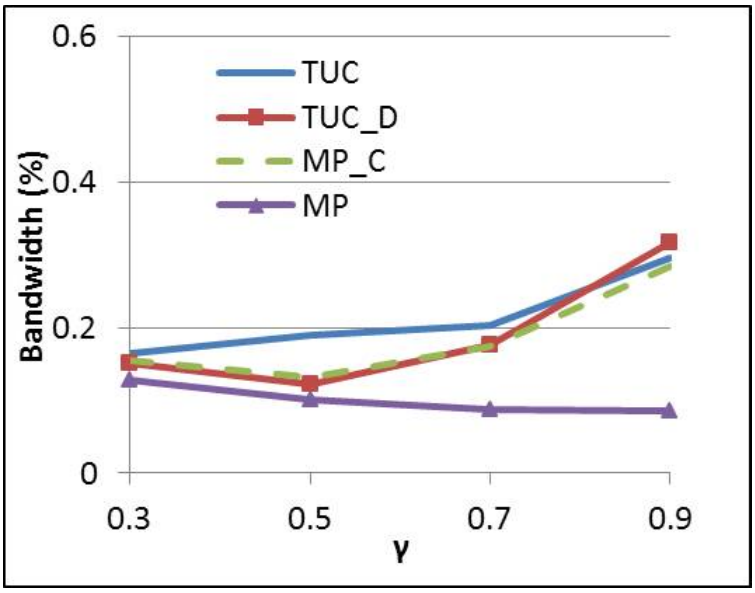

Figure 5.14: Average green bandwidth of the three by three grid network over γ without rerouting

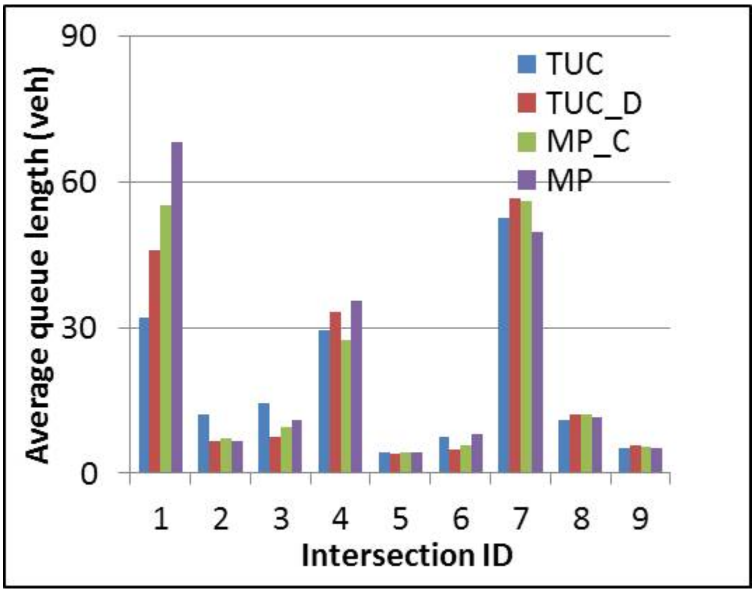

Figure 5.15: Average queue length at intersections of the three by three grid network ($\gamma = 0.9$, $\sigma = 0.3$ without rerouting)

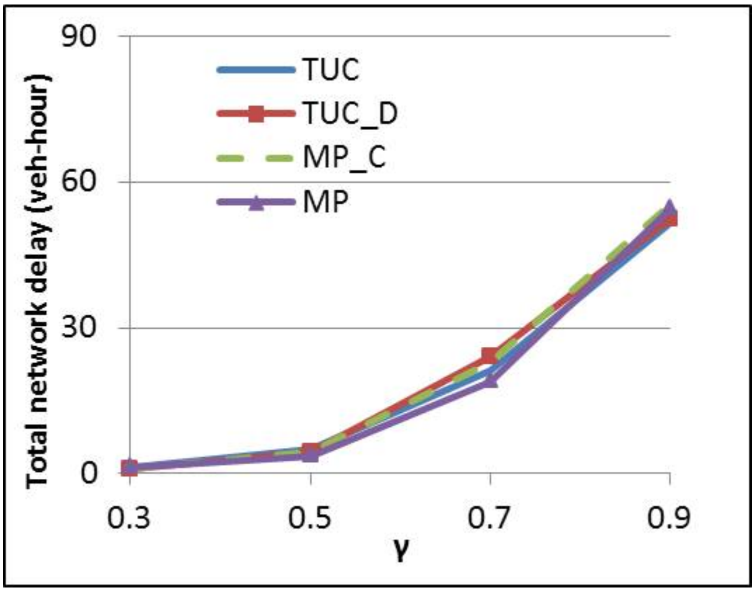

Figure 5.16: Average network delay of the three by three grid network over γ with rerouting

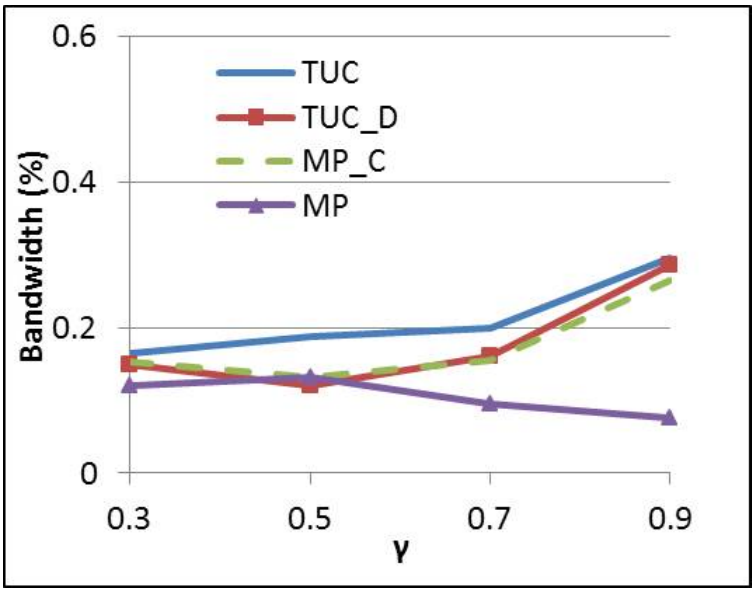

Figure 5.17: Average green bandwidth of the three by three grid network over γ with rerouting

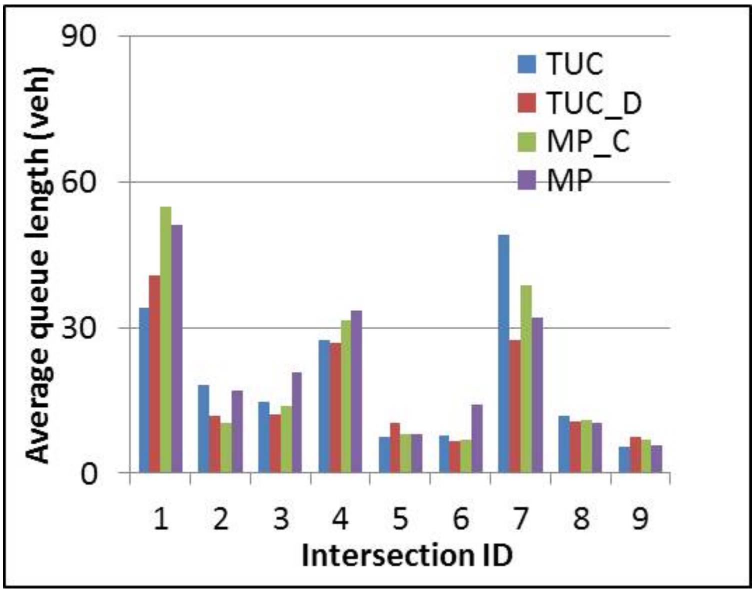

Figure 5.18: Average queue length at intersections of the three by three grid network ($\gamma = 0.9$, $\sigma = 0.3$ with rerouting)

5.4.2 Test under different traffic spatial distributions

In order to investigate further on how rerouting affects centralised and decentralised control systems' performance, the control systems were tested over different traffic spatial distributions by using three sigma values: σ = 0.3, 0.6, 0.9. The test was carried out on the same three by three grid network, where the saturation level $\gamma = 0.7$. According to the definition of σ in Section 5.3.1, $(1-\sigma)$ is the portion of traffic travel straight through the network and the remaining traffic is randomly assigned with other destinations. Figure 5.19 shows the average network delay of Monte Carlo simulation under different sigma values without rerouting. Centralised TUC has the best performance over different σ values. The acyclic MP outperforms cyclic MP and decentralised TUC when σ increases. This means that the acyclic decentralised MP can adapt to different distributed traffic better than the cyclic decentralised systems. When rerouting is allowed (see Figure 5.22), all the decentralised systems have obvious improvements in their network delay. The impact of rerouting on the centralised TUC is not significant, which may due to the predefined settings. Acyclic MP can outperform centralised when σ are non-zero values.

In terms of the bandwidth (see Figure 5.20 and 5.23), centralised TUC formed a lower bandwidth when sigma value increased. As the average bandwidth measured from the horizontal and vertical roads, it represents the bandwidth formed for the traffic travelling straight through the network. By definition of the σ, $(1-\sigma)$ of the traffic will benefit from the straight green bandwidth. However, the higher σ is, the less traffic will travel straight through the network. Decentralised TUC and cyclic

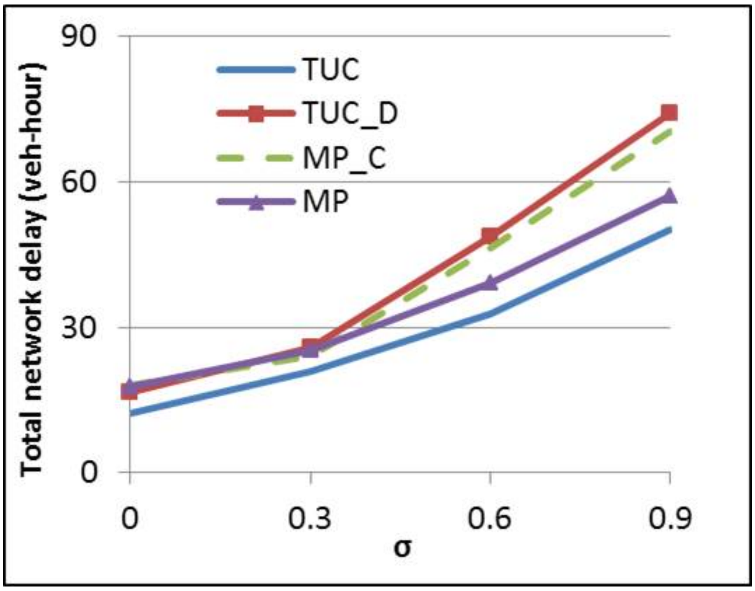

Figure 5.19: Average network delay of the three by three grid network over σ without rerouting

MP formed unnecessary high bandwidth on the straight routes when rerouting is not allowed.

The average queue of the network nodes are showed in Figure 5.21 and 5.24 for $\sigma = 0.7$. The centralised TUC maximised the traffic flows at node 1 and 4 and limited node 7 to minimise the queue from a network view. When rerouting is allowed, centralised TUC does not have much change in the queue through the network. However, acyclic MP have a more evenly distributed queue at each node.

Overall, the test of control systems over different sigma values emphasised the improvement of decentralised systems from rerouting, and also could help to achieve more balanced traffic spatial distribution.

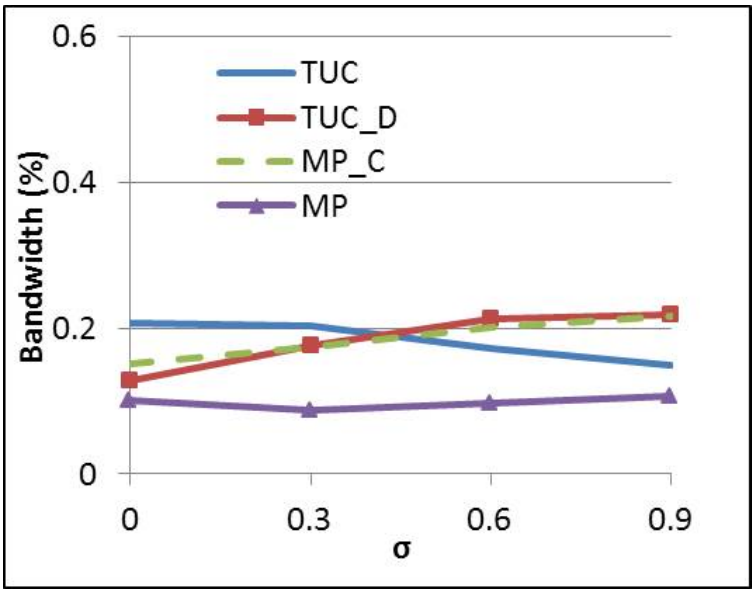

Figure 5.20: Average green bandwidth of the three by three grid network over σ without rerouting

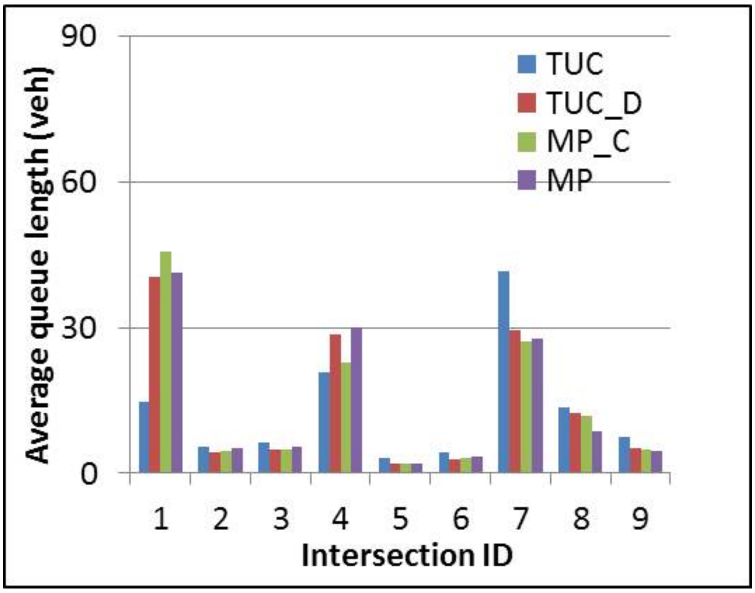

Figure 5.21: Average queue length at intersections of the three by three grid network ($\gamma = 0.7$, $\sigma = 0.7$ without rerouting)

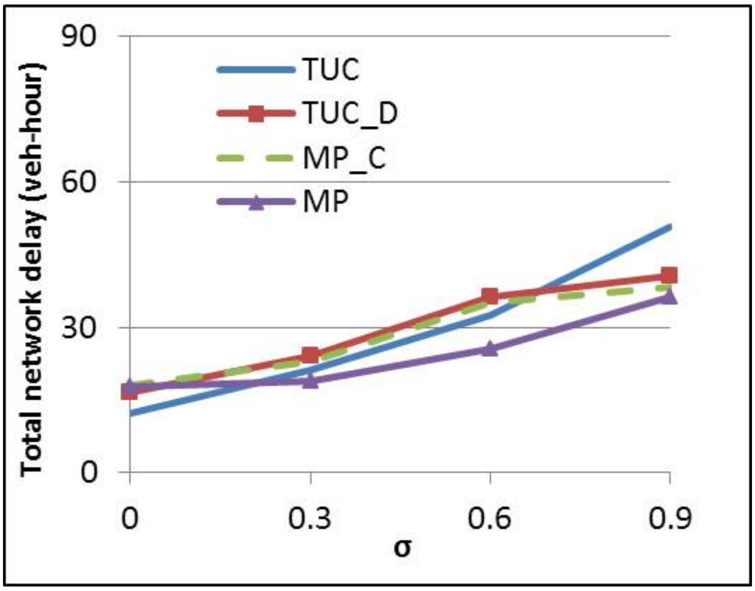

Figure 5.22: Average network delay of the three by three grid network over σ with rerouting

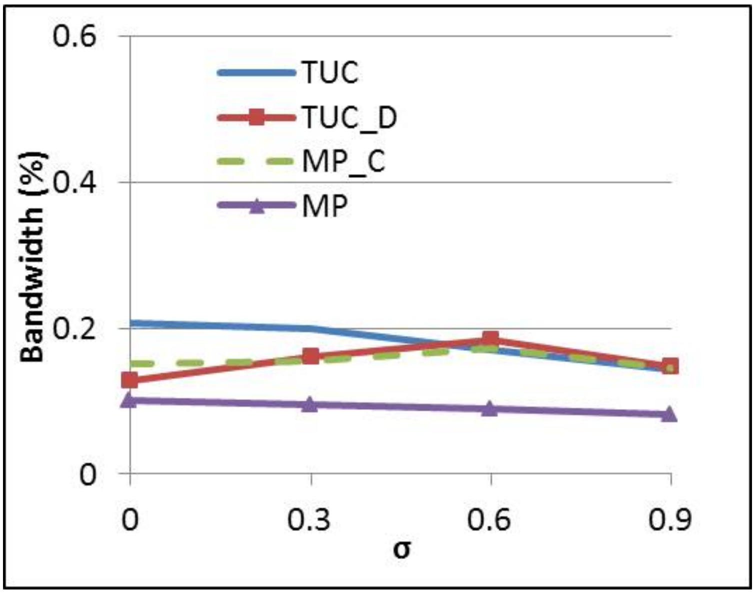

Figure 5.23: Average green bandwidth of the three by three grid network over σ with rerouting

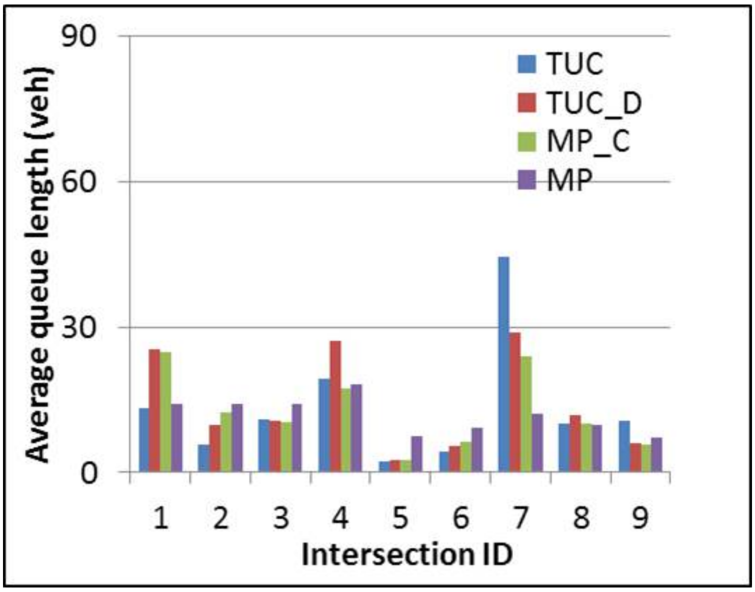

Figure 5.24: Average queue length at intersections of the three by three grid network ($\gamma = 0.7$, $\sigma = 0.7$ with rerouting)

5.4.3 Test on rerouting compliance rate

As rerouting has a great impact on decentralised control systems, the performance of control systems were examined under different rerouting compliance rate. As in a real life scenario, drivers are not always rerouting according to the live traffic conditions. They may stay with the original planned route for many reasons, such as, the driver does not know the alternative routes or the driver is not in a rush to go to the destination. In the following tests, compliance rate equals to 0% means no driver will reroute while 100% means all drivers will reroute respect to traffic conditions. The tests are carried out on the same three by three gird network, where $\gamma = 0.7$ and $\sigma = 0.3, 0.6, 0.9$. The network delay results are showed in Figure 5.25,5.26 and 5.27. The network delays of the decentralised systems are all reduced with the increase of rerouting compliance rate, while the centralised TUC stays steady. When rerouting is not allowed, the centralised TUC outperformed the decentralised systems in the previous sections (e.g. Section 5.3.4). The centralised TUC prioritises the critical parts of the network, which was recognised through the network topology and demand distribution.For example, when the TUC system derives the control gain **L** matrix, the **B** matrix is calculated by considering the road connections in the network. This advantage of the centralised control reduced when drivers are allowed to reroute according to traffic conditions. The distribution of the traffic may not be consistent with the one recognised in TUC. This can explain why TUC's performance slightly dropped in Figure 5.27. In addition, the acyclic MP controlled traffic has a similar response to the rerouting compliance rate under different sigma values. When rerouting compliance rate is 100%, all the network delays of acyclic

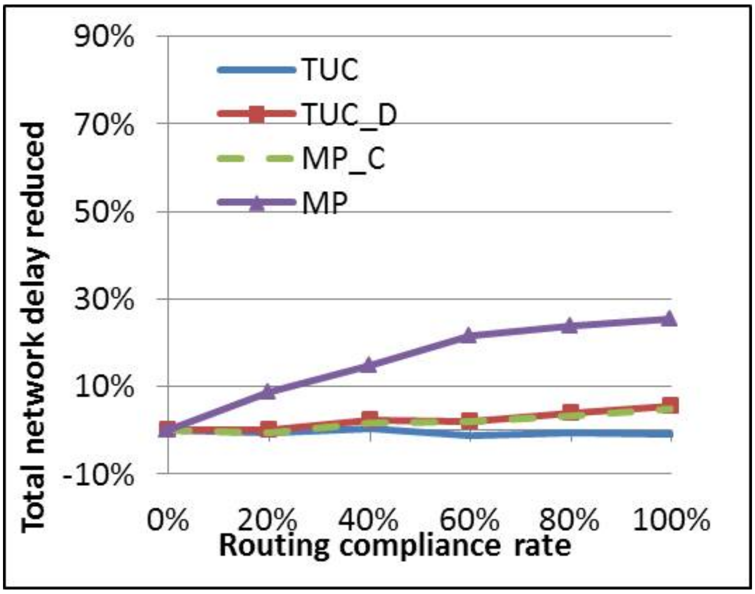

Figure 5.25: Average network delay of the three by three grid network over different rerouting compliance rate $\sigma = 0.3$

MP have improved around 30%. The impact of the rerouting compliance rate in cyclic MP and decentralised TUC largely depend on σ. When σ is low, there is a very limited improvement which can be achieved by rerouting and vice versa.

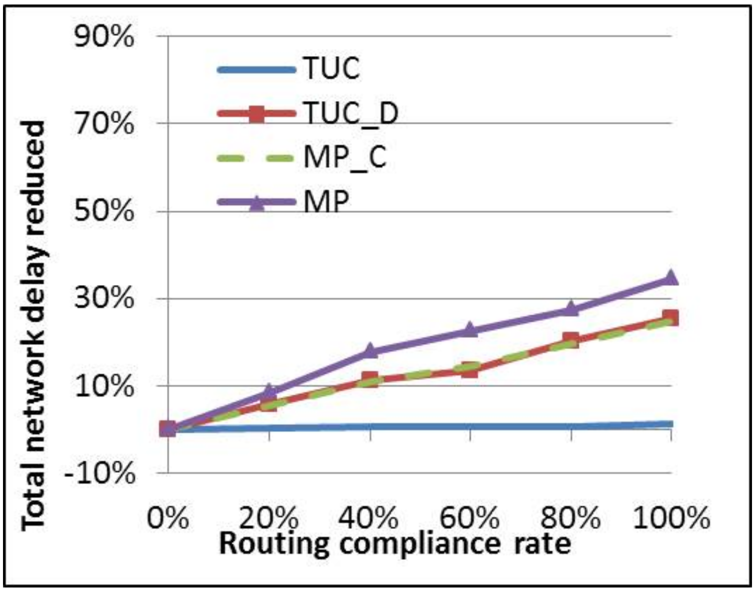

Figure 5.26: Average network delay of the three by three grid network over different rerouting compliance rate $\sigma = 0.6$

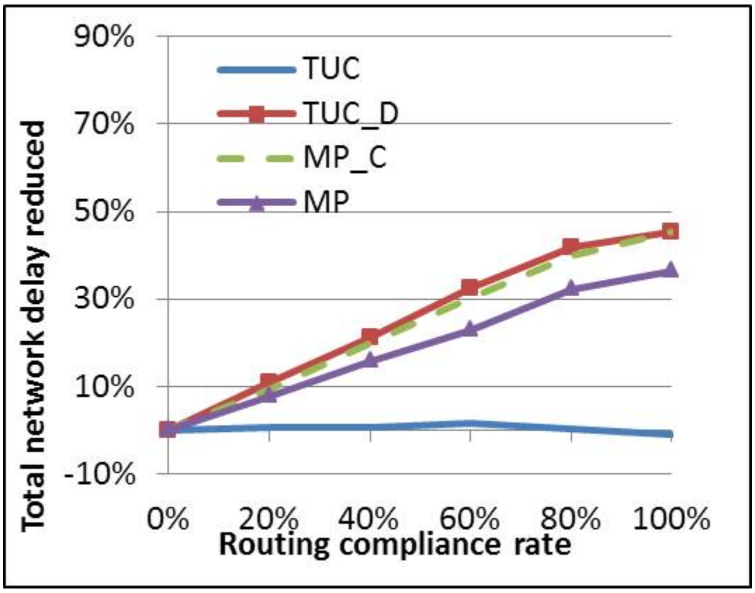

Figure 5.27: Average network delay of the three by three grid network over different rerouting compliance rate $\sigma = 0.9$

5.4.4 Test on a road incident scenario

Both centralised and decentralised control systems are tested on a five by five grid network (see Figure 5.28) with a road incident scenario. Unexpected events can occur on a road network and restrict traffic flow. The aim was to establish how the change of the network structure (road blockage) influences the control systems. The test saturation level γ is set to 0.7 and the spatial distribution parameter σ is set to 0.3. The horizontal roads are the main streets and the vertical roads are the side streets. The demand ratio between main street and side street is 3 : 2. The incident happened at node 19 (highlighted in Figure 5.28) and both link 22 and link 52 were out of service. The choose of the incident location considers its blockage impact on the upstream links and nodes. If the location is too close to the upstream nodes (e.g. node 1,2,6), the traffic will only spill over to the source links and will not affect other network links. The control systems were tested with different incident durations: 4, 8, 12, 16, 20 and 24 minutes. Figure 5.29 and 5.30 are the network delay results under different incident durations. All the control systems' performance deteriorate with the increase in incident duration. Without rerouting, the centralised TUC outperform all the decentralised systems. This is similiar to the findings in [105], which suggested the centralisation and coordination between signal controllers are important for restoring the network performance after disruptions. Decentralised systems could end up with inefficiency and even chaos [105]. However, rerouting improves the performance of all decentralised control systems which is the same as the results from the previous tests (section 5.4.1 and 5.4.2). Acyclic MP has the highest improvement under rerouting and outperforms the centralised TUC. The acyclic MP is the most flexible control system in the test, and this flexibility shows its value when restoring the system performance in a incident event. The acyclic MP here brings new insight on design control system for system resilience management.

In terms of the green bandwidth, the average bandwidth is measured from the straight routes of the network and is plotted in Figure 5.31 and 5.32). Two straight routes, which were blocked by the incident, are excluded in the bandwidth measurement. When rerouting is not allowed, the centralised TUC has a bandwidth around 7% per cycle time and the remaining decentralised control systems' bandwidths are around 5%. This is due to the centralised signal setting prioritised the straight routes, so that most of the traffic still travelled on the straight routes after rerouting. On the other hand, there is less green bandwidth formed on the straight routes under the decentralised systems. The traffic under decentralised systems has changed demand distribution with rerouting, and less vehicles travelled straight after rerouting.

In order to visualise how queue distribution changed after a road incident happened, change in network queues is plotted against distance to the incident's location in Figure 5.33 and 5.34. The x-axis represents the distance from the incident location, and the unit is the number of links. All the upstream nodes of the incident are grouped by their distance to it, so that the y-axis is the average change in queues for each distance group. The change in queue is a ratio of average queue length at 12 minutes blockage case to the no incident case. The change in queue mainly happened on the nodes which are one or two links away from the incident. The centralised TUC has

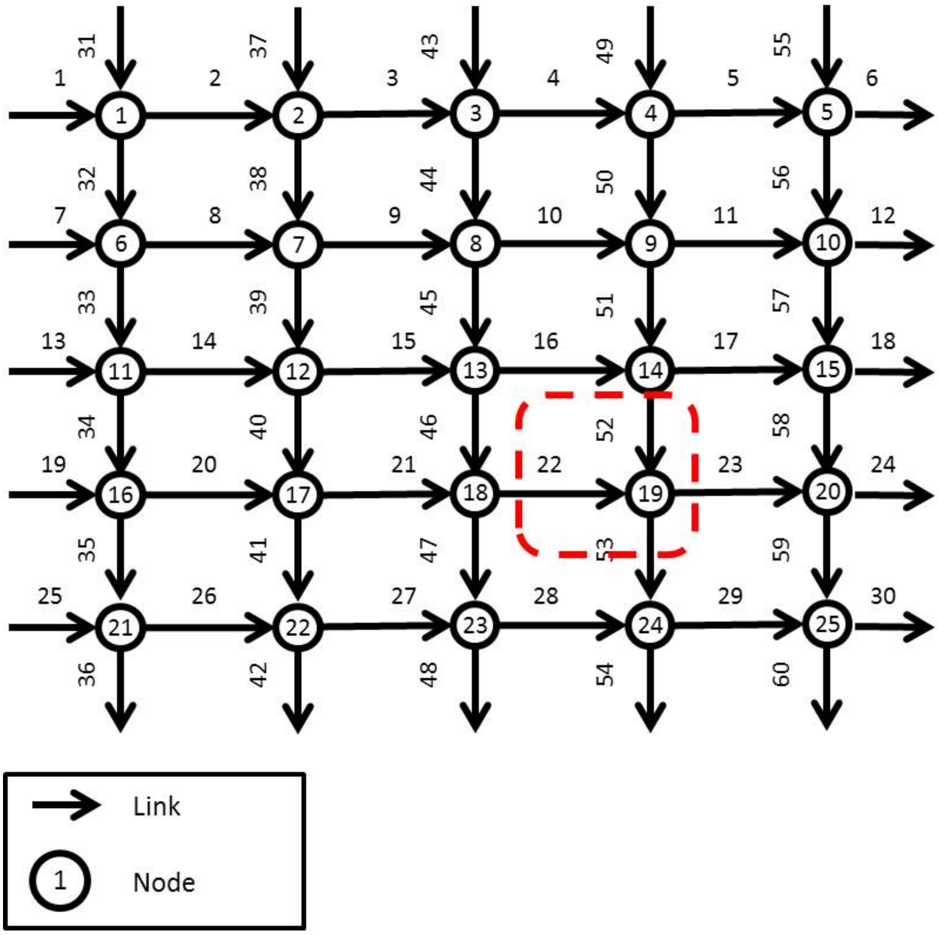

Figure 5.28: Test five by five grid network

a queue change mainly at the nodes directly next to the incident. The decentralised control systems have queue changes at the nodes which are one and two links away from the incident. When rerouting is allowed, all the decentralised control systems have less change in the queue.

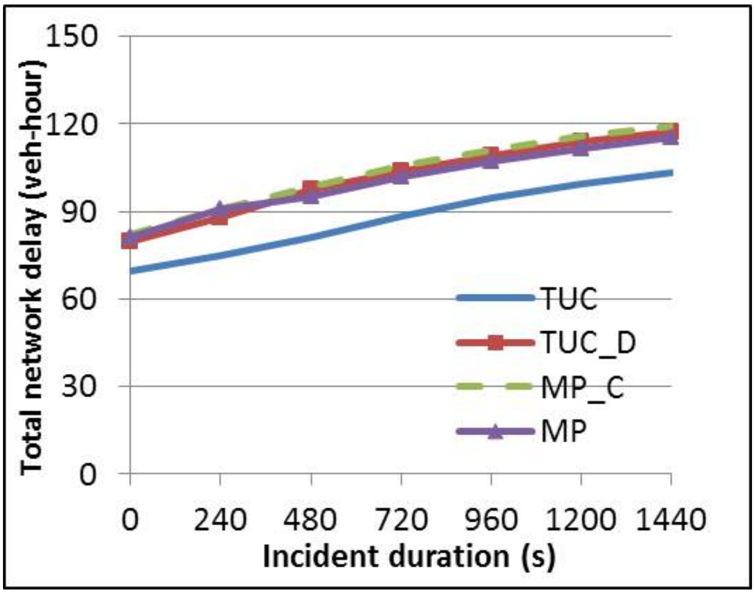

Figure 5.29: Network delay of the road incident scenario without rerouting

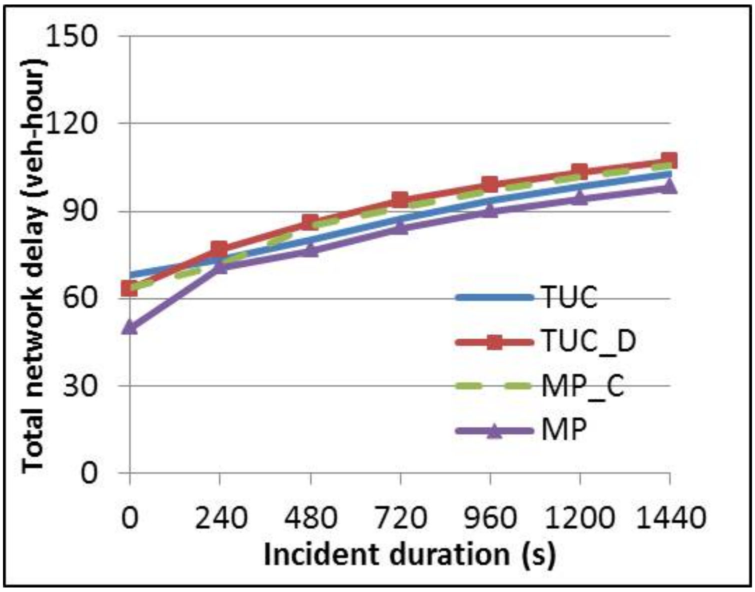

Figure 5.30: Network delay of the road incident scenario with rerouting

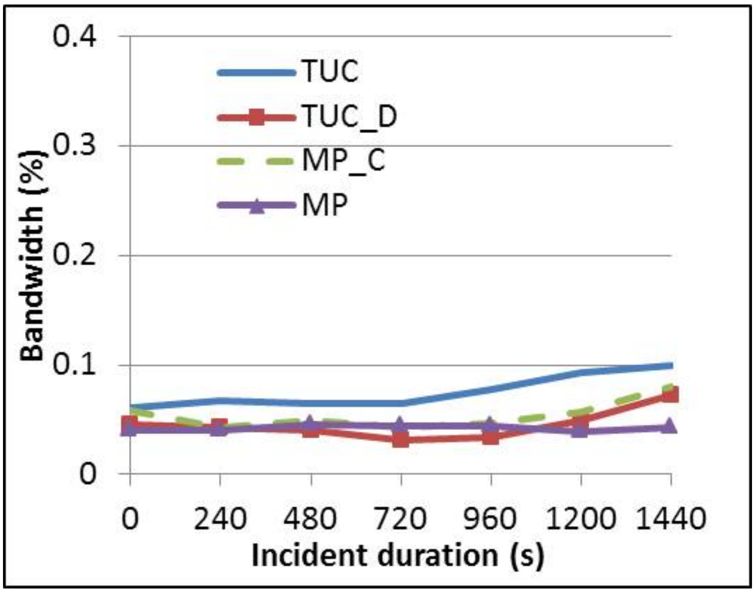

Figure 5.31: Average network bandwidth of the road incident scenario without rerouting

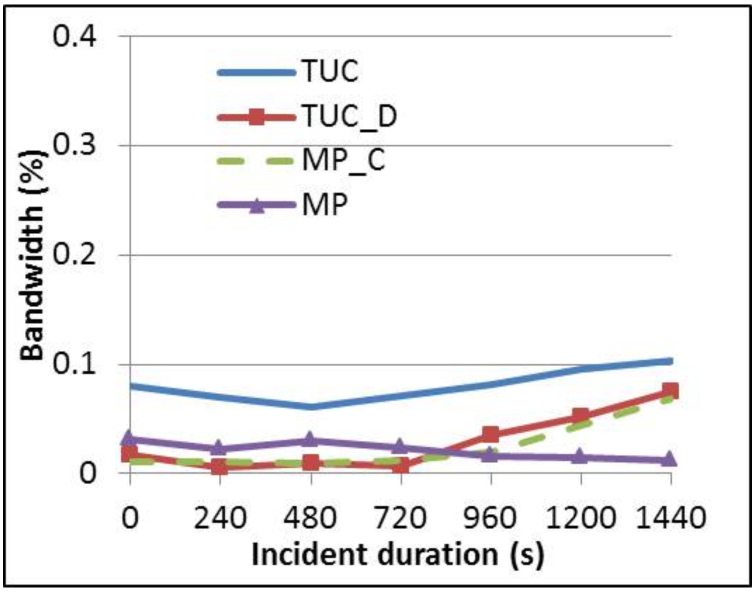

Figure 5.32: Average network bandwidth of the road incident scenario with rerouting

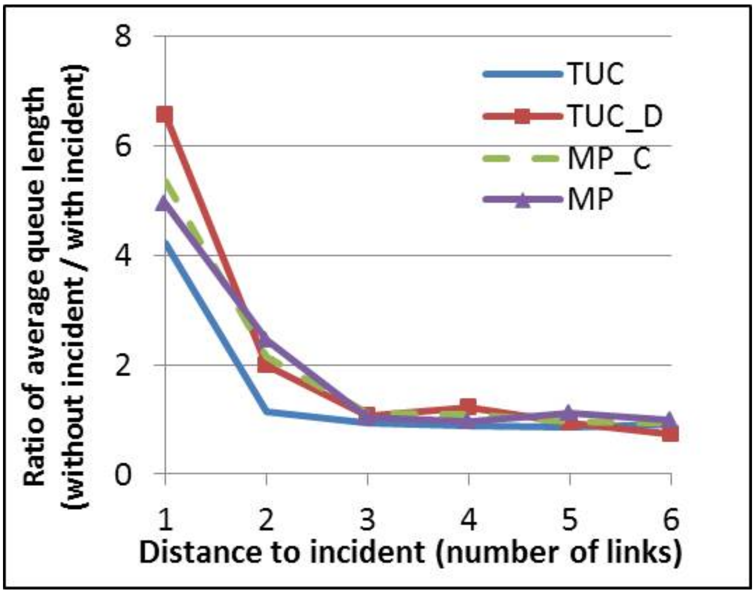

Figure 5.33: Change of network queue distribution without rerouting

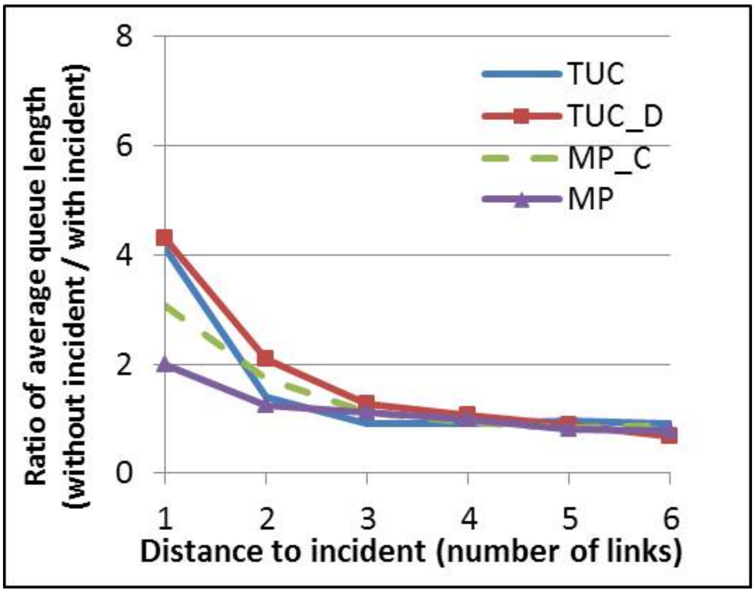

Figure 5.34: Change of network queue distribution with rerouting

5.4.5 Test on London road network

This section considers a London road network and traffic flow data from road detectors to carry out the test between centralised and decentralised traffic signal controls. Bloomsbury area (see Figure 5.35) has been chosen for the test since this is one of the key areas in London with high traffic volumes on Oxford Street for shopping and Kings Cross and St Pancras train stations for travelling to Europe and other parts of the UK. The layout of the network has different features comparing to the other grid networks used in Section 5.4.1, 5.4.2 and 5.4.3. In this network, all the roads have different lengths and capacities, wherein the previous test networks the roads have the same properties. The traffic signal settings are more sophisticated at each intersection since different kinds of the traffic movements are controlled in each signal stage. In the previous tests, all the controllers have the identical settings in traffic movements. In order to import the London road network into SUMO, the network layout is first downloaded from OpenStreetMap[108]. A SUMO tool 'NETCONVERT' can convert the map file from OpenStreetMap (∼.osm) format into a SUMO (∼.net.xml) format or break down into more detailed link (∼.edg.xml), node (∼.nod.xml), connection (∼.con.xml) and traffic signal files (∼.tll.xml). In terms of the real-life traffic flow data of the area, the data is requested from Transport for London. The traffic flow data covers the period from 10:00 am to 12:00 am on the 4th of July in 2011. Figure 5.36 is an example of the measured traffic flow on Euston Road Eastbound and Tottenham Court Road Northbound during the test period. Comparing to the traffic demand used in previous tests, the real demands have more variations through the time. In order to convert plain flow data into SUMO format, a SUMO tool ‘DFROUTER’ can allow a user to compute vehicles’ routes from road detector counts. Once the routes are computed, a SUMO tool ‘DUAROUTER’ can convert them into a route file ($\sim$.rou.xml). The route file in SUMO defines the traffic demand, which has a trip starting time, a route to travel and driver’s characters for each individual vehicle.

The test settings are the same with the previous grid network tests, where four signal controllers (TUC, cyclic Max-pressure (MP_C) and non-cyclic Max-pressure (MP)) are compared in network delay with rerouting. Figure 5.37 shows the network performance results between different controllers. Due to the centralised feature, TUC has the advantage over the other decentralised controls when no rerouting is allowed. The TUC_D and MP_C have similar performance, and it is interesting to see non-cyclic MP performed better than the two cyclic one. This is due to the non-cyclic MP do not have a fixed sequence of green lights given to different traffic movements, and it is more flexible to prioritise the direction with long queues. After rerouting is allowed, it is not surprising that all controller have improvements in their performances. The reason for this improvement is because the minor roads in this London Bloomsbury network create more alternative routes inside the network. Overall, the majority of the test results are consistent with the founding in the previous tests.

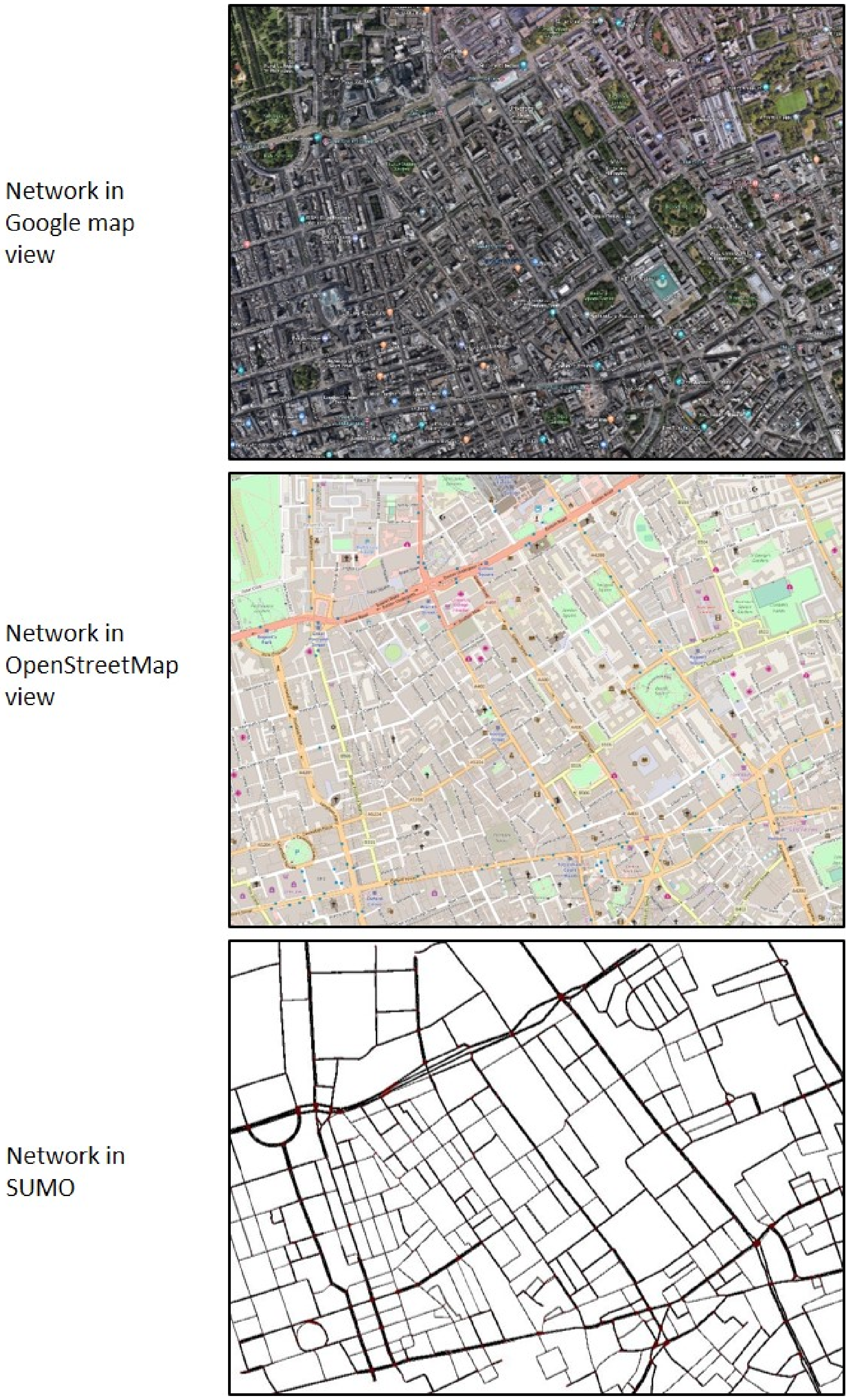

Figure 5.35: London Bloomsbury area test network

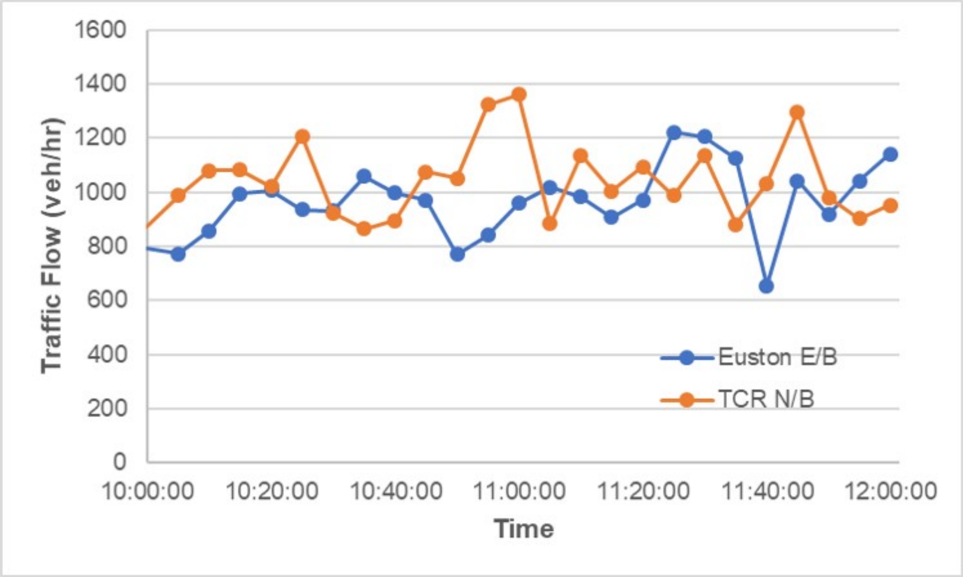

Figure 5.36: An example of measured traffic flow data

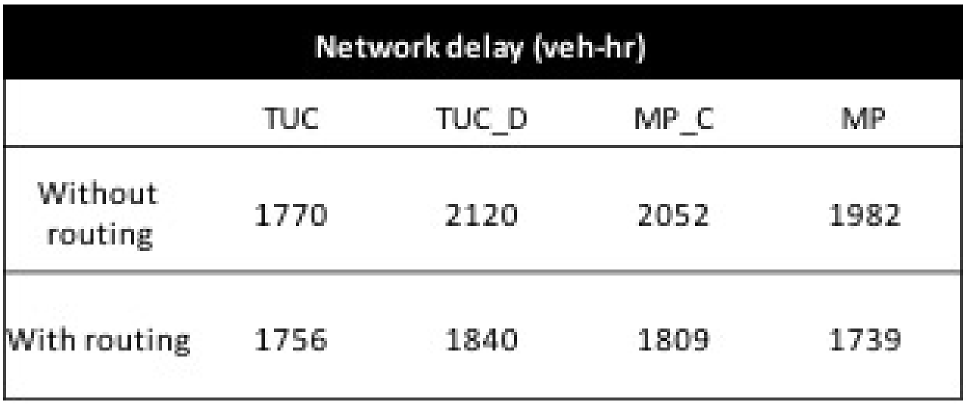

Network delay (veh-hr)				
	TUC	TUC_D	MP_C	MP
Without routing	1770	2120	2052	1982
With routing	1756	1840	1809	1739

Figure 5.37: Test results at the Bloomsbury network

5.4.6 An adaptive TUC system with rerouting control

A new centralised control system is proposed here to test against conventional centralised TUC and decentralised TUC systems. The three TUC systems are tested under different demand levels and distributions on a three by three grid network (see Figure 5.12). In previous tests, centralised TUC was able to outperform decentralised control systems since it considered network topology and demand distribution. However, the decentralised systems received significant improvement in performance when drivers were allowed to reroute respect to traffic conditions. An adaptive centralised system is proposed here to see if the centralised system can also improve its performance by allowing drivers to reroute. The new adaptive centralised control collects real-time demand distribution (through turning ratio ζ) on the test network every signal cycle. The demand distribution will be used to recalculate the control gain matrix **L** of TUC system.

When testing under different demand levels, demand level parameter γ is set to be 0.3,0.5,0.7,0.9 and the distribution parameter σ is fixed to 0.3. The network delay result without rerouting is in Figure 5.38, where the two centralised TUC outperform the decentralised TUC under through all demand levels. The adaptive TUC perform slightly better than the conventional TUC. This is due to the signal setting (**L** matrix) in conventional TUC is derived from the average demand distribution through the entire test period, where the adaptive TUC uses a shorter time interval and update the distribution in real-time. When rerouting is allowed (see Figure 5.39 and 5.40), both decentralised TUC and adaptive centralised TUC have improved in network de-

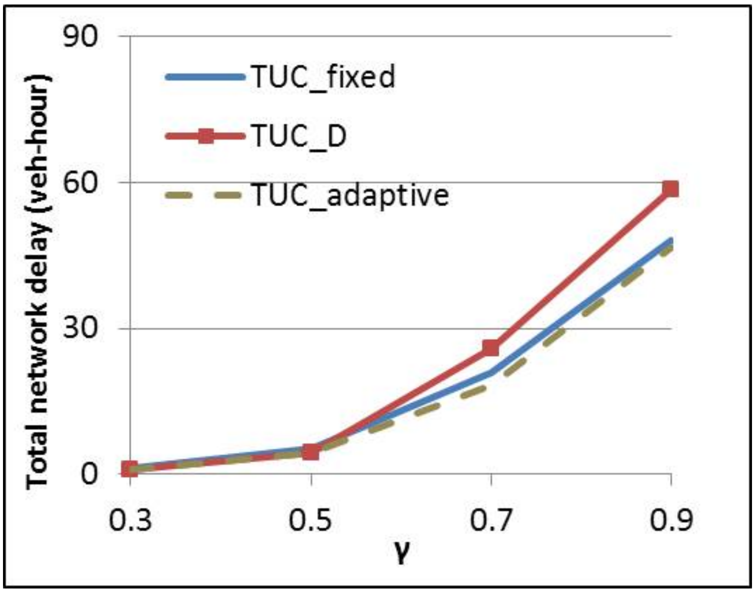

Figure 5.38: Network delay of three TUC systems over γ without rerouting

lay. In this case, giving more flexibility when deriving signal plans in a centralised system, the rerouting can improve its performance.

The second test is carried out under different demand distribution, where the distribution parameter σ is set to be 0,0.3,0.6,0.9 and γ is fixed to 0.7. Figure 5.41 (without rerouting) and Figure 5.42 (with rerouting) show the network delay results. The conventional TUC and the adaptive TUC have similar network delay. When rerouting applies, decentralised TUC has more improvement in the network delay. Figure 5.43 shows that the decentralised TUC improved around 50% when $\sigma = 0.3$, where the adaptive TUC improved 10%. The improvement made by adaptive TUC with rerouting shows the potential of extra efficiency could come from higher degree of flexibility in control.

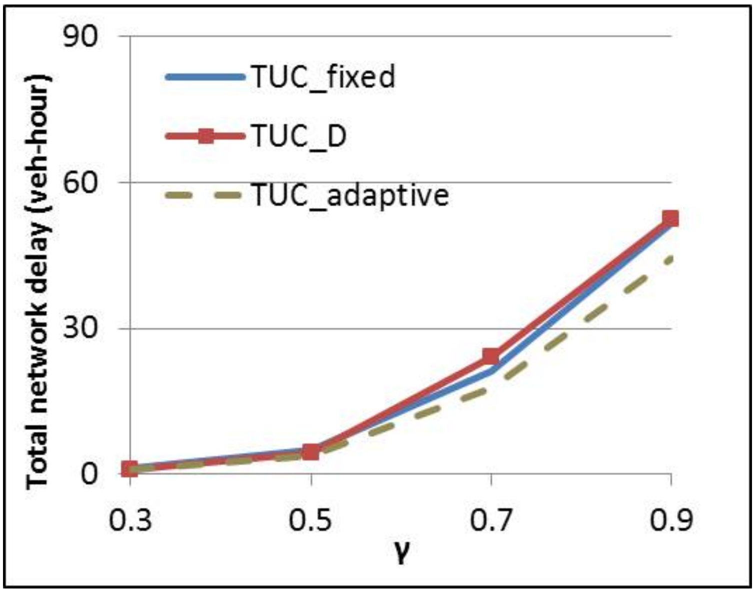

Figure 5.39: Network delay of three TUC systems over γ with rerouting

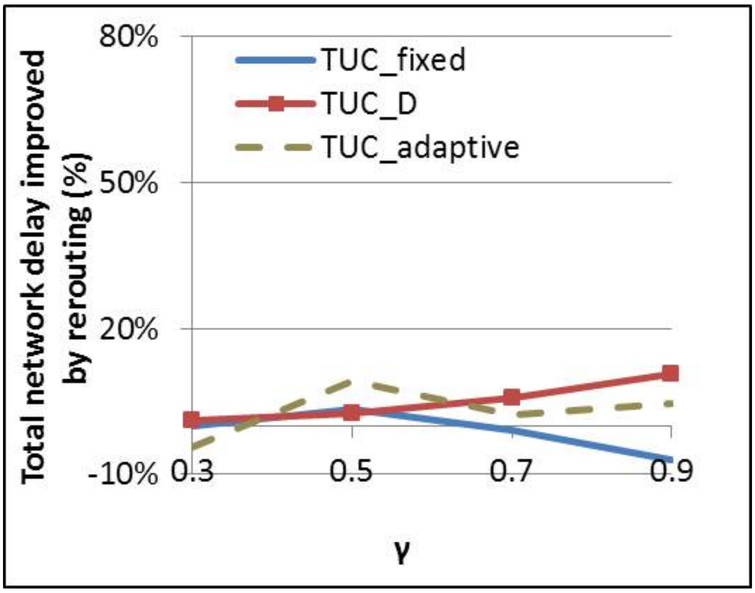

Figure 5.40: Improvement of network delay by rerouting over γ

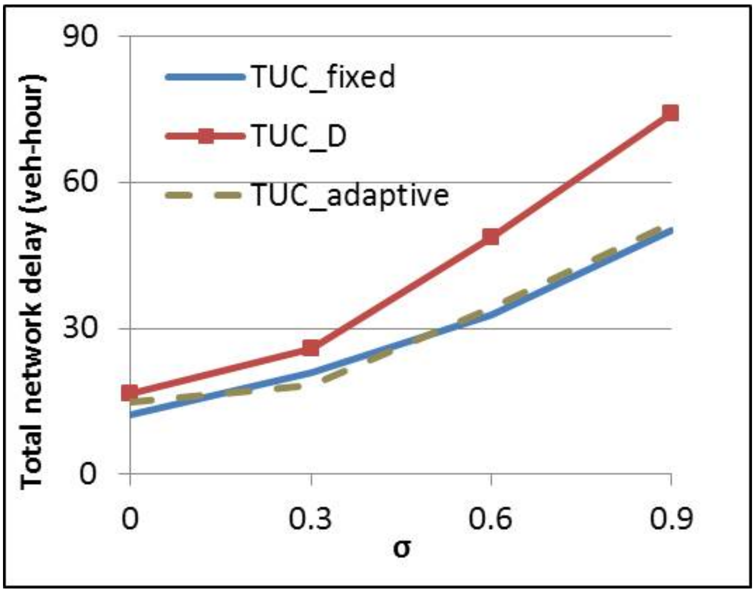

Figure 5.41: Network delay of three TUC systems over σ without rerouting

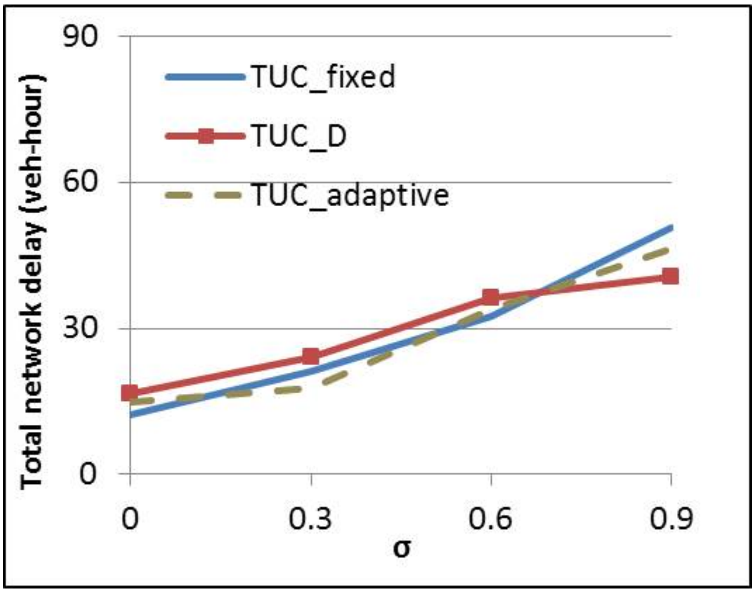

Figure 5.42: Network delay of three TUC systems over σ with rerouting

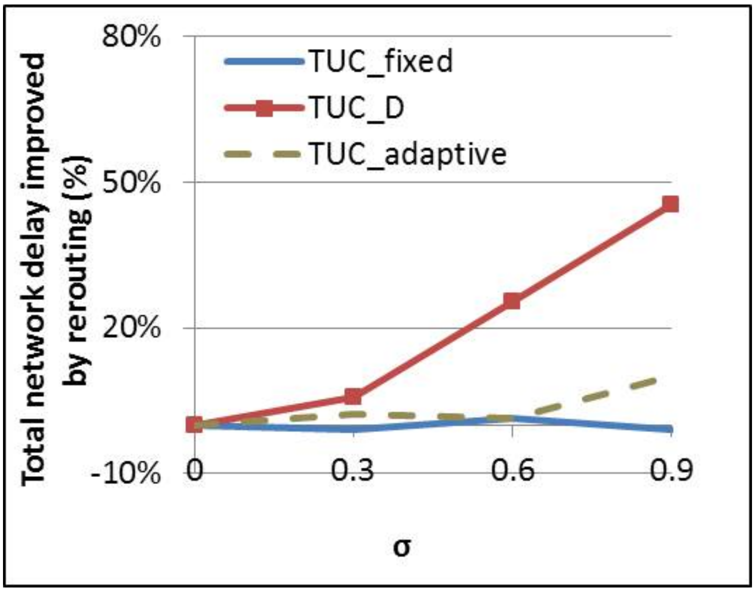

Figure 5.43: Improvement of network delay by rerouting over σ

5.5 Summary

This chapter compared the performance between centralised and decentralised control systems on a microscopic flow model at SUMO. The control systems are tested under different traffic saturation levels and distributions first, and a dynamic rerouting algorithm is implemented to allow traffic rerouting according to the traffic conditions. The results show the improvement in decentralised systems' performance when rerouting is allowed. Between acyclic and cyclic decentralised systems, the acyclic system gained more benefit with rerouting and could outperform the centralised cyclic system in some cases. This highlights the potential of decentralised control which could perform better than the centralised control when degrees of freedom like route choice are allowed in the network. An adaptive centralised system is proposed to capture the change of traffic distribution caused by rerouting. The network delay has also reduced after rerouting in the adaptive centralised system.

Chapter 6

Conclusions and outlook

6.1 Thesis overview

This thesis compares the performance differences between the centralised and decentralised control systems to bring insight of developing an efficient and resilient control system for urban networks.

In order to investigate the performance difference between centralised and decentralised control systems, this study first reviewed the state-of-the-art traffic control systems and chose five control systems for comparison. A brute force approach and genetic algorithm represent centralised control systems, where one control system operates signal controllers for the entire test network. A TUC system and its variant Hybrid system are two semi-decentralised control systems. The reason for them to be semi-decentralised systems is that a part of the signal plans (green split, cycle time) are controlled in a centralised way and the other part (offset) is decentralised.

Max-pressure is a fully decentralised control, where all the signal plans are derived locally and isolated with each intersection of the network.

Both macroscopic and microscopic flow models are built to evaluate the performance of the traffic control systems. In the macroscopic flow model (Cell Transmission Model), traffic is described as a flow and the control systems are compared against different traffic demand levels. The microscopic flow model (Krauss' safe-distance model of SUMO) simulates the movements of each individual vehicle, and the control systems are compared against different traffic demand levels and spatial distributions. In addition, a feedback rerouting algorithm is implemented on the microscopic flow model. This allows the test to mimic drivers' rerouting behaviour with respect to real-time traffic conditions.

By comparing the control systems under macroscopic flow model (CTM), the result shows that green split plans are similar between the centralised and decentralised control. This indicates the benefit of the centralised control from settings of the offset. The centralised offset control has global traffic information, so that the offset can be adjusted frequently and accurately. The decentralised offset control is simply calculated from local queues, and there is no coordination between controllers. The challenge of decentralised offset control is to balance the traffic progression in different directions within a road network, and especially when it is saturated. To solve this issue, a centralised offset control based on a hill climbing algorithm is proposed. It helps to reduce the performance gap between centralised systems and other systems in the test results.

The centralised and decentralised systems are also compared under the microscopic flow model (SUMO), where a feedback rerouting algorithm is added to mimic the drivers' route change behaviour with respect to real-time traffic conditions. The performance differences between the centralised and decentralised systems reduced by increasing the proportion of system users who can reroute according to the traffic conditions. A decentralised system operates each intersection separately, so that is more flexible comparing to the centralised system. The centralised system knew the network flow information, and its signal settings are predefined to prioritise the links which are more likely to be congested. Allowing drivers to reroute will change the traffic spatial distribution through the road network. This is why the decentralised control is more beneficial than the centralised control system. To help the centralised system to be more adaptive to the rerouting behaviour, an adaptive centralised system is proposed. The test results show its improvements over the original centralised system with rerouting.

6.2 Contributions

The first contribution of this study is the comparison test done between centralised and decentralised control systems. This comparison test gave clear visible results to show the performance differences between centralised and decentralised systems. Green split, offset and cycle time are the control parameters used in a signal plan. A centralised brute force approach examined all the feasible signal plans and derived the real global optimum as a bench mark with which to compare. In the global optimum signal plans, the centralised offset is changed frequently and adjusted accurately, which is not the same as the other control systems' signal plan. This leads to the conclusion that offset is the main cause of the performance gap between centralised and decentralised systems.

The second contribution of this study is the proposed centralised offset control which integrates with decentralised control systems. As one of the findings from this study suggested, offset is the main cause of the inefficiency in the decentralised control system, so a centralised offset control based on a hill climbing algorithm is proposed to solve the issue. The hill climbing algorithm searches for efficient network offset plans which can help the network traffic to progress in multiple directions and reduce the total network delay.

Introducing an adaptive centralised system, which is designed to consider the rerouting behaviour of drivers, is the third contribution of the study. In Chapter 5, rerouting behaviour has been found to improve the performance of the decentralised systems. At the same time, there is limited change found in centralised system'performance. This is due to the predefined control matrix **L** prioritises the links which the centralised system thought could have higher demand. The rerouting of the driver changes the traffic spatial distribution, therefore, the centralised system may not perform well when the predefined **L** remains unchanged. The adaptive centralised system allows the control matrix **L** to be updated every signal cycle to change with the traffic distribution. The **L** is updated according to the measured turning ratio at all intersections of the test network. The adaptive centralised system is tested and can perform efficiently with the rerouting of the driver.

6.3 Future work

One of the future works is to integrate traffic demand management into a decentralised traffic management framework. According to the findings by comparing centralised and decentralised control systems, the main cause of the performance gap is in traffic controllers' cooperation (offset control). The offset control has been studied for many years (e.g. MAXBAND [109], MULTIBAND [110] [67]), and many of them focus on maximising the bandwidth for traffic's progression in multiple directions. A recent study [111] shows deriving offset plan according to the traffic demand information (origin-destination flows) can outperform the existing solutions (e.g. MAXBAND and MULTIBAND) on an arterial network. It will be interesting to study how the traffic demand information can be integrated and used properly with decentralised control systems.

The (semi-)decentralised control systems in this study are all feedback control, but further studies can extend to online control or model-based predictive control (MPC) [94] [112]. It will be interesting to decompose and approximate a global control system into a group of local sub systems with interconnections under the MPC framework. There are some possible methods such as: alternative direction method of multipliers (ADMM) [113] [114] [66], sensitivity analysis [57] [115] and approximated functions [12]. A decentralised MPC system may be sensitive to input data quality and traffic information communicated between subsystems.

Appendix A

Genetic Algorithm

This appendix contains the Matlab scripts used in this study. The scripts show the operation processes (reproduction, crossover and mutation) of GA.

```
%% Reproduction
% This script is the reproduction process of GA used in this study.
% Reference: Lo, H.K. and Chow, A.H., 2004. Control strategies for oversaturated traffic. Journal of Transportation Engineering, 130(4), pp.466–478.
%
% 'Fitness' of the chromosomes are evaluated and stochastic universal sampling is carried out.
% The chromosomes with higher 'fitness' have higher chance to be passed on to the next generation.
%
```

```
% TD - [array] Total network delay of all chromosomes
TD_max = max(TD(:));
TD_min = min(TD(:));

if TD_max ~= TD_min
    p = 5;
    FIT_temp = exp((TD_max-TD)/(TD_max-TD_min)*p); % calculate the fitness of chromosomes
    FIT_sum = sum(FIT_temp);
    FIT = FIT_temp/FIT_sum;
    FIT_sorted = sortrows(FIT);
    FIT_cumsum = cumsum(FIT_sorted);

    sample_interval = 1/length(TD)*max(FIT_cumsum);
    sample_points = [sample_interval:sample_interval:max(FIT_cumsum)]';
    FIT_cumsum_mat = FIT_cumsum*ones(1,length(TD));
    sample_point_mat = ones(length(TD),1)*sample_points';
    distance_mat = abs(FIT_cumsum_mat-sample_point_mat); % calculate the distance to sampling points
    [~,index_new_chromosome] = min(distance_mat,[],2);
end

```

```

%% Crossover
% This script shows how GA's crossover process is implemented in this study.
% Reference: Lo, H.K. and Chow, A.H., 2004. Control strategies for oversaturated traffic. Journal of Transportation Engineering, 130(4), pp.466–478.
%
% GA randomly choose two chromosomes as parent chromosomes.
% They will mate and produce two new children chromosomes.
% The crossover/mating process will randomly choose a crossover/cut point.
% First part of parent 1 + second part of parent 2 = child 1
% First part of parent 2 + second part of parent 1 = child 2
% The procedure is continued until every chromosome is mated in the new
% generation.
%
% Chromosome_parent – [structure array] parent chromosomes
% popNum – [constant] number of Chromosomes in test population
% croNum – [constant] number of crossover need to be carried out
% cycNum – [constant] number of cycle in the test period
% contrNum – [constant] number of controller in the network
```

```

croPair = randperm(popNum);
croPair = reshape(croPair,[croNum,2]); % pair up two random Chromosomes for crossover process
Chromosome_child = Chromosome_parent;

for iCro = 1:croNum
    for jCyc = 1:cycNum
        for kContr = 1:contrNum
            croPoint = randi([1 7]); % crossover point
            int_A = Chromosome_child(croPair(iCro,1)).pop(jCyc,kContr);
            int_B = Chromosome_child(croPair(iCro,2)).pop(jCyc,kContr);
            bin_A = dec2bin(int_A,7); % convert integer into 7 bits binary string
            bin_B = dec2bin(int_B,7);
            cut_A = bin_A(croPoint:7);
            cut_B = bin_B(croPoint:7);
            bin_A(croPoint:7) = cut_B;
            bin_B(croPoint:7) = cut_A;

            Chromosome_child(croPair(iCro,1)).pop(jCyc,kContr) =
        bin2dec(bin_A);
      Chromosome_child(croPair(iCro,2)).pop(jCyc,kContr) = bin2dec(bin_B);
    end
  end
end



%% Mutation
% This script is the reproduction process of GA used in this study.
% Reference: Lo, H.K. and Chow, A.H., 2004. Control strategies for oversaturated traffic. Journal of Transportation Engineering, 130(4), pp.466—478.
%
% Chromosome — [structure array] include chromosomes of the entire population
% popNum — [constant] number of Chromosomes in test population
% cycNum — [constant] number of cycle in the test period
% contrNum — [constant] number of controller in the network

mutRate = 0.005;
```

```
TotBits = popNum*cycNum*contrNum*7; % Total bits number of the whole chromosome population
mutNum = round(TotBits*mutRate); % number of bits will be mutated
bits_loc = randperm(TotBits,mutNum); % bits locations for mutation

for i = 1: length(bits_loc)
    bit_temp = bits_loc(i);
    bit_iPop = ceil(bit_temp/(cycNum*contrNum*7));
    bit_temp = bit_temp-(bit_iPop-1)*(cycNum*contrNum*7);
    bit_iCyc = ceil(bit_temp/(contrNum*7));
    bit_temp = bit_temp-(bit_iCyc-1)*(contrNum*7);
    bit_iContr = ceil(bit_temp/7);
    bit_ind = bit_temp-(bit_iContr-1)*7;

    bit_string = dec2bin(Chromosome(bit_iPop).pop(bit_iCyc,bit_iContr),7);
    switch bit_string(bit_ind)
        case '1'
            bit_string(bit_ind) = '0';
        case '0'
            bit_string(bit_ind) = '1';
    end
    Chromosome(bit_iPop).pop(bit_iCyc,bit_iContr) = bin2dec(
        bit_string);
end
```

Appendix B

TUC: split control

This appendix contains the Matlab scripts used in this study. The scripts show how to derive control gain (L matrix) of LQR problem and how to apply green split constraints.

```
%% TUC Split Control – derive control gain of LQR
% This script creates control gain (L matrix) for the Linear–Quadratic Regulator used for TUC system's split control.
%
% delta_t – [constant] a time interval of one time step
% Link – [structure array] contains link information, such as link length,saturation flow rate and jam density.
% Node – [structure array] contains node/intersection information, such as incoming links, outgoing links, turning ratios.
% Contr – [structure array] contains signal controller information, such as controller location and signal timing
```

```
   plans.
% SinkLink – [array] a list of sink links ID.

% convert network links' turning ratio matrix
TurnMatrix = zeros(length(Link.Length));
for iContr = 1: length(Contr)
    iNode = Contr(iContr).Node;
    inLinks = Node(iNode).InLink;
    outLinks = Node(iNode).OutLink;
    turnRatios = Node(iNode).TurnRatio;
    for iLink = 1:length(inLinks)
        for jLink = 1:length(outLinks)
            TurnMatrix(inLinks(iLink),outLinks(jLink)) =
               turnRatios(iLink,jLink);
        end
    end
end

% B matrix – diagonal matrix of 'minus' saturation flow rate
B_mat = zeros(length(Link.Length));

for iNode = 1:length(Node)
    inLinks = Node(iNode).InLink;
    outLinks = Node(iNode).OutLink;
    for iLink = 1: length(inLinks)
        for jLink = 1: length(outLinks)
            uLink = inLinks(iLink);
            dLink = outLinks(jLink);
            B_mat(dLink,uLink) = B_mat(uLink,dLink)+TurnMatrix(
               uLink,dLink)*Link.SatFlow(uLink)*delta_t;
        end
    end
end

for iLink = 1:length(Link.Length)
    B_mat(iLink,iLink) = -1*Link.SatFlow(iLink)*delta_t;
end

% A matrix - identity matrix
A_mat = eye(length(Link.Length));
A_mat(SinkLink,:) = 0;
B_mat(SinkLink,:) = 0;

% S matrix - diagonal weighting matrix
S_elem = 1./(Link.Length.*Link.kjam);
S_mat = diag(S_elem);
```

```

% R matrix — diagonal weighting matrix
R_mat = (0.001)*eye(length(Link.Length));

% Matlab built—in function dlqr
% Linear—quadratic (LQ) state—feedback regulator for discrete—time state—space system
[L_mat] = dlqr(A_mat,B_mat,S_mat,R_mat);




%% TUC Split Control — apply green split constraints
% This script applies the green split constraints to the timing plan dervied from LQR
% Reference: Diakaki, Christina. "Integrated control of traffic flow in corridor networks." Ph. D. Thesis, Department of Production Engineering and Management, Technical University of Crete (1999).
%
% CycleTime — [constant] cycle time value
% LostTime — [constant] lost time per stage
% g_min_without_LostTime — [constant] minimum green split value
```

```
   exclude lost time
% g_Stage — [array] include green splits of all stages

StageNum = size(g_Stage,1);
AuxVarB = CycleTime—LostTime∗StageNum;
SetH = [1:StageNum];
StopSign = 0;

while StopSign ~= 1
    % Step 2: Calculate auxiliary variable A
    AuxVarA = (AuxVarB — sum([g_Stage(SetH)]))/length(SetH);
    % Step 3: Calculate modified green split
    for i = 1: length(SetH)
        g_Stage(SetH(i)) = g_Stage(SetH(i))+AuxVarA;
    end

    % Step 4: Define auxiliary set P and N
    AuxSetP = [];
    AuxSetN = [];
    maxStgTSnoLT = CycleTime — LostTime∗StageNum —
       g_min_without_LostTime∗(StageNum—1);
    for i = 1: length(SetH)
        if g_Stage(SetH(i)) > maxStgTSnoLT
```

```
            AuxSetP = [AuxSetP,SetH(i)];
        elseif g_Stage(SetH(i)) < g_min_without_LostTime
            AuxSetN = [AuxSetN,SetH(i)];
        end
    end
    % Step 5: Check if auxiliary set P and N are empty
    if isempty(AuxSetP) == 1 && isempty(AuxSetN) == 1
        StopSign = 1;
        % Step 6: Calculate auxiliary variablr D and d
    else
        AuxVarD = sum(g_Stage(AuxSetP))-length(AuxSetP)*
           maxStgTSnoLT;
        AuxVard = length(AuxSetN)*g_min_without_LostTime-sum(
           g_Stage(AuxSetN));

        % Step 7: apply maximum green split constraint
        if AuxVarD >= AuxVard
            g_Stage(AuxSetP) = maxStgTSnoLT;
            SetH(ismember(SetH,AuxSetP))=[];
            AuxVarB = AuxVarB - length(AuxSetP)*maxStgTSnoLT;
        end

        % Step 8: apply minimum green split constraint
        if AuxVarD <= AuxVard
            g_Stage(AuxSetN) = g_min_without_LostTime;
            SetH(ismember(SetH,AuxSetN))=[];
            AuxVarB = AuxVarB - length(AuxSetN)*
               g_min_without_LostTime;
        end

        % Step 9: STOP, with error message
        if AuxVarD ~= AuxVard && isempty(SetH) == 1
            error('The admissible region for green light time is
               empty.');
        end

        % Step 10: STOP with the optimal solution
        if AuxVarD == AuxVard
            StopSign = 1;
        end
    end
end

g_Stage = round(g_Stage);
```

References

[1] United Nations. Department of Economic and Social Affairs. Population Division. *World Urbanization Prospects: The 2014 Revision*. UN, 2015.

[2] Department for Transport. Road traffic forecasts 2015. [Accessed on: 10 Jan 2016].

[3] INRIX. INRIX traffic scorecard. `http://inrix.com/scorecard/`, 2016. [Accessed on: 19 Jun 2017].

[4] A.H.F. Chow, A. Santacreu, I. Tsapakis, G. Tanasaranond, and T. Cheng. Empirical assessment of urban traffic congestion. *Journal of Advanced Transportation*, 48(8):1000–1016, 2014.

[5] Siemens PLC Peek Traffic Ltd and TRL Limited. SCOOT.

[6] T. Le, P. Kovács, N. Walton, H.L. Vu, L.L.H. Andrew, and S.S.P. Hoogendoorn. Decentralized signal control for urban road networks. *Transportation Research Part C: Emerging Technologies*, 2015.

[7] J. Li and M.H. Zhang. Coupled linear programming approach for decentral-

ized control of urban traffic. *Transportation Research Record: Journal of the Transportation Research Board*, (2439):83–93, 2014.

[8] P. Varaiya. *The max-pressure controller for arbitrary networks of signalized intersections*. Springer, 2013.

[9] H. Prothmann, S. Tomforde, J. Branke, J. Hähner, C. Müller-Schloer, and H. Schmeck. *Organic traffic control*. Springer, 2011.

[10] S. Lammer and D. Helbing. Self-control of traffic lights and vehicle flows in urban road networks. *Journal of Statistical Mechanics: Theory and Experiment*, P04019, 2008.

[11] L.B. de Oliveira and E. Camponogara. Multi-agent model predictive control of signaling split in urban traffic networks. *Transportation Research Part C: Emerging Technologies*, 18(1):120–139, 2010.

[12] A.H.F. Chow. Optimisation of dynamic motorway traffic via a parsimonious and decentralised approach. *Transportation Research Part C*, 55:69–84, 2015.

[13] J.J. Olstam and A. Tapani. Comparison of car-following models. Technical report, 2004.

[14] R.E. Chandler, R. Herman, and E.W. Montroll. Traffic dynamics: studies in car following. *Operations Research*, 6(2):165–184, 1958.

[15] D.C. Gazis, R. Herman, and R.B. Potts. Car-following theory of steady-state traffic flow. *Operations Research*, 7(4):499–505, 1959.

[16] D.C. Gazis, R. Herman, and R.W. Rothery. Nonlinear follow-the-leader models of traffic flow. *Operations Research*, 9(4):545–567, 1961.

[17] A.D. May. Non-integer car-following models. *Highway Research Record*, 199(3):19–32, 1967.

[18] H. Ozaki. Reaction and anticipation in the car-following behavior. In *Proceedings of the 13th International Symposium on the Theory of Road Traffic Flow*, pages 349–366, 1993.

[19] M. Brackstone and M. McDonald. Car-following: a historical review. *Transportation Research Part F: Traffic Psychology and Behaviour*, 2(4):181–196, 1999.

[20] L.A. Pipes. An operational analysis of traffic dynamics. *Journal of Applied Physics*, 24(3):274–281, 1953.

[21] S.P. Hoogendoorn and P.H.L. Bovy. State-of-the-art of vehicular traffic flow modelling. *Proceedings of the Institution of Mechanical Engineers, Part I: Journal of Systems and Control Engineering*, 215(4):283–303, 2001.

[22] W. Leutzbach. *Introduction to the theory of traffic flow*. Springer, 1988.

[23] G.F. Newell. A simplified car-following theory: a lower order model. *Transportation Research Part B: Methodological*, 36(3):195–205, 2002.

[24] L. Leclercq. Hybrid approaches to the solutions of the âĂĲlighthill–whitham–richardsâĂİ model. *Transportation Research Part B: Methodological*, 41(7):701–709, 2007.

[25] R. Wiedemann. Simulation des strassenverkehrsflusses. Technical report, 1974.

[26] PTV Group. VISSIM 5.40 user manual, 2011.

[27] B.D. Greenshields, J.R. Bibbins, W.S. Channing, and H.H. Miller. A study of traffic capacity. In *Proceedings of the 14th annual meeting of the highway research board*, volume 14, pages 448–477, 1935.

[28] H. Greenberg. An analysis of traffic flow. *Operations Research*, 7(1):79–85, 1959.

[29] L.C. Edie. Car-following and steady-state theory for noncongested traffic. *Operations Research*, 9(1):66–76, 1961.

[30] G. F. Newell. A simplified theory of kinematic waves in highway traffic: I general theory, ii queuing at freeway bottlenecks, iii: multi-destination flows. *Transportation Research Part B*, 27:281–313, 1993.

[31] C. F. Daganzo. The cell transmission model: A dynamic representation of highway traffic consistent with the hydrodynamic theory. *Transportation Research Part B: Methodological*, 28(4):269–287, 1994.

[32] M.J. Lighthill and G.B. Whitham. On kinematic waves. ii. a theory of traffic flow on long crowded roads. In *Proceedings of the Royal Society of London A: Mathematical, Physical and Engineering Sciences*, volume 229, pages 317–345. The Royal Society, 1955.

[33] P.I. Richards. Shock waves on the highway. *Operations Research*, 4(1):42–51, 1956.

[34] S.K. Godunov. A difference method for numerical calculation of discontinuous solutions of the equations of hydrodynamics. *Matematicheskii Sbornik*, 89(3):271–306, 1959.

[35] H.J. Payne. Models of freeway traffic and control. *Mathematical models of public systems*, pages 51–61, 1971.

[36] M. Papageorgiou, J.M. Blosseville, and H. Hadj-Salem. Modelling and real-time control of traffic flow on the southern part of boulevard peripherique in paris: Part i: Modelling. *Transportation Research Part A: General*, 24(5):345–359, 1990.

[37] D. Helbing. Gas-kinetic derivation of navier-stokes-like traffic equations. *Physical Review E*, 53(3):2366, 1996.

[38] M. Papageorgiou. Some remarks on macroscopic traffic flow modelling. *Transportation Research Part A: Policy and Practice*, 32(5):323–329, 1998.

[39] F.V. Webster. Traffic signal settings. Technical report, 1958.

[40] Dennis I Robertson. Transyt: a traffic network study tool. 1969.

[41] Transport Research Laboratory. TRANSYT - Traffic Network and Isolated Intersection Study Tool (Version 15). `trlsoftware.co.uk/products/junction_signal_design/transyt`, 2015. [Accessed on: 30 Jul 2015].

[42] N.H. Gartner, J.D.C. Little, and H. Gabbay. Mitrop: a computer program for simultaneous optimisation of offsets, splits and cycle time. *Traffic Engineering & Control*, 17(8/9), 1976.

[43] K.W. Huddart and E.D. Turner. Traffic signal progression - GLC combination method. *Traffic Engineering & Control*, 8(8), 1969.

[44] M.C. Bell and R.D. Bretherton. Ageing of fixed-time traffic signal plans. In *International Conference On Road Traffic Control*, 1986.

[45] D. Robertson and R. Bretherton. Optimizing networks of traffic signals in real time-the scoot method. *IEEE Transactions on Vehicular Technology*, 40(1):11–15, 1991.

[46] P.B. Hunt, D.I. Robertson, R.D. Bretherton, and R.I. Winton. Scoot-a traffic responsive method of coordinating signals. Technical report, 1981.

[47] P.R. Lowrie. The sydney coordinated adaptive traffic system-principles, methodology, algorithms. In *International Conference on Road Traffic Signalling, 1982, London, United Kingdom*, number 207, 1982.

[48] Roads and Maritime Services. An introduction to SCATS: SCATS 6 âĂŞ functional description. `http://www.scats.com.au/files/an_introduction_to_scats_6.pdf`, 2011. [Accessed on: 30 Oct 2015].

[49] N.H. Gartner. *OPAC: A demand-responsive strategy for traffic signal control*. Number 906. 1983.

[50] L.C. Liao. *A review of the optimized policies for adaptive control strategy (OPAC)*. California PATH Program, Institute of Transportation Studies, University of California at Berkeley, 1998.

[51] P. Mirchandani and L. Head. A real-time traffic signal control system: architecture, algorithms, and analysis. *Transportation Research Part C: Emerging Technologies*, 9(6):415 – 432, 2001.

[52] P. Mirchandani and F. Wang. RHODES to intelligent transportation systems. *Intelligent Systems, IEEE*, 20(1):10–15, Jan 2005.

[53] C. Diakaki. *Integrated control of traffic flow in corridor networks*. PhD thesis, Technical University of Crete, 1999.

[54] C. Diakaki, M. Papageorgiou, and K. Aboudolas. A multivariable regular approach to traffic responsive network-wide signal control. *Control Engineering Practice*, 10:183–195, 2002.

[55] UTOPIA: Optimizing traffic flows across the road network. `https://www.swarco.com/mizar-en/Products/Urban-Systems/UTOPIA`. [Accessed on: 23 Oct 2015].

[56] UTOPIA - Urban traffic control system architecture. `http://ftp.citilabs.com/sites/default/files/files/3_Swarco.pdf`. [Accessed on: 23 Oct 2015].

[57] M. Rinaldi and C.M.J. Tampère. An extended coordinate descent method for

distributed anticipatory network traffic control. *Transportation Research Part B: Methodological*, 80:107–131, 2015.

[58] N.E. Marinica. *Distributed estimation and control of interacting hybrid systems for traffic applications*. PhD thesis, Ghent University, 2014.

[59] S. Lämmer and D. Helbing. Self-stabilizing decentralized signal control of realistic, saturated network traffic. Santa Fe Institute, 2010.

[60] R.T. Van Katwijk. *Multi-agent look-ahead traffic-adaptive control*. PhD thesis, Delft University of Technology, 2008.

[61] T. Wongpiromsarn, T. Uthaicharoenpong, Y. Wang, E. Frazzoli, and D. Wang. Distributed traffic signal control for maximum network throughput. In *Intelligent Transportation Systems (ITSC), 2012 15th International IEEE Conference on*, pages 588–595. IEEE, 2012.

[62] M.R. Crabtree. MOVA traffic control manual. *Application guide:Issue D*, 2011.

[63] Hong Lo. A novel traffic signal control formulation. *Transportation Research Part B*, 33:433 – 448, 1999.

[64] G. Gomes and R. Horowitz. Optimal freeway ramp metering using the asymmetric cell transmission model. *Transportation Research Part C*, 14(4):244 – 262, 2006.

[65] K. Aboudolas, M. Papageorgiou, and E. Kosmatopoulos. Store-and-forward

based methods for the signal control problem in large-scale congested urban road networks. *Transportation Research Part C*, 17:163–174, 2009.

[66] S. Timotheou, C.G. Panayiotou, and M.M. Polycarpou. Network traffic signal control with nonconvex alternating direction method of multipliers formulations. *Transportation Research Record: Journal of the Transportation Research Board*, (2490):11–20, 2015.

[67] N.H. Gartner, S.F. Assman, F. Lasaga, and D.L. Hou. A multi-band approach to arterial traffic signal optimization. *Transportation Research Part B: Methodological*, 25(1):55–74, 1991.

[68] N.H. Gartner and C. Stamatiadis. Arterial-based control of traffic flow in urban grid networks. *Mathematical and computer modelling*, 35(5-6):657–671, 2002.

[69] J.H. Holland. Adaptation in natural and artificial systems. 1975. *Ann Arbor, MI: University of Michigan Press and*, 1992.

[70] H. Lo and A. H. F. Chow. Control strategies for over-saturated traffic. *ASCE Journal of Transportation Engineering*, 130:466–478, 2004.

[71] TRAVOLUTION in Ingolstadt. `http://www.travolution-ingolstadt.de`. [Accessed on: 21 Oct 2015].

[72] M. Dorigo, V. Maniezzo, and A. Colorni. Ant system: optimization by a colony of cooperating agents. *IEEE Transactions on Systems, Man, and Cybernetics, Part B (Cybernetics)*, 26(1):29–41, 1996.

[73] R. Putha, L. Quadrifoglio, and E. Zechman. Comparing ant colony optimization and genetic algorithm approaches for solving traffic signal coordination under oversaturation conditions. *Computer-Aided Civil and Infrastructure Engineering*, 27(1):14–28, 2012.

[74] J. Wu, A. Abbas-Turki, and A. El Moudni. Cooperative driving: an ant colony system for autonomous intersection management. *Applied Intelligence*, 37(2):207–222, 2012.

[75] Z. Cong, B. De Schutter, and R. Babuška. Ant colony routing algorithm for freeway networks. *Transportation Research Part C: Emerging Technologies*, 37:1–19, 2013.

[76] F. Glover. Future paths for integer programming and links to artificial intelligence. *Computers & operations research*, 13(5):533–549, 1986.

[77] F. Glover and M. Laguna. *Tabu SearchâĹŮ.* Springer, 2013.

[78] T. Hu and L. Chen. Traffic signal optimization with greedy randomized tabu search algorithm. *Journal of Transportation Engineering*, 138(8):1040–1050, 2012.

[79] N. Metropolis, A.W. Rosenbluth, M.N. Rosenbluth, A.H. Teller, and E. Teller. Equation of state calculations by fast computing machines. *The journal of chemical physics*, 21(6):1087–1092, 1953.

[80] S. Memoli, G.E. Cantarella, S. de Luca, and R. Di Pace. Network signal

setting design with stage sequence optimisation. *Transportation Research Part B: Methodological*, 100:20–42, 2017.

[81] F. Glover, M. Laguna, E. Taillard, and D. de Werra. *Tabu search*. Baltzer Basel, 1993.

[82] H. Lo and A.H.F. Chow. Control strategies for over-saturated traffic. *ASCE Journal of Transportation Engineering*, 130:466–478, 2004.

[83] W.B. Powell. *Approximate Dynamic Programming - Solving the Curses of Dimensionality*. Wiley, Hoboken, New Jersey, 2010.

[84] A.H.F. Chow, S. Li, W.Y. Szeto, and D.Z.W. Wang. Modelling urban traffic dynamics based upon the variational formulation of kinematic waves. *Transportmetrica B*, 3(3):169–191, 2015.

[85] A. H. F. Chow, A Santacreu, I Tsapakis, G Tanasaranond, and T Cheng. Empirical assessment of urban traffic congestion. *Journal of Advanced Transportation*, 48(8):1000 – 1016, 2014.

[86] R. Sanchez, R. Horowitz, and P. Varaiya. Analysis of queue estimation methods using wireless magnetic sensors. *Transportation Research Record*, 2229:34–45, 2011.

[87] D.C. Gazis. *Traffic theory*, volume 50. Springer Science & Business Media, 2002.

[88] C. Diakaki, V. Dinopoulou, K. Aboudolas, M. Papageorgiou, E. Ben-Shabat, E. Seider, and A. Leibov. Extensions and new applications of the traffic-

responsive urban control strategy: coordinated signal control for urban networks. *Transportation Research Record*, 1856:202–211, 2003.

[89] C. Diakaki, V. Dinopoulou, K. Aboudolas, M. Papageorgiou, E. Ben-Shabat, E. Seider, and A. Leibov. Extensions and new applications of the traffic-responsive urban control strategy: coordinated signal control for urban networks. *Transportation Research Record*, 1856:202–211, 2003.

[90] A. Kouvelas, K. Aboudolas, M. Papageorgiou, and E. Kosmatopoulos. A hybrid strategy for real-time traffic signal control of urban road networks. *IEEE Transactions on Intelligent Transportation Systems*, 12:884–894, 2011.

[91] M. J. Smith. A local traffic control policy which automatically maximises the overall travel capacity of an urban road network. *Traffic Engineering and Control*, 21(6):298–302, 1980.

[92] A. Kouvelas, J. Lioris, S. Fayazi, and P. Varaiya. Maximum pressure controller for stabilizing queues in signalized arterial networks. *Transportation Research Record*, 2421:133–141, 2014.

[93] L. Tassiulas and A. Ephremides. Stability properties of constrained queueing systems and scheduling policies for maximum throughput in multihop radio networks. *IEEE transactions on automatic control*, 37(12):1936–1948, 1992.

[94] K. Aboudolas, M. Papageorgiou, A. Kouvelas, and E. Kosmatopoulos. A rolling-horizon quadratic-programming approach to the signal control problem in large-scale congested urban road networks. *Transportation Research Part C*, 18:680–694, 2010.

[95] T. Le, P. Kovacs, N. Walton, H. Vu, and L. Andrew. Decentralised signal control for urban road networks. *Transportation Research Part C*, 58:431–450, 2015.

[96] R. Sanchez, R. Horowitz, and P. Varaiya. Analysis of queue estimation methods using wireless magnetic sensors. *Transportation Research Record*, 2229:34–45, 2011.

[97] D. Krajzewicz, J. Erdmann, M. Behrisch, and L. Bieker. Recent development and applications of sumo - simulation of urban mobility. *International Jounral on Advanced in Systems and Measurements*, 5(3&4), 2012.

[98] D. Krajzewicz. *Traffic Simulation with SUMO âĂŞ Simulation of Urban Mobility*, volume 145. Springer, 2010.

[99] S. Krauss. *Microscopic modeling of traffic flow: Investigation of collision free vehicle dynamics*. PhD thesis, Universitat zu Koln., 1998.

[100] R.E. Allsop. Some possibilities for using traffic control to influence trip distribution and route choice. In *Transportation and Traffic Theory, Proceedings*, volume 6, 1974.

[101] M.J. Smith. Traffic control and route-choice; a simple example. *Transportation Research Part B: Methodological*, 13(4):289–294, 1979.

[102] R. Liu and M. Smith. Route choice and traffic signal control: A study of the stability and instability of a new dynamical model of route choice and traffic

signal control. *Transportation Research Part B: Methodological*, 77:123–145, 2015.

[103] M. J. Smith, R. Liu, and R. Mounce. Traffic control and route choice: Capacity maximisation and stability. *Transportation Research Part B: Methodological*, 81:863–885, 2015.

[104] B. G. Heydecker and J. D. Addison. Analysis of dynamic traffic equilibrium with departure time choice. *Transportation Science*, 39(1):39–57, 2005.

[105] A.H.F. Chow, K. Han, and K. Achuthan. An agent-based analysis of transport network vulnerability and resilience with provision of travel information. In *The Sixth International Symposium on Dynamic Traffic Assignment*, 2016.

[106] TraCI4Matlab: A implementation of the traci interface for matlab. `http://uk.mathworks.com/matlabcentral/fileexchange/44805-traci4matlab?requestedDomain=www.mathworks.com`, note = [Accessed on: 17 Oct 2017].

[107] A.H.F. Chow and R. Sha. Performance analysis of centralized and distributed systems for urban traffic control. *Transportation Research Record: Journal of the Transportation Research Board*, (2557):66–76, 2016.

[108] OpenStreetMap. `http://www.openstreetmap.org/`. [Accessed on: 30 Oct 2017].

[109] J.D.C. Little, M.D. Kelson, and N.H. Gartner. Maxband: A program for set-

ting signals on arterials and triangular networks. In *Transportation Research Record 795*, pages 40–46. TRB, 1981.

[110] N.H. Gartner, S.F. Assmann, F. Lasaga, and D.L. Hous. Multiband–a variable-bandwidth arterial progression scheme. Number 1287, 1990.

[111] T. Arsava, Y. Xie, and N.H. Gartner. Arterial progression optimization using od-band: Case study and extensions. *Transportation Research Record: Journal of the Transportation Research Board*, (2558):1–10, 2016.

[112] E. Camponogara and H.F. Scherer. Distributed optimization for model predictive control of linear dynamic networks with control-input and output constraints. *IEEE Transactions on Automation Science and Engineering*, 8(1):233–242, 2011.

[113] J. Haddad, B. De Schutter, D. Mahalel, I. Ioslovich, and P. Gutman. Optimal steady-state control for isolated traffic intersections. *IEEE Transactions on automatic control*, 55(11):2612–2617, 2010.

[114] J. Reilly and A.M. Bayen. Distributed optimization for shared state systems: applications to decentralized freeway control via subnetwork splitting. *IEEE Transactions on Intelligent Transportation Systems*, 16(6):3465–3472, 2015.

[115] M. Rinaldi, W. Himpe, and C.M.J. Tampère. A sensitivity-based approach for adaptive decomposition of anticipatory network traffic control. *Transportation Research Part C: Emerging Technologies*, 66:150–175, 2016.